

**WATER INDUCED EROSION OF MINE WASTE:  
COMPLICATING CHARACTERISTICS AND PREDICTIVE TOOLS**

by

BEVIN J. HARRISON

B.Sc., The University of Victoria, 1996

A THESIS SUBMITTED IN PARTIAL COMPLETION OF THE  
REQUIREMENTS FOR THE DEGREE OF

MASTERS OF APPLIED SCIENCE

in

THE FACULTY OF GRADUATE STUDIES  
(Department of Civil Engineering)

We accept this thesis as conforming to the required standard

THE UNIVERSITY OF BRITISH COLUMBIA

August 2003

©Bevin J. Harrison, 2003

In presenting this thesis in partial fulfilment of the requirements for an advanced degree at the University of British Columbia, I agree that the Library shall make it freely available for reference and study. I further agree that permission for extensive copying of this thesis for scholarly purposes may be granted by the head of my department or by his or her representatives. It is understood that copying or publication of this thesis for financial gain shall not be allowed without my written permission.

Department of Civil Engineering

The University of British Columbia  
Vancouver, Canada

Date Aug. 15 2003

## **ABSTRACT**

The results of erosion of sediment loading from mine waste deposits extend far beyond the mine footprint itself. Material that migrates into local rivers degrades water quality and the habitats of many wildlife species dependent on it. Predicting erosion rates to take the appropriate prevention and remediation steps is key to minimizing the off-site impacts of migrating mine waste. This study comprises an in-depth review of the detachment and transport mechanisms of water induced erosion. It evaluates the current tools available for predicting the rates of water induced erosion for their use in the mining industry and explores the relationships, limits and threshold conditions under which water induced erosion is accelerated. A sensitivity analysis of the Water Erosion Prediction Project (WEPP) model is provided for a generic oxide/sulphide mine in South East Asia to demonstrate not only the model sensitivity but also its applicability to industries outside the agricultural realm for which it was originally developed.

## TABLE OF CONTENTS

ABSTRACT .....	II
TABLE OF CONTENTS .....	III
LIST OF TABLES.....	VIII
LIST OF FIGURES .....	IX
ACKNOWLEDGMENTS .....	XI
1. INTRODUCTION .....	1
2. EROSION THEORY .....	5
2.1 Definitions .....	5
2.1.1 Erosion.....	5
2.1.2 Sedimentation .....	6
2.1.3 Soil Erosion, Soil Loss, Sediment Yield and Sediment Delivery Ratio (SDR) .....	6
2.1.4 Upland Erosion .....	7
2.1.5 Types of Erosion.....	8
2.2 Soil Erosion Rates.....	9
2.3 Hydrologic Factors in Soil Erosion .....	11
2.3.1 Precipitation.....	11
2.3.2 Runoff Generation .....	12
2.4 Types of Soil Erosion .....	12
2.4.1 Interrill Erosion.....	13
2.4.2 Rill Erosion.....	15
2.4.3 Gully Erosion.....	16
2.4.4 Channel Erosion.....	17
2.4.5 Piping or Tunnel Erosion.....	17
2.4.6 Mass Movements .....	18
2.5 Interrill and Rill Erosion Relationships .....	18
2.5.1 Sediment Continuity Equation.....	19



2.5.2	Relationship Between Detachment and Transport .....	21
2.5.3	Detachment By Rainfall .....	23
2.5.4	Transport By Rainfall .....	27
2.5.5	Detachment By Runoff.....	27
2.5.6	Detachment Capacity, $D_C$ .....	28
2.5.7	Actual Detachment, $D_A$ .....	30
2.5.8	Physically Based Detachment Equation .....	31
2.5.9	Transport By Runoff.....	32
2.6	Future Research .....	39
3.	FACTORS AFFECTING SOIL EROSION: RELATIONSHIPS, LIMITS AND THRESHOLDS.....	42
3.1	Factors Affecting Soil Erosion .....	42
3.2	Climate.....	43
3.2.1	Effects on Erosion.....	43
3.3	Hydrology.....	46
3.3.1	Runoff.....	46
3.3.2	Infiltration and Seepage.....	50
3.3.3	Entrapped Air.....	54
3.3.4	Surface Seals and Surface Crusts .....	55
3.4	Soil Physical Properties .....	57
3.4.1	Soil Texture, Structure and Strength .....	58
3.4.2	Bulk Density and Unit Weight .....	66
3.5	Chemical and Mineralogical Properties.....	69
3.5.1	Organic Material.....	69
3.5.2	Clay Content and Exchangeable Cations.....	70
3.6	Soil Hydrologic Properties .....	74
3.7	Landscape .....	75
3.7.1	Slope Gradient .....	75
3.7.2	Slope Length.....	79
3.7.3	Slope Shape .....	81

3.7.4	Examples of Erosion Impacts .....	81
3.8	Land Use .....	82
3.8.1	Cover .....	83
3.8.2	Terraces .....	85
3.9	Summary .....	86
4.	EROSION MODELS .....	91
4.1	Empirically Based Erosion Prediction Equations .....	92
4.1.1	Universal Soil Loss Equation (USLE) .....	92
4.1.2	Revised Universal Soil Loss Equation (RUSLE) .....	96
4.1.3	Modified Universal Soil Loss Equation (MUSLE) .....	99
4.1.4	Other USLE Modifications .....	100
4.2	Overview of Erosion Simulation Models .....	101
4.3	Physically Based Erosion Models .....	103
4.3.1	Water Erosion Prediction Project (WEPP) .....	103
4.3.2	Griffith University Erosion System Template (GUEST) .....	105
4.3.3	European Soil Erosion Model (EUROSEM) .....	114
4.4	Other Erosion Simulation Models .....	123
4.4.1	Agricultural Nonpoint Source Pollution (AGNPS) .....	123
4.4.2	Areal Non-Point Source Watershed Environment Response Simulation (ANSWERS) .....	123
4.4.3	Chemicals, Runoff and Erosion from Agricultural Management Systems (CREAMS) .....	125
4.4.4	Erosion Productivity Impact Calculator (EPIC) .....	126
4.4.5	Kinematic Runoff and Erosion Model (KINEROS) .....	127
4.4.6	Kentucky Erosion Model (KYERMO) .....	127
4.4.7	Limburg Soil Erosion Model (LISEM) .....	129
4.4.8	Modeling Within-Storm Sediment Dynamics (MWISED) .....	130
4.4.9	Productivity Index (PI) .....	131
4.4.10	RillGrow 1 and 2 .....	131
4.4.11	Water and Tillage Erosion Model (WATEM) .....	132

4.5	Summary.....	132
5.	WATER EROSION PREDICITON PROJECT MODEL: OVERVIEW .....	138
5.1	Background.....	138
5.2	Scope and Application.....	140
5.3	Model Structure .....	140
5.3.1	Climate Generation.....	142
5.3.2	Winter Hydrology.....	144
5.3.3	Hydraulics of Overland Flow .....	146
5.3.4	Hillslope Surface Hydrology .....	147
5.3.5	Water Balance and Percolation.....	149
5.3.6	Subsurface Hydrology .....	151
5.3.7	Soils .....	153
5.3.8	Plant Growth.....	154
5.3.9	Residue Decomposition and Management .....	155
5.3.10	Hillslope Erosion .....	156
5.3.11	Irrigation .....	161
5.4	Limitations of the WEPP Model.....	161
6.	WATER EROSION PREDICTION PROJECT MODEL: APPLICATION.....	167
6.1	WEPP Required Parameters .....	167
6.2	Field vs. Laboratory Evaluation .....	167
6.3	Setting Up a Field Study .....	168
6.4	Laboratory Experimentation.....	170
6.5	Parameter Estimation.....	171
6.5.1	Interrill Erodibility ( $K_i$ ).....	171
6.5.2	Rill Erodibility ( $K_r$ ).....	172
6.5.3	Critical Shear Stress ( $\tau_c$ ).....	173
6.5.4	Effective Hydraulic Conductivity Parameter ( $K_e$ ).....	173
6.6	Sensitivity Analysis Using the WEPP Model.....	174
6.6.1	Site Background.....	175

6.6.2 WEPP Model Input Parameters: Estimation of Suitable Ranges.....	175
6.6.3 Results of Sensitivity Analysis .....	187
7. CONCLUSIONS .....	213
REFERENCES .....	217
APPENDIX I .....	229

## LIST OF TABLES

Table 2.1 Average Interrill and Rill Erosion For 1982 and 1992 (Uri, 2001).....	10
Table 3.1 Sediment Classification .....	58
Table 3.2 Soil Erodibility Based on Critical Shear Values .....	64
Table 3.3 Soil Characteristics .....	67
Table 3.4 Grainsize Distribution.....	67
Table 3.5 Ranges of CEC for various soil textures (Flanagan and Nearing, 1995) ..	71
Table 3.6 Summary of Factors Affecting the Erosion Process.....	87
Table 4.1 Erosion Model Summary .....	134
Table 6.1 Uniform Slope Profile to Concave Slope Profile .....	179
Table 6.2 Structural Characteristics Varied in the WEPP Sensitivity Analysis .....	179
Table 6.3 Pohnpei Island Characteristics.....	181
Table 6.4 Climate Parameters for Pohnpei Island and South East Asia.....	181
Table 6.5 WEPP Soil Layer Characteristics .....	186

## LIST OF FIGURES

Figure 2.1 Types of Erosion Based on Erosive Agents (Lal, 1990).....	12
Figure 2.2 Conceptual Model of the Soil Erosion Process (Meyer and Wischmeier, 1969).....	20
Figure 3.1 Factors Affecting Soil Erosion (Modified from Lal, 1990) .....	43
Figure 3.2 Runoff Generation (Owoputi, 1994) .....	48
Figure 3.3 Soil Texture Triangle (Ballard, 1999).....	59
Figure 3.4 Conceptual model showing the effect of slope gradient on delivery rate during interrill erosion (Foster and Meyer, 1972a) .....	76
Figure 3.5 Slope Shapes (Modified from Lal, 1990).....	81
Figure 4.1 Soil Erosion Prediction Using GUEST Technology (Yu <i>et al.</i> , 1997) ..	106
Figure 4.2 EUROSEM Model Description (Morgan <i>et al.</i> , 1998) .....	116
Figure 5.1 WEPP Model Structure (Modified from Flanagan and Nearing, 1995)	141
Figure 6.1 Baseline Tailings or Waste Rock Pile Design.....	176
Figure 6.2 Single and Multiple Lift Configurations of Uniform Slope.....	177
Figure 6.3 Concave Slope Configuration .....	179
Figure 6.4 Location of Pohnpei Island (Graphic Maps, 2001) .....	180
Figure 6.5 Comparison of Soil Loss for Different Slope Shapes .....	189
Figure 6.6 Comparison of Runoff for Single Raise Uniform Hillslopes with Differing Slope Gradients and Bench Lengths.....	190
Figure 6.7 Comparison of Soil Loss for Single Raise Uniform Hillslopes with Differing Slope Gradients and Bench Lengths.....	190
Figure 6.8 Comparison of Runoff for Single Raise Uniform Dams with Differing Slope Gradients and Bench Lengths.....	192
Figure 6.9 Comparison of Soil Loss for Single Raise Uniform Dams with Differing Slope Gradients and Bench Lengths.....	192
Figure 6.10 Comparison of Runoff for Single and Multiple Raise Uniform Hillslope Configurations with Differing Slope Gradients.....	193
Figure 6.11 Comparison of Soil Loss for Single and Multiple Raise Uniform Hillslope Configurations with Differing Slope Gradients.....	194
Figure 6.12 Comparison of Soil Loss for Single and Multiple Raise Hillslopes and Dams of Uniform and Concave Slope Shapes with Differing Slope Gradients .....	195
Figure 6.13 Comparison of Runoff for Uniform and Concave Hillslope Under 100-year Continuous Simulation Climate Conditions .....	196
Figure 6.14 Comparison of Soil Loss for Uniform and Concave Hillslopes Under 100-year Continuous Simulation Climate Conditions.....	197
Figure 6.15 Comparison of Single Event Soil Loss for Uniform and Concave Hillslopes .....	198
Figure 6.16 Comparison of Interrill Erodibility and the Effect on Soil Loss for 3H:1V Hillslopes of Linear and Concave Configuration .....	199

Figure 6.17 Comparison of Interrill Soil Loss for Various Single Event Storm Intensities.....	202
Figure 6.18 Comparison of Soil Loss for Uniform and Concave Hillslopes for Differing Rill Erodibility Factors .....	203
Figure 6.19 Comparison of Runoff for Single Raise Uniform and Concave Hillslopes for Differing Effective Hydraulic Conductivity Values .....	204
Figure 6.20 Comparison of Soil Loss for Single Raise Uniform and Concave Hillslopes for Differing Effective Hydraulic Conductivity Values.....	205
Figure 6.21 Effect of Single Storm Rainfall Intensity on Runoff for Single Raise Uniform 3H:1V Hillslopes Under Differing Effective Hydraulic Conductivities .....	206
Figure 6.22 Effect of Single Storm Rainfall Intensity on Soil Loss for Single Raise Uniform 3H:1V Hillslopes Under Differing Effective Hydraulic Conductivities .....	206
Figure 6.23 Effects of Sand Concentration on Average Annual Runoff.....	207
Figure 6.24 Effect of Sand Concentration on Average Annual Soil Loss.....	208

## **ACKNOWLEDGMENTS**

I would like to take this opportunity to thank the following organizations, influential people and friends.

- Klohn Crippen Consultants Ltd., for providing some of the financial support and the leave of absence required for me to complete this degree.
- Dr. Barbara Lence of the Department of Civil Engineering at UBC, supervisor, for her willingness to take on an unusual student and a topic outside her field of expertise. Thanks to Barbara for her time, constant encouragement, ideas, support and reviewing.
- Dr. Les Lavkulich for his consultation time and scientific background on the topic of erosion.
- Seoris Harrison, my Mom for living unconditionally with me, my stress and my mess for the past two years.
- Alex Harrison, my Dad for always asking me “so are you finished yet?”
- Friends especially Pam, Karin, Karyn and my sister Erin who, even though they didn’t see me much, were there when I could tear myself away. I am looking forward to starting my life back up.
- Finally, Mike Scholz, for his patience, support and encouragement.



## 1. INTRODUCTION

The migration and loss of fertile soil from agricultural and forestry areas due to erosion is of great concern worldwide. It is well known that when exposed to water and wind, soil will migrate and likely be deposited in streams, reservoirs and ultimately the ocean causing sedimentation and reducing water quality. The slow rate of soil formation and the accelerated erosion process due to anthropogenic influences may result in a loss of fertile soil forever. In the past, the investigation of erosion on non-agricultural lands was limited to a few studies of erosion on construction sites (Wischmeier *et al.*, 1971; Wischmeier and Smith, 1978). Recently, increased concern for the migration of mine wastes to the surrounding environment has led to the investigation into the erosion impacts of the mining industry on the receiving environment. This thesis is designed to synthesize the information related to the factors that contribute to the accelerated water erosion process while providing, where possible, the threshold conditions under which the erosion of mine waste material takes place. A critique of the available erosion prediction technologies with respect to their applicability to the mining industry is also provided so that the selection of an appropriate model will reflect the dominant factors that accelerate water erosion of mine waste.

Since the inherent chemical and physical toxicity of mine waste materials makes it necessary for them to be contained, the current practice for limiting the migration of toxic by-products from mining and milling during mine operation and post-closure is to concentrate the material in tailings or spoil piles and cover them with earthen material. A mixture of vegetation and rip-rap (coarse rock) can be used to stabilize the material and limit the penetration of oxygen and/or water depending on the climatic regime and the reactivity of waste material being contained. This practice is becoming increasingly accepted as covers can be designed to blend into the

surrounding landscape. However, the effects of water erosion on bare, exposed mine wastes begins long before covers and rehabilitation can be considered. The accurate prediction of erosion and sedimentation rates during mine operation allows for the establishment of cost-effective maintenance schedules and appropriate sedimentation pond design to ensure that mine waste does not migrate off-site.

Erosion processes occur under several sets of conditions and are a function of the erodibility of the material (material properties) and the erosivity, the potential ability of an agent (rainfall, overland flow and/or seepage) to cause erosion. Though past research has focused on determining these relationships for forestry and agriculture, some application of the current erosion science to mining has been undertaken for coal mine spoil in Australia and the eastern United States. Very limited research has been conducted on the erosion of tailings resulting from oxide and sulphide mining. As a result, the observations and conclusions for mining operations provided in this study are based on a synthesis of a variety of mining and non-mining published cases.

The goals of this study are to investigate the processes of erosion that cause the physical migration of mine waste from stockpiles in which they are originally stored. More specifically, this study aims to:

- Provide a detailed overview of the physical nature of the erosion process as it is currently understood in the literature;
- Discuss the characteristics that complicate the water induced erosion process, establish the general conditions under which accelerated erosion appears to occur and provide, where possible, the threshold conditions under which erosion takes place;
- Provide a summary of the models available for predicting erosion rates and document their limitations in application to the field of mine waste;

- Conduct a sensitivity analysis of the Water Erosion Prediction Project (WEPP) model using a generic mine waste storage facility; and
- Provide guidelines for conducting either field or laboratory scale experiments to estimate the erodibility parameters that are required as input to the WEPP model.

An overview of the theory of erosion mechanics is provided in Chapter 2, taking into account the types of detachment and transport capacity equations that have been derived to explain the water erosion. The complexities of the water erosion processes, as they interact with environmental factors is discussed in Chapter 3, with particular attention focussed on outlining threshold conditions where possible. Chapter 4 provides a summary of the water erosion prediction models available, highlighting their limitations and application to the mining industry. An in depth explanation of the Water Erosion Prediction Project (WEPP) model, the most attractive model available for estimating mine waste erosion, is given in Chapter 5. Chapter 6 details the results of a sensitivity analysis of the WEPP model for a mine waste site in South East Asia and provides an explanation of how to set up a successful erosion prediction experiment to estimate the parameters necessary to use the WEPP model. Finally, Chapter 7 provides the conclusions of the study.

This thesis is composed of information that is designed for use by two types of readers. For the casual reader who wishes to gain a general understanding of the water erosion process and acquire a quick impression of the current technologies available for erosion prediction, a review of Chapters 2 and 4 is recommended. The summary table at the end of Chapter 3 also provides a quick reference for the list of factors that complicate the erosion processes outlined in Chapter 2. For the more knowledgeable technical reader, the detailed discussion of the complicating erosion characteristics in Chapter 3 presents the more pertinent issues for designing and carrying out a successful erosion estimating analysis. The background information

provided in Chapter 5 supplements the example of the use of the WEPP model provided in Chapter 6. The results of the WEPP sensitivity analysis as well as guidance for determining input parameters for the WEPP model presented in Chapter 6, are necessary reading for any erosion prediction study using this model.

## **2. EROSION THEORY**

This chapter introduces the topic of erosion and provides definitions of the key terms encountered when discussing the erosion processes. The hydrologic factors required to initiate water erosion are first discussed followed by an overview of the types of erosion and the theory behind several of the erosion processes. The conditions that complicate the erosion prediction process and the environmental factors that affect the magnitude of the erosion processes are discussed in Chapter 3.

### **2.1 Definitions**

The following definitions provide the basic background for discussing the topic of water erosion.

#### **2.1.1 Erosion**

Bates and Jackson (1984) define erosion as the “wearing away of soil and rock by weathering, mass wasting and the action of streams, glaciers, waves, wind and underground water.” In keeping with this definition, Selby (1993) recognizes that

$$\text{Erosion} = f(\text{Erodibility, Erosivity}), \quad [2.1]$$

where erodibility is the vulnerability of the soil or rock to the processes of erosion and erosivity is the potential ability of an agent to cause erosion. The erosivity agents include the eroding power of raindrops, flowing water and sliding or flowing earth masses each of which initiate the broader mechanisms of detachment and transport that together define the erosion process. Though not a factor in the removal of soil particles from the soil mass, deposition plays a significant role in the erosion cycle by making sediment available for future erosion events.

When the erosive forces of raindrop impact or flowing water exceed a soil particle's resistance to dislodging from the soil mass, detachment occurs (Foster, 1982). The entrainment and movement of sediment from its original location by raindrop splash or overland flow is called transport while deposition occurs when the transport capacity of a given flow is not great enough to transport a sediment load of a given particle size (Foster, 1982).

Some sources of sediment available for detachment, transportation and deposition include natural geological erosion sites (badlands), agricultural areas, forestry road cuts, construction sites, surface mined land and mine waste deposits. Sediment can be deposited at many stages throughout the transport process including but not limited to, the toe of slopes, streams or reservoirs, vegetation traps or simply at changes in slope gradient (Foster, 1982).

### **2.1.2 Sedimentation**

The action of depositing sediments due to the inability of the flow to transport that sediment is called sedimentation. Sedimentation has significant economic, environmental and social implications in that it causes a reduction in the storage capacity of reservoirs, contributes to eutrophication of lakes and increases the turbidity of the receiving water. Thus, sedimentation is often used as a measure of water quality. Some scientists believe that sedimentation is the major cause of concern for which erosion is simply the initial stage (Lal, 1990).

### **2.1.3 Soil Erosion, Soil Loss, Sediment Yield and Sediment Delivery Ratio (SDR)**

The distinction between soil erosion, soil loss and sediment yield is important when quantifying the amount of sediment removed from a hillslope or watershed during an erosion event and interpreting model output. The definitions in the literature are not universal. For the purposes of this study, the following definitions are used. Soil

erosion is the gross removal of soil by the erosive agents (Lal, 1990). Soil loss according to Nearing *et al.* (1994) is the amount of soil lost in a specific time period over an area of land which has experienced net soil loss (the difference between the amount of soil dislodged and the amount deposited). Soil loss is expressed in units of mass per unit area such as t/ha or kg/m<sup>2</sup>. It may be given for a single storm event or an average value for a number of years and is of interest for on-site effects of erosion. The fraction of sediment which leaves a specified area of land in a given time period is the sediment yield. It refers to the mass of sediment that crosses a boundary such as the edge of a field or outlet of a watershed. Any sediment deposited in the transporting waterways of a watershed does not contribute to the sediment yield. Sediment yield may be expressed in units of total mass (kg), mass per unit width of the boundary (kg/m) or mass per unit area (t/ha or kg/m<sup>2</sup>). Sediment yield is important in term of off-site effects of erosion including siltation of sedimentation ponds, streams and reservoirs.

Sediment yield is usually not available as a direct measurement but is estimated by using either the sediment delivery ratio (SDR) or the flow transport capacity (Yulianti, 1996). The SDR is expressed as a percent of gross soil erosion by water that is delivered to a watershed outlet or a particular point in the drainage system (Renard *et al.*, 1994). It is computed as the ratio of sediment yield at the watershed outlet or point of interest to the gross erosion in the entire watershed. Gross erosion includes sheet, rill, gully and channel erosion each of which are discussed in detail in Section 2.4 (Renard *et al.*, 1994). Flow transport capacity is the amount of sediment that can be transported by a given flow.

#### **2.1.4 Upland Erosion**

Any area where overland flow could be generated and incorporated into a hydrologic model is considered to be an upland area (Foster and Meyer, 1972a). Erosion in

upland areas is also referred to as hillslope erosion. The processes of erosion that occur on hillslope areas involve not only the detachment of the soil particles, but also the transport of this material downslope.

### 2.1.5 Types of Erosion

The following basic definitions of each of the erosion processes will be discussed in greater detail in subsequent sections.

**Rill Erosion** - soil erosion that occurs in numerous, randomly occurring, small, channels measuring only a few centimeters wide and deep (Brady and Weil, 1996). Rills may follow tillage marks or develop like drainage networks of rivers in a large basin;

**Interrill Erosion** - soil erosion that occurs through the removal of a thin, relatively uniform layer of soil particles from areas between rills (Foster, 1982);

**(Classical) Gully Erosion** - soil erosion that occurs in a gully, a rill that cannot be removed by regular tillage (Meyer *et al.*, 1975). Gullies evolve by means of erosion of the gully bottom, through the advancement of the gully upslope (head-cut migration) and erosion of gully walls. This type of erosion implies a movement of sediment by water erosion and gravity;

**Ephemeral Gully** - a short-lived rill that may reappear in the same place once tillage has removed it. The movement of sediment occurs by channelized flow;

**Channel Erosion** - movement of soil by the action of streamflow (Foster, 1982);

**Pipe or Tunnel Erosion** - the rapid subsurface flow of water removing soil material (Foster, 1982); and

**Landslide Erosion** - the movement of soil en masse by gravity (Foster, 1982).



Though the interrill and rill erosion processes are the focus of this research, the definitions of the other erosion processes are provided here for completeness.

## **2.2 Soil Erosion Rates**

New soil formation or the development of soil from parent material is a slow process measured on a geological time scale. According to Lal (1990:3), "it takes hundreds of thousands of years to develop the equivalent of a 5-cm layer of fertile soil. Natural soil formation rates have been reported in the range of 0.01 to 0.10 mm depth/year, approximately 0.15 to 1.5 t/ha/year assuming a dry density of 1.5 t/m<sup>3</sup> (Williams, 2002b). The natural erosion process also takes place on a geologic time scale and together, these processes contribute to shaping the landscape.

Since the climatic conditions and soil properties themselves contribute to the soil erosion process, the rates of natural and accelerated erosion vary both spatially and temporally. As a result the rates of the natural soil erosion process have been reported as range values. According to Brady and Weil (1996), natural soil erosion amounts to approximately 0.2 to 0.5 t/ha/year in the United States. Williams (2002b) reports natural soil erosion rates of 0.75 t/ha/year in Australia. Both approximations fall within the range of soil formation rates reported above, suggesting a natural equilibrium.

Though accelerated erosion or erosion that exceeds this natural rate can occur in nature, due to landslides and other episodic erosion events, accelerated rates are largely caused by anthropogenic influences that make the soil more susceptible to the actions of water and wind (Brady and Weil, 1996). The human induced soil erosion process is generally more drastic and rapid than natural erosion events. In exposed agricultural areas for example, the equivalent of 1 cm depth of topsoil over a given area may be lost in a single rainstorm or windstorm (Lal, 1990).

The values in Table 2.1 provide some estimates for average combined interrill and rill erosion rates in agricultural areas in the United States for the years of 1982 and 1992.

**Table 2.1 Average Interrill and Rill Erosion For 1982 and 1992 (Uri, 2001)**

LAND USE BY YEAR	HECTARES (Millions)	WATER EROSION (t/ha/year)
<b>1982</b>		
Cropland	170.3	10.3
Highly Erodible Cropland	50.6	19.1
Cultivated	41.9	22.1
Non-cultivated	8.7	5.0
Non-highly Erodible Cropland	119.7	6.5
Cultivated	106.3	7.0
Non-cultivated	13.4	1.0
<b>1992</b>		
Cropland	154.7	7.8
Highly Erodible Cropland	42.7	14.6
Cultivated	33.5	17.3
Non-cultivated	9.1	4.3
Non-highly Erodible Cropland	112.0	5.3
Cultivated	98.1	6.0
Non-cultivated	13.9	1.0

The rates of erosion between 1982 and 1992 have clearly decreased due to active soil conservation measures. These values are supported by Bhuyan *et al.* (2002) who report water erosion rates of >13 t/ha/year on cultivated row crops in the United States. In the humid tropics, on cultivated slopes of 30 %, Sheng (1989) reports soil loss rates can be between 100 and 200 t/ha/yr without practicing conservation measures.

Acceptable soil loss tolerances or “the maximum level of soil erosion that will permit a high level of crop productivity to be sustained economically and indefinitely” are in the range of 4 to 11 t/ha/year according to Wischmeier and Smith (1978:3). As indicated by the average values reported in Table 2.1, some of the highly erodible

croplands in the United States do not fall within this tolerance range. In addition, the acceptable soil erosion rates provided by Wischmeier and Smith (1978) far exceed the natural soil creation rate quoted above.

The tolerable erosion rates from rehabilitated mine slopes from the Bowen Basin Coal fields in Central Queensland, Australia is 12 to 40 t/ha/year (Williams, 2002b). Erosion rates from other human impacted areas such as construction sites have also been estimated. In Maryland and Virginia Chen (1974) reports a range of soil losses from 120 to 500 t/ha/year from construction sites. These rates again far exceed the estimated natural soil formation rates. The literature does not provide soil erosion rates for bare, exposed mine waste material.

## **2.3 Hydrologic Factors in Soil Erosion**

In order for erosion to take place, two driving hydrologic factors are required. First, water must be added to the soil surface through precipitation and second, runoff must be generated either above or below the ground surface. In a watershed situation, runoff can be divided into overland-flow and channel-flow whereas hillslope erosion is limited to the mechanisms of overland flow. The hydrologic factors and their effects on the soil erosion process are discussed in more detail in Section 3.3.

### **2.3.1 Precipitation**

It is generally assumed that important rainfall factors including kinetic energy, rainfall intensity and drop size distribution can either be measured directly or estimated stochastically (Foster and Meyer, 1972a; Al-Durrah and Bradford, 1982; Owoputi, 1994). The addition of precipitation as snow complicates the erosion process when snowmelt begins. Snowmelt adds significant amounts of stored water to the volumes of overland flow increasing the potential for erosion (Renard *et al.*, 1994).

### 2.3.2 Runoff Generation

Though rainfall plays a dominant role in detaching soil material, runoff is more significant in detaching and transporting material downslope (Yu and Rose, 1999). Rainfall at an intensity that is greater than the infiltration rate of a soil produces runoff as Hortonian overland flow (Nakano *et al.*, 1986). Other methods of runoff generation include saturation overland flow whereby percolation deep into the soil profile is prevented due to a low permeability layer close to the surface. As rainfall continues, the soil storage capacity is filled until the water table rises to become coincident with the soil surface. Any further addition of rainfall generates runoff. Runoff generation by means of Hortonian excess and saturation overland flow significantly increase the soil erosion rates above those accomplished by rainfall alone.

### 2.4 Types of Soil Erosion

Figure 2.1 shows the erosion types based on their major causes.

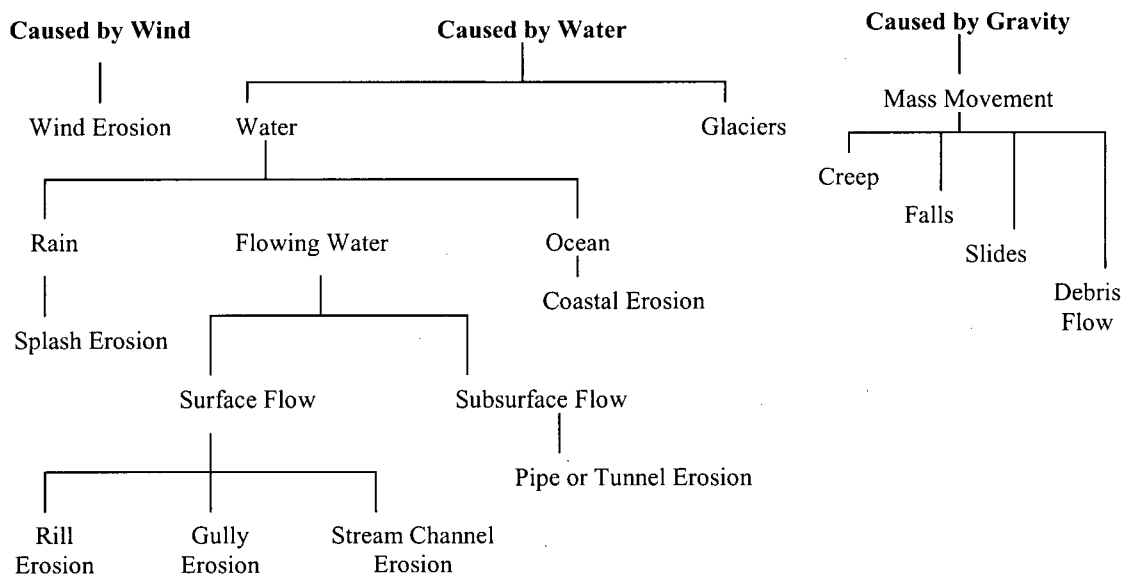


**Figure 2.1 Types of Erosion Based on Erosive Agents (Lal, 1990)**

The erosion processes caused by wind and gravity are not the subjects of this research. An evaluation of the types of water induced erosion processes encountered in the mining industry is presented below.

Sections 2.4.1 through 2.4.6 provide a discussion of the types of erosion that would be effective in mobilizing sediment in the mined landscape. Of the hillslope erosion processes, the interrill and rill erosion processes are the most frequently occurring processes in water erosion. Interrill and rill erosion are further defined using the following four sub-processes:

1. Detachment by rainfall;
2. Transport by rainfall;
3. Detachment by runoff; and
4. Transport by runoff.

It is important to note that the basic principles governing the interrill and rill erosion processes remain the same when the soil is exposed regardless of the land use (Wischmeier and Smith, 1978).

#### **2.4.1 Interrill Erosion**

Interrill erosion is sometimes incorrectly classified as a less severe stage of the erosion process than rill erosion (Foster, 1982). This misconception arises because uniform layers of soil particles are removed from interrill areas which are often less noticeable than the small channels that develop as rill erosion occurs. Since the removal of consecutive layers of soil particles characterizes the interrill erosion process, it is often referred to as sheet erosion. In addition, the interrill erosion process is initiated as soon as a rainfall event begins due to soil detachment by raindrop impact. Rill erosion; however, commences once infiltration rates have

slowed and concentrated overland flow can generate sufficient depth and velocity to entrain and transport sediment (Foster, 1982).

Of the four sub-processes listed in Section 2.4 above, the interrill erosion process is governed by the detachment of sediment by raindrop impact and the transport of sediment by both raindrop splash and thin, sheet or overland flow to rills (Meyer, 1981). Since both the depth and flow rates of sheet flow are small on interrill areas, the flow shear stress is also small. As a result, any additional detachment of soil particles due to overland flow on interrill areas is neglected since the flow energy is consumed transporting soil material and is therefore unavailable for additional detachment (Foster and Meyer, 1972a).

Overland flow in interrill areas alone can transport only the smallest particle sizes. However, the kinetic energy of the raindrop impacting the soil is transferred to the soil surface, inducing the separation of soil particles (Fan and Wu, 2001) while also creating localized turbulence in the thin overland flow (Owoputi, 1994). These combined rainfall disturbances make it possible for larger particles to be entrained in the flow. Since splash detachment is the primary factor in soil availability to interrill flow transport and significantly increases the transport capacity of the thin sheet flow (Foster, 1982; Grosh, 1994), it is concluded that rain intensity rather than rainfall amount is more important in causing erosion in interrill areas (Watson and Laflen, 1986). It should be noted that although raindrop splash can deliver sediment directly to rills, the rate of occurrence is low. Often the minor effect of splash erosion is combined with the major effect of sediment movement by overland flow when characterizing sediment delivery from interrill to rill areas (Meyer, 1981).

The amount of sediment detached by raindrops and transported by overland flow are inter-related. The amount of sediment that raindrops will be able to detach depends on the depth of the overland flow. If the depth of the overland flow is greater than

one-third the diameter of the impacting raindrop, detachment by the raindrop will not occur (Fan and Wu, 2001). Also, the injection of soil particles into the overland flow caused by raindrops will be affected by the amount of sediment already being transported by the overland flow (i.e. sediment concentration).

Though interrill and rill erosion are independent processes, the severity of rill erosion depends on the sediment input from interrill areas (Foster, 1982). Deposition in rills will occur when the influx of sediment from interrill areas is greater than the flow transport capacity in rills (Foster, 1982). However, if the influx of sediment from interrill areas is less than the transport capacity of the flow in rills, detachment occurs. Even with the addition of sediment from interrill areas, detachment will also occur when the flow is able to maintain sufficient erosive forces to overcome the soil resistance of the soil to erosion (Foster and Meyer, 1972a).

#### **2.4.2 Rill Erosion**

Rill erosion is the process of sediment movement due to concentrated flow within the rill itself (Foster, 1982). When the velocity and turbulence of overland flow become great enough, rill formation takes place (Warrington *et al.*, 1989). However, the locations where rills develop are largely unknown. Some authors try to predict the locations where rills will develop (Nakano *et al.*, 1986; Favis-Mortlock, 2002); however, since rill behavior during erosion events is not understood, predicting the location and formation of rills remains unexplained (Nakano *et al.*, 1986).

Of the four sub-processes listed in Section 2.4 above, detachment and transport by raindrop impact can be neglected since the water depth in rills is generally sufficient to dampen the erosive effects of raindrops. Although there is evidence that raindrops do aid in the ability of overland flow to transport additional sediment, the studies

supporting this have been conducted on interrill areas. Overland flow or rill flow is therefore the main cause of soil detachment and transport in a rill.

If the sediment inflow to a newly formed rill channel is less than the transport capacity of the rill flow and if the erosive forces of the flow exceed the resistance of the soil to detachment, rill erosion occurs. Most downslope movement of upland sediment is by flow in rills since the transport capacity of the deeper overland flow is greater than the transport capacity of thin sheet flow produced in interrill areas. Selby (1993) reports that rills are both collection areas for interrill sediment and transporting vessels for those sediments removed from rill walls and floors. Rill erosion is then the primary agent for sediment transport on slopes with little vegetation.

#### **2.4.3 Gully Erosion**

Rills and gullies can be distinguished only by their sizes. When a rill becomes so large that it cannot be removed by ordinary tillage practices, it is called a gully (Meyer *et al.*, 1975). However, with the evolution of tillage machinery over the history of agriculture, the distinction between rills and gullies has become dependent on the tillage practices and equipment. Press and Siever (1985) define a gully as a small steep sided valley or erosion channel greater than 0.3 m across, greater than 0.6 m deep and characterized by steep-sided erosion scarps several feet high. Due to the constant instability and catastrophic movement of gully sides, gully walls are devoid of vegetation ((Falk, 1985).

Gully erosion and mass wasting are the most impressive forms of erosion simply due to their magnitude. However, these processes only dominate in especially vulnerable areas, particularly steep, geologically young landscapes where the underlying material is mechanically weak and unconsolidated (El-Swaify and Fownes, 1989).



The setting and factors causing these forms of erosion are qualitatively understood but not quantitatively predictable (Falk, 1985).

Gully erosion is affected by the same combination of the sub-processes mentioned in Section 2.4 for rills. Unlike the continuous erosion that is a feature of rilling, gully erosion has been observed to occur in pulses. Pulsing events occur when the gully banks are undercut by the flow in the gully and the weight of the overhang exceeds the soil strength causing the overhang to slough off into the flow. Factors including the location of the phreatic surface, soil moisture content and movement, overburden loads and soil strength are important in these slope stability type failures (Foster, 1982). The sloughed material is mobilized through the gully system by the flow provided that the flow transport capacity is adequate to move the accumulated sediment. If the flow transport capacity is too low, the material remains in the gully bottom and helps stabilize the banks against further failures (Foster, 1982).

#### **2.4.4 Channel Erosion**

Channel erosion is a complex topic that is not investigated in detail in this study. The erosion of channels is determined using empirical river sediment transport and sediment yield relationships. These relationships are based on more fundamental hydraulic principles and aim to explain the changes in river morphology. Sediment transport relationships described by such authors as Yalin (1963), Bagnold (1966) and Govers (1987) have been modified for use in rill and interrill erosion theory and as a result have been incorporated into the discussion that follows.

#### **2.4.5 Piping or Tunnel Erosion**

The primary difference between piping or tunnel erosion and other forms of erosion caused by water is that piping or tunnel erosion is initiated due to subsurface flow. The concentrated hydraulic removal of subsurface soil creates underground

passageways in the natural landscape and earthworks structures. Typically, tunnel erosion occurs in semi arid and arid climates caused by water flowing rapidly through the shrinkage cracks (Selby, 1993). Cracking clays with high shrink-swell capacity are more prone to tunnel erosion than soils with high exchangeable sodium percentages (Selby, 1993). Determining sites of tunnel initiation and the variety of the initiation mechanisms make tunnel erosion an insidious and enigmatic process. Since the primary focus of this study is surface erosion, the process of pipe and tunnel erosion is mentioned here for completeness, and not investigated in detail.

#### **2.4.6 Mass Movements**

The force of gravity causes the downhill movement of sediment and distinguishes the erosion caused by mass movements from other types of surface erosion. However, other influencing factors such as slope gradient, the nature of the surface material and the water content determines whether these episodes occur quickly on some slopes and slowly on others (Press, 1985). When sediment is transported by water, it is simply a component of the overland flow. However, in the process of landslide erosion, large volumes of the soil body experience coherent movement as in rapid landslides or slow soil creep (Marshall *et al.*, 1996). The mechanisms behind mass movements are not discussed in detail here; however, it is recognized that portions of the theory used to describe the movement of soil en masse is relevant in the discussion of rill and gully erosion.

### **2.5 Interrill and Rill Erosion Relationships**

The following sections provide some of the equations that are used to describe the erosion sub-processes as they relate to interrill and rill erosion. The sediment continuity equation adopted by most erosion specialists is described in Section 2.5.1 and the relationship between detachment and transport required to solve the continuity equation are given in the sections that follow.

### 2.5.1 Sediment Continuity Equation

The conservation of mass equation for sediment discharge from a control volume is the governing equation used to describe dynamic upland, surface water erosion process by many researchers (Foster and Meyer, 1972a). Foster (1982) presents the equation as follows

$$\frac{\delta(G)}{\delta(x)} + \rho_s \frac{\delta(Cy)}{\delta(t)} = D_i + D_r \quad [2.2]$$

Where

- $G$  = sediment load (M/T/L)
- $x$  = distance downslope (L)
- $\rho_s$  = mass density of sediment particles (M/L<sup>3</sup>)
- $C$  = sediment concentration (L<sup>3</sup>/L<sup>3</sup>)
- $y$  = flow depth (L)
- $t$  = time (T)
- $D_i$  = rate of interrill delivery to rills (M/T/ L<sup>2</sup>)
- $D_r$  = rate of rill detachment (M/T/L<sup>2</sup>)

The  $\delta G/\delta x$  term represents the buildup or loss of sediment load with distance and the  $\delta(Cy)/\delta t$  term represents the storage rate of sediment in the flow depth (Foster, 1982). Dispersion is neglected in Equation [2.2].

Recognizing that quasi-steady sediment movement can be assumed, the sediment storage term drops out and Equation [2.2] can be re-written as

$$\frac{\delta(G)}{\delta(x)} = D_i + D_r \quad [2.3]$$

Where all variables are defined above.

Equations [2.2] and [2.3] above explain the conceptual model as first presented by Meyer and Wischmeier (1969) as shown in Figure 2.2.

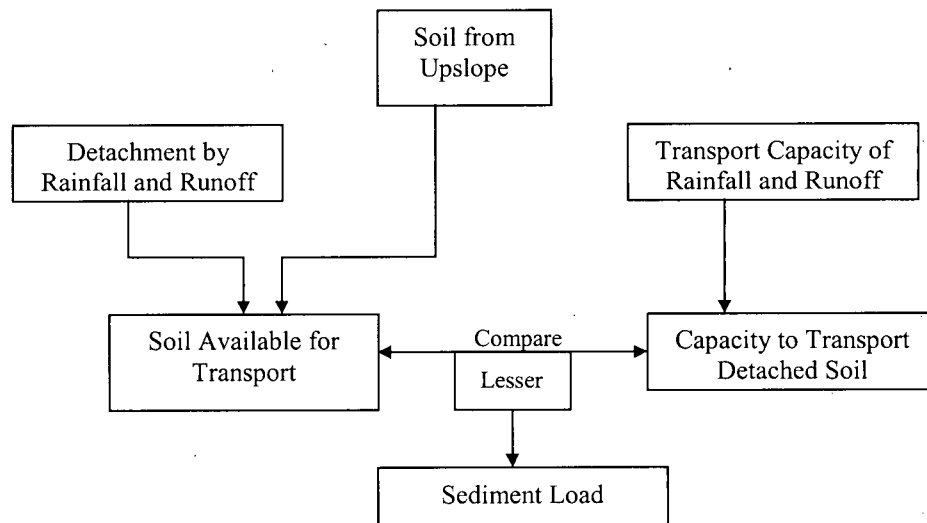


**Figure 2.2 Conceptual Model of the Soil Erosion Process (Meyer and Wischmeier, 1969)**

In this model, the sediment from upslope combined with that detached by rainfall and runoff becomes the material that is available for transport. The transport capacity of rainfall and runoff dictate the ability of overland flow to transport detached soil. The sediment load is determined when the lesser of the soil available for transport or the capacity of the flow to transport the detached material are

compared resulting in either a detachment limiting or transport limiting scenario. The relationship between detachment and transport is explained in more detail in Section 2.5.2. The terms for interrill and rill detachment ( $D_i$  and  $D_r$ ) are also investigated in more detail since the relationships between them and the mechanisms of detachment and transport dictate the magnitude of erosion that takes place.

## 2.5.2 Relationship Between Detachment and Transport

The following equation describes the relationship between detachment and transport of material in a single rill based on a hypothetical case of uniform flow in an infinitely long channel (Foster and Meyer, 1972a).

$$\frac{D_A}{D_C} + \frac{G}{T_C} = 1 \quad [2.4]$$

Where

$D_A$  = actual rill detachment rate (M/T/L<sup>2</sup>)  
 $D_C$  = rill detachment capacity (M/T/L<sup>2</sup>)  
 and all other variables are defined above.

When  $D_A < 0$ , detachment or erosion is taking place and when  $D_A > 0$ , deposition is occurring.

Equation [2.4] shows that there is a complimentary relationship between the actual rate of rill detachment ( $D_A$ ) that occurs due to overland flow and the transport rate or sediment load that the flow is carrying ( $G$ ). Since the sediment load cannot be negative, the term  $G/T_C$  cannot be negative and the maximum value that  $D_A/D_C$  can attain is unity.  $D_A/D_C$  reaches unity when flow without sediment ( $G = 0$ ) enters an erodible section of hillslope and the actual detachment occurs at a maximum possible rate called the detachment capacity,  $D_C$ .

As the actual detachment rate increases and therefore the sediment being transported ( $G$ ) increases, the amount of additional detachment that can take place decreases

since the energy within the flow is increasingly spent on transporting newly detached material. The implications of this relationship are affected by the interaction between rill and interrill sediment load and delivery as well as the detachment and transport relationships within the rill itself. For example, if the sediment load in the rill flow is low, a majority of the flow's energy will be used to detach material and the detachment rate of the rill flow will be close to maximum or detachment capacity. However two simultaneous situations occur to alter this detachment and transport relationship. First eroded sediment from interrill areas is delivered to the rill causing the energy of the rill flow to be partially consumed in transporting the newly acquired interrill sediment. Since part of the energy of the rill flow is now required to transport interrill sediment, the energy available to detach additional material within the rill is reduced and the actual detachment rate decreases. Second, if the rill flow were to continue downslope without the addition of interrill sediment, the rill detachment rate would decrease until, if the channel length were long enough, the detachment becomes essentially zero. However, since interrill sediment is delivered to rills, the actual rill detachment rate drops more quickly. If the sediment detachment rate decreases to zero, then the sediment transport rate has reached a maximum, called the transport capacity. The transport capacity is the situation in which the flow over an erodible surface is neither detaching nor depositing sediment (Foster and Meyer, 1972a).

As the explanation of Equation [2.4] indicates, flow with little or no sediment load will be more erosive than a flow with large sediment loads. This conclusion agrees with research conducted in the river sediment transport field indicating that critical velocities and shear stresses are indicators of channel stability (erosion and deposition). Some theory suggests that detachment due to the abrasion of sediment-laden flow occurs (Schroeder, 1987) however there is little evidence of its significance in upland erosion (Foster and Meyer, 1972a).

The rate of detachment of cohesionless material at the head of a slope where flow is introduced depends on the sediment load of the added flow. However, the sediment load at the end of the slope is independent of the sediment load of the inflow. The decrease in erosion rate with distance downslope, indicates a decrease in detachment as the sediment load increases (Foster and Meyer, 1972a).

It was indicated previously that if the actual detachment rate is greater than zero, deposition occurs. It should be noted however, that a deposition capacity cannot be defined in the same manner as a detachment capacity since there is no upper limit to the sediment load in the flow (Foster and Meyer, 1972a).

### **2.5.3 Detachment By Rainfall**

Soil detachment occurs due to both rainfall and runoff. Soil detachment due to raindrop impact is a function of rainfall and soil characteristics as well as the depth of overland flow. Drop diameter, velocity and rainfall intensity determines the amount of kinetic energy transferred to the soil surface causing the detachment of soil particles from the soil mass. The force of the raindrop impacting the soil surface increases with the depth of thin sheet flow up to a depth of one-third the median drop diameter (Fan and Wu, 2001). Once the flow exceeds this depth, the force of raindrop impact is dissipated and the raindrop energy is absorbed in the flow depth reducing its ability to dislodge soil particles (Toy and Foster, 1998). As a result, detachment due to rainfall is considered to be negligible in rills, gullies and stream channels and is discussed here in relation to interrill erosion.

Numerous studies have been conducted to estimate the rate of soil detachment due to raindrop impact (Meyer and McCume, 1958; Gilley, 1982; Gilley and Finkner, 1985; Turner *et al.*, 1985; Truman and Bradford, 1993) and the resulting equations include an empirical constant for soil characteristics called the soil erodibility factor. One of

the more commonly applied equations that describe the interrill detachment rate is a power function of rainfall intensity (Meyer, 1981; Foster, 1982). Foster (1982) provides the following equation for estimating the rate of soil detachment on interrill areas.

$$D_i = cK_i I^a \quad [2.5]$$

Where

$K_i$  = soil erodibility factor for detachment by raindrop impact  
(MT/L<sup>4</sup>)

$I$  = rainfall intensity (L/T)

$c$  and  $a$  = constants  
and all other variables are defined above.

Equation [2.5] has been modified in many ways including for example, by the addition of a factor describing the amount of ground cover shielding the bare soil and therefore reducing the erosive ability of raindrops. Foster (1982) provides a description of some of the modifications made to this equation to suit various conditions.

The range of values for the constant  $a$ , depend on the soil characteristics. However, few studies have been conducted to relate soil splash or detachment to individual soil properties (Watson and Laflen, 1986). Meyer (1981) reports that the exponent of the power function relating rainfall erosivity to rainfall intensity is related to clay content. Bubenzer and Jones (1971) found that percent clay is a better indicator of splash erosion than particle size, aggregate index, bulk density, organic matter or moisture content. Other reported soil characteristics that have been related to raindrop detachment are soil type and size of structural aggregates (Rose, 1961) as well as aggregate size, stability and surface area (Yamamoto and Anderson, 1973).



Soil detachment and transport processes in interrill areas have not been clearly separated since most methods measure the degree of soil splash, which includes both detachment and transport. However, not all detached particles are transported far enough to be measured (Grosh, 1994). Equation [2.5] not only represents the detachment of soil from interrill areas, it also quantifies the amount of sediment delivered from interrill areas to rills (Owoputi, 1994).

Slope gradient is known to affect the soil detachment by raindrops. Several equations are reported that attempt to incorporate the effects of slope on interrill erosion (Gilley and Finkner, 1985). Neal (1938) reports the following equation for detachment by raindrops incorporating the effects of slope.

$$D_i = K_i I^a S_f \quad [2.6]$$

Where

$$S_f = a(\sin \theta)^b + c \quad [2.7]$$

and

$S_f$  = interrill slope gradient factor

$\theta$  = slope angle

$b$  = constants

and all other variables are defined above.

However, studies that conclude that there is soil loss at a zero slope gradient (Foster and Meyer, 1972a; Lattanzi *et al.*, 1974) contradict the relationship defined in Equation [2.6]. Here the exponent implies that at a zero slope gradient there would be no detachment by interrill processes.

Some equations attempt to relate detachment by rainfall to the soil shear strength. Chorley (1959) originally defines this relationship. Watson and Laflen (1986) show that the shear strength of the soil varies depending on whether the measurement is

taken before or after the rainfall event and therefore a range of equations are derived. Al-Durrah and Bradford (1981) develop the following relationship based on measurement of shear strength for the detachment due to a single raindrop.

$$D_S = a + b \left( \frac{KE}{\tau} \right) \quad [2.8]$$

Where

$D_S$  = amount of soil detached (M/drop)  
 $KE$  = kinetic energy of the raindrop ( $ML^2/T^2$ )  
 $\tau$  = soil shear strength ( $ML/T^2$ )  
 and all other variables are defined above.

The soil and raindrop parameters are derived from the results of a silt loam soil only (Al-Durrah and Bradford, 1981), and therefore the equation has been refined to be applicable to a wider range of soils.

Gilley (1982) derives the only physically based equation for assessing detachment by raindrops. The equation is based on the principles of point pressure or the pressure acting at the soil water interface, directly below the drop impact and is related to the normal component of velocity for inclined surfaces.

$$D_i = 0.2K_D V_I^2 \left( \frac{d_e}{h} \right)^{1.83} \cos^2 \theta \quad [2.9]$$

Where

$K_D$  = soil detachment factor (No units provided)  
 $V_I$  = drop impact velocity (L/T)  
 $d_e$  = equivalent drop diameter (L)  
 $h$  = water depth (L)  
 and all other variables are defined above.

Although this equation is useful for assessing the relative importance of such factors as overland flow depth and rainfall characteristics, it is difficult to apply due to the difficulty in measuring the individual characteristics (Gilley, 1982). In addition, it is unclear whether the soil detachment factor,  $K_D$  provided in Equation [2.9] above is

similar to the soil erodibility factor,  $K_i$  used in for example, Equation [2.5], as well as many of the other interrill erosion equations published in the literature.

Other equations provided in the literature suggest the use of parameters such as rainfall kinetic energy, raindrop volume or the density of water to estimate the erosion rate for interrill areas. A complete list of these equations can be found in Gilley (1982) and Gilley and Finkner (1985). Equations [2.5] through [2.8] above and the equations provided in Gilley and Finkner (1985) are derived through regression analysis. Therefore, the physical nature of the soil erodibility factor due to raindrop impact is not well understood.

#### **2.5.4 Transport By Rainfall**

As indicated above, transport by rainfall may occur on interrill areas where raindrop splash transfers soil particles from interrill areas directly to rills. Mathematical formulations describing this process have not been developed. Foster and Meyer (1972a) postulate that rill density is more significant in this erosion process than the distance that the particles are splashed. For example, if rills comprise 10% of the landscape, then the amount of sediment transferred to rills by raindrop splash is 10% of that detached. However, if rills cover 80% of the landscape then 80 % of the material detached during raindrop impact will be transferred to rills.

#### **2.5.5 Detachment By Runoff**

Again, the sediment detachment equations reported in the literature are regression equations. The physical meaning behind them has not been developed largely due to the limited understanding of the process of sediment detachment by overland flow. There are two components of detachment by runoff explained below, the detachment capacity,  $D_C$  and the actual detachment rate,  $D_A$ . These components are limited to the rill areas since as explained in Section 2.4.1 above, the flow energy in interrill

areas is consumed in transporting detached material and energy is unavailable for additional detachment.

### 2.5.6 Detachment Capacity, $D_C$

It is believed that the detachment of soil particles occurs when the shear stress of the overland flow exceeds the resistance of the soil to the flow and the soil particle is pulled away from the soil mass. The shear stress of the overland flow is a function of the flow depth and velocity. If the flow depth and velocity in interrill and rill areas is significant, detachment will occur. However, since the flow depth in interrill areas is not significant in causing detachment, the detachment capacity equations found in the literature have been developed to apply to rill areas only where overland flow depth is nearly always significant.

The following equation relates the detachment capacity ( $D_C$ ) of the flow in rill areas to the flow shear stress and the critical shear stress of the soil.

$$D_C = K_r (B\tau - \tau_{cr})^a \quad [2.10]$$

Where

- $K_r$  = rill erodibility factor (T/L)
  - $\tau$  = flow shear stress (M/T<sup>2</sup>L)
  - $\tau_{cr}$  = critical shear stress of the soil (M/T<sup>2</sup>L)
  - $B$  = constant
- and all other variables are defined above.

Of the parameters required to solve for detachment capacity in Equation [2.10], only  $\tau$  has physical meaning since it can be related to overland flow. The critical shear stress of the soil ( $\tau_{cr}$ ) is described by Foster (1982) as "fictitious" since it is especially difficult to evaluate and depends on such non-uniform factors as the number of rills, the distribution of flow between the rills and the variation of shear stress in time and space within the rills (Foster, 1982). Yalin (1963) concludes that

the critical tractive force does not exist based on the “difficulty or impossibility of defining, accurately, the so-called ‘critical’ values (Yalin, 1963:223). Owoputi (1994) concludes that since  $K_r$ ,  $\tau_{cr}$ ,  $B$  and  $a$  do not represent any physical factors, it is impossible to predict their response to changes in factors causing erosion rates.

Forms of Equation [2.10] are used in such erosion prediction models as WEPP, KYERMO and CREAMS. WEPP provides a means of determining appropriate values of  $K_r$  and  $\tau_{cr}$  while the form of the equation used in the CREAMS model includes values for the constants  $a$  and  $B$ . KYERMO requires the user to provide values for  $K_r$  though no procedure is recommended for parameter estimation (Owoputi, 1994).

Foster (1972a) conclude that because of the assumptions made in the Yalin (1963) sediment transport relationship, it appears to be an equation that expresses detachment per unit area per unit time as long as the appropriate critical shear stress is chosen. If the bed shear stress is large compared to the critical shear stress, detachment capacity can be expressed as shown in Equation [2.11].

$$D_C = K_r \tau^{2/3} \quad [2.11]$$

Where all variables are defined above.

Other authors indicate that including the critical shear stress value does provide a better fit to the measured sediment concentration. However, in some areas where the flow shear stress is far in excess of the soil critical shear, Equation [2.11] may be appropriate.

Although the concept of detachment capacity is different from that of transport capacity Equation [2.11] has been used by many authors to estimate the transport

capacity of overland flow. Equation [2.11] is an approximation of the Yalin (1963) sediment transport equation discussed in Section 2.5.9.1.

### 2.5.7 Actual Detachment, $D_A$

By plugging Equation [2.10] into Equation [2.4] the actual detachment rate is derived as expressed in Equation [2.12].

$$D_r = K_r (B\tau - \tau_{cr})^a \left( 1 - \frac{G}{T_C} \right) \quad [2.12]$$

Where all variables are defined above.

The relationships described in Section 2.5.2 between detachment and transport are preserved in Equation [2.12].

Foster (1982) proposes the following equation to describe the deposition of suspended sediment from the flow.

$$D_E = Av(G - T_C) \quad [2.13]$$

Where

- $D_E$  = deposition rate ( $M/L^2/T$ )
- $A$  = constant
- $v$  = particle settling velocity ( $L/T$ )
- and all other variables are defined above.

Application of this equation implies that once the sediment transport capacity is filled, deposition occurs at the settling velocity rate of the particles.

Rose (1997) uses the following equation, which is similar to that presented by Foster (1982).

$$D_E = vC \quad [2.14]$$

Where all variables are defined above.

Before either detachment or deposition can take place a flow shear stress exceeding the critical stresses must be achieved. The critical conditions of transport capacity are discussed in Section 2.5.9.

### 2.5.8 Physically Based Detachment Equation

There are two types of forces acting to dislodge particles or aggregates of particles from the soil mass, external forces from raindrop impact and overland flow and internal forces including those induced by seepage. The external forces comprise the forces normal and parallel to the soil surface. The internal forces affect the equilibrium of the soil particles depending on the direction of seepage flow and are influenced by the effects of cohesion and self-weight (Owoputi, 1994).

The only physically based detachment equation describes the vector sum of all of the forces acting on the mass of soil particles (Owoputi, 1994). Once the net upward force is greater than zero, soil detachment occurs and this removal continues at the magnitude of the net upward force. The equation derived by Owoputi (1994) is based on a force balance for a single soil particle. However, since the focus of the study by Owoputi (1994) is the applicability of the detachment equation to assessing soil erodibility, full determination of the external forces is not required.

For purely cohesionless sands and silts, the detachment equation is expressed as follows.

$$D_r = \frac{F_{TM} \left( \frac{1-G}{T_C} \right)}{\frac{1}{\lambda} + \frac{g}{\lambda\beta} \left( (1+w_c)\Gamma_1 - (\Gamma_1 - i\Gamma_2) \frac{\rho_w}{\rho_s} \right)} \quad [2.15]$$

Where

- (ML/T<sup>2</sup>)  $F_{TM}$  = external force acting under the unit weight of flow
- $\lambda$  = constant for each soil type and slope position
- $g$  = acceleration due to gravity (L/T<sup>2</sup>)
- $\beta$  = initial acceleration with which the particles can move from the bed (L/T<sup>2</sup>)
- $w_c$  = water content by weight
- $\Gamma_1$  and  $\Gamma_2$  = net upward forces acting on the soil particles (ML/T<sup>2</sup>)
- $i$  = hydraulic gradient
- and all other variables are defined above.

The factors describing the detachment rate also describe the soil erodibility and therefore by removing the external forces from the equation, the remaining variables would describe the erodibility of the soil. The following equation describes the erodibility of a cohesionless soil.

$$K_D = \frac{1}{\frac{1}{\lambda} + \frac{g}{\lambda\beta} \left( (1 + w_c)\Gamma_1 - (\Gamma_1 + i\Gamma_2) \frac{\rho_w}{\rho_s} \right)} \quad [2.16]$$

Where all variables are defined above.

A factor for the effects of cohesion would have to be added to Equation [2.16] to make it applicable to soils that exhibit cohesion; however, this severely complicates the erodibility process since cohesion is a function of other parameters such as clay content.

### 2.5.9 Transport By Runoff

Flow incision and therefore net erosion, will only occur when the transport capacity of overland flow is sufficient to remove material that is transported into the flowpath from the interrill areas (Govers, 1987). The relationship between detachment capacity and transport capacity of overland flow in rills was discussed in Section



2.5.2. Here, a complimentary relationship between detachment capacity and transport capacity indicates that as the detachment capacity of the flow decreases, the transport rate approaches a maximum value called the transport capacity.

Many of the physically based erosion prediction models developed recently rely on the principle of sediment transport capacity (Govers, 1987). Transport capacity was first investigated in relation to flow transport in rivers. Features such as the river flow regime and bed gradient differ considerably from upland erosion conditions. As a result, utilizing the existing sediment transport relationships in hillslope erosion prediction models requires modifications to the empirical coefficients. Of the sediment transport relationships developed for river flow, the Yalin Equation (Yalin, 1963) is determined by Foster and Meyer (1972b) to be the most appropriate relationship since it fit the data for overland flow most appropriately. Since then, the modified Yalin Equation has been used in many of the physically based erosion prediction models to estimate transport capacity. Such models include the WEPP, ANSWERS, CREAMS and KYERMO discussed in detail in Chapter 4. Sediment transport relationships that are not taken directly from river applications are derived through statistical experimental data of overland flow conditions. Only the GUEST erosion prediction model uses a theoretically derived sediment transport capacity relationship based on stream power expressed in terms of sediment concentration rather than solids discharge (Rose, 1997).

The equation used to predict sediment transport capacity of overland flow distinguishes the physically based erosion prediction models from one another. The equations are grouped here according to the basic parameter used to calculate sediment discharge. These parameters include flow shear stress, unit stream power and power functions of slope, rainfall intensity and flow rate (Owoputi, 1994).

### 2.5.9.1 Flow Shear Stress

The early river transport relationships rely on the concept of excess shear stress. Transport capacity is the difference between the actual shear stress and the critical shear stress necessary to initiate particle movement (Govers, 1987). Equation [2.17] describes the flow shear stress ( $\tau$ ).

$$\tau = \gamma_w S_{EGL} R \quad [2.17]$$

Where

$$\begin{aligned} \gamma_w &= \text{unit weight of water (M/L}^2\text{T}^2\text{)} \\ S_{EGL} &= \text{slope of the energy grade line (L/L)} \\ R &= \text{hydraulic radius (L)} \\ &\text{and all other variables are defined above.} \end{aligned}$$

The slope of the hydraulic gradeline is often approximated by the slope of the land surface and the hydraulic radius is often approximated by the depth of flow.

Since rapid deposition occurs in areas where the flow becomes ponded, it was concluded that detached particles primarily move as bedload and therefore the transport capacity of the flow is expressed by bedload formulae. The Yalin (1963) Equation has been used to estimate the bed load transport rate under steady uniform flow for sediment of the same size. The equation relates the sediment transport capacity to land slope and flow rate and has been modified to determine rill flow transport capacity as shown in Equation [2.18].

$$T_c = K_T \tau^{2/3} \quad [2.18]$$

Where

$$\begin{aligned} K_T &= \text{soil transport factor} \\ &\text{and all other variables are defined above.} \end{aligned}$$

Equation [2.18] is the same as Equation [2.11] used to calculate to the detachment capacity of the flow. Both equations include a factor that explains the susceptibility of the soil to detachment or transport while recognizing that the flow shear stress far exceeds the critical shear stress of the soil.

### 2.5.9.2 Stream Power

The concept of stream power was first introduced by Bagnold (1966) and relies on the balance of energies rather than the balance of forces to define sediment transport processes. Stream power is the “amount of energy dissipated per unit of time and per unit of bed surface” (Govers, 1987:51). Stream power can be expressed as either the effective stream power, i.e. the power available to the flow per unit bed area as proposed by Bagnold (1966) or the unit stream power, i.e. the power per unit weight of water as Yang (Yang, 1972) proposed.

The expression for effective stream power is Equation [2.19] (Bagnold, 1966).

$$\Omega_e \sim \frac{(\omega - \omega_{cr})^{1.5}}{h^{2/3}} \quad [2.19]$$

Where

- $\Omega_e$  = effective stream power ( $ML^2/T^3$ )
- $\omega$  = stream power ( $ML^2/T^3$ )
- $\omega_{cr}$  = critical stream power ( $ML^2/T^3$ )
- and all other variables are defined above.

Equation [2.19] is expressed in an alternate form in Equation [2.20], which can be compared more directly with Equation [2.22].

$$\Omega_e = \gamma_w ShV \quad [2.20]$$

Where

- $\Omega_e$  = unit stream power per bed area ( $M/T^3/$ )

$S$  = slope (L/L)  
 $V$  = velocity of overland flow (L/T)  
 and all other variables are defined above.

Transport capacity in interrill areas is assumed to be proportional to the stream power as shown by (Gilley, 1982; Gilley and Finkner, 1985)

$$T_C = K_T \gamma_w S h V \quad [2.21]$$

Where all variables are defined above.

The unit stream power described as the power per unit weight of water (Yang, 1972).

$$\Omega_w = S V \quad [2.22]$$

Where

$\Omega_w$  = unit stream power per unit weight of water ( $\text{ML}^2/\text{T}^3$ )  
 and all other variables are defined above.

Yang (1972) uses some experimental data to develop the transport capacity relationship based on the total sediment concentration as a function of stream power. The total sediment concentration in this equation is the maximum sediment concentration in the overland flow.

$$\log C_T = A + B \log \left( \frac{\Omega_w}{\omega} - \frac{\Omega_{wc}}{\omega} \right) \quad [2.23]$$

Where

$C_T$  = total sediment concentration ( $\text{M}/\text{L}^3$ )  
 $\Omega_{wc}$  = critical stream power per unit weight of water ( $\text{ML}^2/\text{T}^3$ )  
 and all other variables are defined above.

Moore and Burch (1986) conclude that the formula proposed by Yang (1972) gives promising results for sediment transport capacity of overland flow in interrill and rill areas.

### 2.5.9.3 Power Functions

Several power functions are derived expressing the sediment transport capacity of overland flow with other variables. Such variables include

- flow rate and slope;
- flow depth and slope;
- slope, shear velocity and grain size;
- flow rate, slope and rainfall intensity; and
- flow rate, slope, rainfall intensity and shear stress.

The equations derived for turbulent river transport are explored by Julien and Simons (1985) in order to determine their applicability to the laminar conditions of overland flow. Using dimensional analysis and data fitting, they determine that the original equations are unsuitable and recommend Equation [2.23].

$$T_C = Q^a S^b I^c \left( 1 - \frac{\tau_{cr}}{\tau} \right)^d \quad [2.23]$$

Where

$Q$  = flow rate ( $L^3/T$ )

$d$  = constant

and all other variables are defined above.

The transport capacity equations developed by Guy *et al.* (1987) utilize the impacts of runoff (first term on the right hand side of Equations [2.24] and [2.25]) and rainfall (second term on the right hand side of Equations [2.24] and [2.25]). In interrill areas, Guy *et al.* (1987) finds raindrops contribute 85 % to transport capacity.

$$T_C = AS^{a_1}Q^{a_2} + BI^{b_1}S^{b_2} \quad [2.24]$$

$$T_C = DS^{d_1}(Q - Q_{cr})^{d_2} + EI^{e_1}Q^{e_2}S^{e_3} \quad [2.25]$$

Where

$Q_{cr}$  = critical flow rate ( $L^3/T$ )

$A, a_1, a_2, B, b_1, b_2, D, d_1, d_2, E, e_1, e_2$  and  $e_3$  = constants  
and all other variables are defined

above.

Equation [2.26] is an example of the use of a power function relating sediment transport to both flow rate and slope. Recognizing that the same hydraulic parameters used in sediment transport prediction in rivers are of fundamental importance to sediment transport prediction in overland flow, Govers (1987) develops Equation [2.26] was.

$$T_C = Aq^bS^c \quad [2.26]$$

and all other variables are defined above.

Equation [2.26] is used as the sediment transport capacity relationship in the EUROSEM model discussed in more detail in Chapter 4.

Many equations have been proposed to describe the transport capacity of overland flow and many are based on original research for stream and river channel stability. Like the detachment equations, all of the transport capacity relationships are based on regression analysis and no single equation has been generally agreed upon to provide the most suitable results. Alonso *et al.* (1981) concludes that the original sediment transport capacity relationships are suitable for gully and channel erosion. This conclusion is acceptable because the depth of flow in gullies and channels in upland areas dampens the effects of raindrop impact (Owoputi, 1994). Therefore the use of river sediment transport relationships for overland flow particularly in interrill

areas is likely not correct as Gilley and Fickner (1985) propose when utilizing the Yang (1972) stream power function.

## **2.6 Future Research**

Much research is required to be able to define the erosion process in more physical terms. The current equations identified in this chapter, are extremely site specific due to their empirical nature and are often sensitive to uncertainties in data collection and modeling. Since many of the modeling packages available for upland erosion prediction rely on the equations described in Section 2.5, a suitable, versatile erosion model does not yet exist. Understanding the physical process of water induced erosion can be achieved through studies of the threshold conditions under which the individual erosion processes take place. Several of these characteristics are discussed in Chapter 3.

## CHAPTER 2 – LIST OF SYMBOLS

SYMBOL	DESCRIPTION
$G$	sediment load
$x$	distance downslope
$\rho_s$	mass density of sediment particles
$C$	sediment concentration
$y$	flow depth
$t$	time
$D_i$	rate of interrill delivery to rills
$D_r$	rate of rill detachment
$D_A$	actual rill detachment rate
$D_C$	rill detachment capacity
$K_i$	soil erodibility factor for detachment by raindrop impact
$I$	rainfall intensity
$S_f$	interrill slope gradient factor
$\theta$	slope angle
$D_S$	amount of soil detached
$KE$	kinetic energy of the raindrop
$\tau$	soil shear strength
$K_D$	soil detachment factor (No units provided)
$V_I$	drop impact velocity
$d_e$	equivalent drop diameter
$h$	water depth
$K_r$	soil erodibility factor
$\tau$	flow shear stress
$\tau_{cr}$	critical shear stress of the soil
$D_E$	deposition rate
$v$	particle settling velocity
$F_{TM}$	external force acting under the unit weight
	of flow
$\lambda$	constant for each soil type and slope position
$g$	acceleration due to gravity



particles	$\beta$	initial acceleration with which the
		can move from the bed
particles	$w_c$	water content by weight
	$\Gamma_1$ and $\Gamma_2$	net upward forces acting on the soil
	$i$	hydraulic gradient
	$\gamma_w$	unit weight of water
	$S_{EGL}$	slope of the energy grade line
	$R$	hydraulic radius
	$K_T$	soil transport factor
		$\Omega_e$ effective stream power
	$\omega$	stream power
	$\omega_{cr}$	critical stream power
water	$\Omega_e$	unit stream power per bed area
	$S$	slope
	$V$	velocity of overland flow
	$\Omega_w$	unit stream power per unit weight of
	$C_T$	total sediment concentration
	$\Omega_{wc}$	critical stream power per unit weight of
		water
	$Q_{cr}$	critical flow rate
	$A, a, a_1, a_2$	constants
	$B, b, b_1, b_2$	constants
	$c$	constant
	$D, d, d_1, d_2$	constants
	$E, e_1, e_2, e_3$	constants

### **3. FACTORS AFFECTING SOIL EROSION: RELATIONSHIPS, LIMITS AND THRESHOLDS**

Our understanding of soil, climate and vegetation separately is robust. The interactions between these domains lead to complexities that can be described, but are not as well quantified. For example, it is understood that rain will infiltrate into the soil matrix; however, measuring the infiltration rate has lead to many different approaches with varying degrees of accuracy. The complexities due to the interaction between these domains are then compounded when they are used to explain and predict dependent phenomena such as water induced erosion.

This chapter discusses the passive factors that contribute to the natural erosion process including climate, hydrology, soil properties and landscape characteristics and investigates these factors in terms of the relationships, limits and boundaries that cause accelerated erosion to take place. It provides where possible the similarities and differences in the passive factors that result in variations in erosion rates on lands disturbed by mining. A summary of these impacts and effects on erosion is provided in Table 3.6 at the end of the chapter.

#### **3.1 Factors Affecting Soil Erosion**

Both active and passive factors influence and accelerate the soil erosion process. The active factors are limited to human land use activities that accelerate the erosion process including, but not limited to, agriculture, forestry, construction and mining. The passive factors include site specific, environmental conditions such as climate, hydrology, soil conditions and slope that contribute to natural soil erosion. Figure 3.1 shows the properties of the active and passive processes that cause erosion.

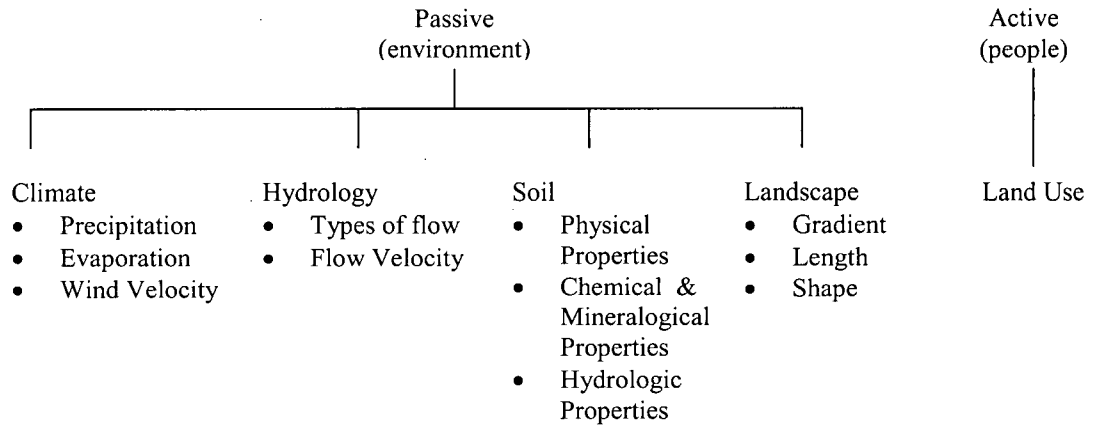


**Figure 3.1 Factors Affecting Soil Erosion (Modified from Lal, 1990)**

Modern erosion research continues to seek to understand the effects of active erosion processes and of passive relationships. It is recognized that severe erosion dominates tropical areas with young stratigraphy and steep slopes, characteristics often observed in landscapes disturbed by mining. In the sections that follow several general conclusions are drawn regarding the conditions under which the dominant erosion processes take place and these conclusions are extended to include anthropogenic effects.

## **3.2 Climate**

Climate is the driving force behind the erosion of soil of any type. It has spatial and temporal variation; however, it is one of the more easily measured and quantified erosion parameters. The factors affecting climate are precipitation, evaporation and wind velocity.

### **3.2.1 Effects on Erosion**

The ability of the climate to initiate erosion and increase the erodibility of the soil is accomplished through precipitation effects including rainfall characteristics such as intensity, drop size distribution, storm duration, kinetic energy and momentum (Al-

Durrah and Bradford, 1982). Wind velocity and direction, soil water balance and mean annual and seasonal temperatures as well as relative humidity and evapotranspiration indirectly contribute to soil erosion (Lal, 1990). For example, wind direction and velocity increase the erosive potential of rainfall by “driving” raindrops against a slope. A negative soil water balance in combination with high seasonal temperatures for example, provide ideal conditions for developing a surface crust, thus increasing the resistance of the soil to soil erosion. However, the reduction in infiltration due to the surface seal increases the volume and velocity of overland flow, potentially increasing the erosion rate. Of course the effects that rainfall and temperature have on erosion rates are highly dependant on the soil properties and the land use.

#### **3.2.1.1 Examples of Erosion Impacts**

Interrill erosion begins with the onset of rainfall. Therefore, numerous rainfall simulation studies have been reported in the literature using a variety of rainfall simulators, rainfall intensities and storm duration to examine interrill erosion rates. It should be noted that the erosion rates predicted under simulated rainfall, using rainfall/runoff plots do not mimic the natural environment exactly. However, these studies provide the fastest results utilizing a minimum of resources (Meyer and McCume, 1958).

Very early in the erosion research, it was concluded that rainfall intensity rather than rainfall amount or duration is more important in causing erosion (Nichols and Sexton, 1932). Section 2.5.3 describes the relationship between rainfall and erosion resulting in the mathematical expression relating rainfall intensity to interrill erosion (Equation [2.5]). The exponent of the power function relating rainfall intensity to interrill soil loss rate ranges between 1.6 and 2.3 (Meyer, 1981) depending on the soil and surface conditions, including slope. Foster (1982) reports a range between

1.3 and 2.0 and Watson and Laflen (1986) report values between 1.36 and 2.54 again due to variations in soil texture and slope. Bare, tilled, silt and silt loam soils have intensity exponents ranging from 1.85 to 2.21 while for clay and silty clay soils, exponents range from 1.63 to 1.73 for rainfall intensities above 10 mm/hr. Meyer (1981) concludes that overall an exponent of 2.0 is applicable for the power law relationship for silt, silt loam, loam and sandy loam soils. Fan and Wu (2001) however, test the exponent of the rainfall intensity for six soils under high rainfall intensities (35 mm/hr, 60 mm/hr, 90 mm/hr and 120 mm/hr) in Taiwan. They conclude that above slope gradients of 25 % the exponent of 2.0 is too high and a range of 0.78 to 1.72 is more appropriate in predicting interrill erosion rates. The relationship adopted by many of the new erosion simulation models uses an intensity exponent of 2.0 (Flanagan and Nearing, 1995).

Meyer (1981) also concludes that the influence of intensity on erosion is greater for soils with low clay content. The lesser effect of intensity on high clay soils is presumed to be due to greater soil cohesion, which slows the rate of soil detachment and produces large aggregates difficult to transport as raindrop splash. Therefore, for soils with greater than 20 % clay the exponent of 2.0 is only appropriate at high rainfall intensities and the exponent decreases with increasing clay content.

In addition to intensity, rainfall energy is also important for causing interrill erosion. Young and Wiersma (1973) conclude that the major force initiating soil detachment is the impact of falling raindrops. They show that an 89 % reduction in rainfall energy without a reduction in rainfall application rate decreases the soil loss from interrill areas by between 90 % and 94 % for silt loam to sandy loam soils, respectively. Such a reduction can be accomplished by maintaining a vegetative cover over an erodible soil surface as discussed further in Section 3.8.1.

Since interrill erosion is made up of both transport by raindrops (splash) and transport by thin, sheet overland flow, the effect that rainfall intensity has on each has been investigated (Meyer, 1981). It is concluded that rainfall intensity affects soil loss by runoff much more than soil loss by splash. Doubling rainfall intensity slightly more than doubles sediment moved by splash and quintuples sediment carried by runoff (Meyer, 1981). Overall however, it has been concluded that separating sediment detached by splash from sediment detached by runoff is seldom necessary and interrill erosion is often quantified by that material transported to rill areas (Meyer, 1981).

### **3.3 Hydrology**

The interaction of climate and soil properties as well as land use combine to create the runoff, infiltration and seepage that characterize the hydrologic component that affects soil erosion. As shown in Figure 3.1, the hydrologic factors that affect soil erosion are the type of flow and the flow velocity.

#### **3.3.1 Runoff**

As indicated in Section 2.3.2, runoff can play two roles in the soil erosion process. Not only does runoff have the potential to cause erosion, it is the main agent responsible for the transport of the eroded sediment downslope and off-site.

##### **3.3.1.1 Effects on Erosion**

Horton (1933) proposed a concept describing runoff generation as overland flow where the rainfall intensity exceeds the ability of the soil to accept water through infiltration. For a considerable period after its publication, Horton's theory of overland flow was considered to be the primary source of runoff at the ground surface and influenced many hydrologic models for decades thereafter (Sloan and Moore, 1984). However, as the physics of groundwater flow became increasingly

well understood, the probability of Hortonian overland flow was recognized to be limited to very specific situations (Dunne *et al.*, 1975). Thus, runoff production deviated from the Hortonian overland flow concept and expanded to include subsurface storm flow and saturation overland flow (Dunne *et al.*, 1975). These mechanisms of runoff production have been recognized to be influenced by such conditions as topography, soil antecedent moisture content, soil surface conditions, soil profile stratification with the occurrence of a perched water table and the presence or absence of pipe flow (Owoputi, 1994). Though the relative contribution of these mechanisms in the production of runoff has remained controversial, it is agreed that the energy available during overland flow events is significant in causing hillslope erosion.

Hortonian overland flow is generated due to saturation from above, when precipitation exceeds infiltration (Horton, 1933). It generally occurs on soils with low infiltration rates such as agricultural land, exposed soil surfaces without vegetation, deserts and urban areas (Sloan and Moore, 1984) and would therefore be expected on fine grained, compacted mine waste sites. Forested watersheds in humid regions; however, do not generally experience overland flow as Hortonian excess. Rather, subsurface storm flow and/or saturation overland flow likely prevail in these areas (Dunne *et al.*, 1975; Sloan and Moore, 1984).

Subsurface storm flow is affected by many of the factors listed above. A soil profile in a steeply sloping watershed, having a near-surface high hydraulic conductivity layer underlain by a less permeable boundary layer some distance below the surface quickly draws water into the soil profile while the less permeable layer creates a barrier to water percolation forming a perched water table. The water then moves along the less permeable layer causing runoff to occur below the ground surface as shown in Figure 3.2.

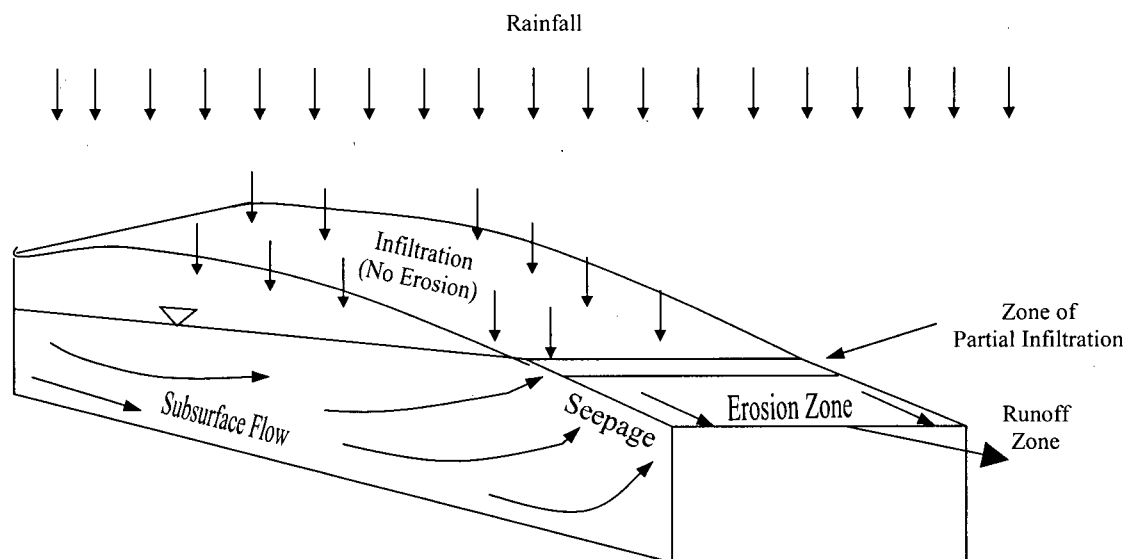


**Figure 3.2 Runoff Generation (Owoputi, 1994)**

The below ground pathway is effective in reducing the erosive forces of flowing water at the ground surface and therefore reduces hillslope soil erosion rates. However, subsurface flow is the major cause of pipe or tunnel erosion. It likely emerges in local streams making a significant contribution to the channel storm hydrograph and channel erosive processes depending on residence time within the soil profile.

In hillslope erosion, the point at which the lateral subsurface flow and the hillslope profile intersect is known as a seepage zone. At this point, the lateral subsurface storm flow is said to “daylight”. This seepage zone or daylight point is the location at which return flow becomes overland flow and is able to run off the soil surface at much greater velocities than are possible underground (Dunne *et al.*, 1975) increasing the erosive potential of what was once subsurface water. The soil type and profile will influence the return flow volume and generally the quantity of return flow is insignificant in well-drained, deep, permeable soils. However, as the storm size increases, so does the rate of return flow (Dunne *et al.*, 1975). The location of



the daylight point is also significant in the gully erosion process as the erosive headcut moves upslope as the phreatic surface moves upslope. This relationship is further discussed in Section 3.3.2.1 with its impacts on erosion discussed in Section 3.3.2.2.

If the lateral subsurface flow is unable to remove the incoming rainwater, due to for example flat topography or insufficient hydraulic conductivity, the soil water storage increases, causing a rise in the water table. In a completely saturated profile, the water table is coincident with the ground surface as often occurs in low-lying areas. The runoff generated from the combination of a high water table with either return flow from a seepage zone or precipitation is called saturation overland flow having high erosive potential (Dunne *et al.*, 1975).

The soil surface conditions and the soil structure itself can significantly impact the volume of runoff generated by altering the soil permeability. For example, plant roots penetrating the soil profile can create a different response of overland flow and subsurface flow than would a soil without plant root biomass (Dunne *et al.*, 1975). Plant roots may offer significant macro-pore pathways that, when the plants die back, can increase subsurface flow and reduce surface erosion.

Since the connection between runoff and either surface or subsurface flow has been recognized as the major contributor to soil erosion, the effects of topography was one of the first variables studied in erosion mechanics (Zingg, 1940). These topographic effects include slope length, gradient and soil roughness. For example, the higher the surface slope generally, the greater the overland flow velocity and the greater the gradient of exiting subsurface flow (Owoputi, 1994). As the rate of overland flow increases, so does the energy available for soil detachment and transport.

### **3.3.1.2 Examples of Erosion Impacts**

The velocities for overland flow are typically in the range of 0.015 m/s to 0.3 m/s and are great enough to move silts and fine sands (Selby, 1993). Due to the shallow depth of flow however, these velocities are difficult to measure in field applications. Instead, using the stream power concept as described in Section 2.5.9.2 with the knowledge of average peak runoff rates and hillslope geometry, critical slope angles above which flow driven erosion processes become dominant can be estimated. In tropical steeplands, a stream power greater than  $0.1 \text{ W/m}^2$  is shown to coincide with flow driven erosion processes (Yu *et al.*, 1999). Slope angles greater than critical determined using this stream power threshold indicate that rainfall impact is only a minor contributor to soil erosion.

### **3.3.2 Infiltration and Seepage**

Storm infiltration into hillslopes produces seepage in the downstream areas resulting in interrelated effects on erosion. These effects are dependent on soil properties including compaction, grain size and crusting as well as soil moisture.

#### **3.3.2.1 Effects on Erosion**

Infiltration is the rate at which the rainwater is accepted and transmitted through the soil (Lal, 1990) and is important in predicting the amount of runoff that will be generated during a rainstorm as explained in the Section 3.3.1.1. The infiltration rate is affected by the degree of soil compaction and the ability of the soil to develop a surface seal. Infiltration capacities are reported to range between 2 mm/hr to 2500 mm/hr (Selby, 1993). The amount of runoff generated is commonly correlated to the amount of erosion that takes place due to the process of overland flow. Infiltration has also been reported to directly influence the stability conditions of soil (Owoputi, 1994). Due to the downward migration of surface water through the soil surface and

into the soil profile, the infiltrating water tends to lock soil particles into position causing an increase in resistance of soil to erosion (Owoputi, 1994).

The upward movement of subsurface or groundwater flow as well as the emergence of infiltrated water from the walls of rills and gullies is called return flow, seepage or exfiltration. The zone of saturation, having positive pore water pressure and an exfiltration gradient characterizes a seepage zone (Huang and Laflen, 1996). As explained in Section 3.3.1.1, when seepage water runs overland it is recognized as one of the components of runoff contributing to the volume of erosion. However, since return flow areas are characterized by significant externally directed hydraulic gradients, the role of seepage in accelerating the erosion process is its potential to increase soil instability and induce soil sloughing rather than causing excessive shear stresses to induce soil erosion. The extent to which seepage conditions change the erodibility of the soil however, is largely unknown (Stolte *et al.*, 1990). One additional argument suggests that the force accompanying seepage out of the hillslope cannot aid erosion since the force disappears once the soil particle becomes unstable, again supporting the argument that the primary role of seepage in erosion is particle instability (Owoputi, 1994).

It is well known that soil detachment is a balance between the hydraulic stresses from rainfall and surface flow and the soil strength resisting these erosive stresses (Huang and Laflen, 1996). Detachment begins when the erosive forces exceed the soil strength and detachment increases when the difference between erosive forces and soil strength increases. Thus, the ability of the soil to resist erosion depends on its shear strength, which is governed by effective stresses. Positive pore water pressure reduces the effective stress between soil particles reducing soil strength (Huang and Laflen, 1996). Effective stresses are lowest in soils under an upward hydraulic gradient since exfiltration works against gravity and soil cohesion to reduce the contacts between soil particles. Though not as low as the effective stress

in soils of the seepage zone, effective stress is also low in saturated soils, but highest in soils in which infiltration is occurring.

In addition, as soil moisture is reduced from saturation and the soil suction enters negative pore water pressures, soil detachment by raindrops decreases rapidly (Huang and Laflen, 1996). Therefore, erosion rates in the field are thought to be dependent on the moisture regime of the hillslope, not just the slope gradient and soil types (Owoputi, 1994; Huang and Laflen, 1996) and soil types can have drastically different erosion rates depending on moisture regime. After a rain event stops and the soil profile begins to drain, surface tension pulls particles together, increasing the cohesive strength and therefore reducing the erodibility and erosion rates.

#### **3.3.2.2 Examples of Erosion Impacts**

Determining the flow gradient at different locations on the soil surface with the use of a numerical seepage model demonstrates the effects of seepage and infiltration on erosion and soil erodibility (Owoputi, 1994). Here, seepage flux is highest at the toe end of the slope and decreases upslope. Therefore, it is expected that if the soil erodibility is affected by seepage, then the soil erodibility would be highest at the toe end and decrease upslope. Owoputi (1994) visually observes the greatest amount of soil erosion at the toe end of the slope and this zone of active erosion moves upslope with time. The movement of the active zone upslope indicates that the effective soil erodibility at the toe end decreased with time causing active erosion to seek soil particles upslope that could be more easily detached. When the flow gradient is compared over a range of slope gradients, the soil erodibility increased as the slope gradient increased. This implies that a greater slope gradient would experience a greater increase in erodibility for the same change in flow gradient.

Though return flow is considered one of the components of runoff, its ability to erode soil material independently of rainfall induced runoff is negligible since the shear stress it applies to the soil surface is negligible. Owoputi (1994) considers seepage flow separately from runoff rates caused by rainfall. When combined, it was assumed that seepage and runoff from rainfall would be additive. However, the average total runoff rates were less than the combined total from the seepage and rainfall induced runoff by between 30 % and 60 % depending on the slope. While the rainfall itself increases the runoff rate increasing shear stress on the soil surface and therefore increasing erosion, the rainfall also increases the hydraulic head in the soil. This increase in hydraulic head in the soil reduces the difference between the externally applied seepage head and the hydraulic head, therefore reducing the runoff rates caused by seepage alone and reducing the total runoff observed.

Owoputi (1994) also observes that as time goes on, the erosion rates of the material decrease while the runoff stays the same. There are two possible explanations for this. First, it is possible that the raindrop impact causes an increase in compaction of the soil material causing runoff to remain high, but reducing its ability to mobilize material. The second factor is the reduction in impact of seepage velocity due to the upslope migration of the seepage and therefore the erosion face. The erosion moves upslope from the toe end towards the point where the water table intersects the slope profile, which is the upper bound of the eroding surface. Since there is a reduction in seepage velocity as the seepage face moves upslope and erodibility is a function of seepage velocity, then erodibility would decrease with time and so would erosion, which is observed.

When several slope gradients are compared, the seepage velocity at the toe end of the steepest slope is the greatest. Thus it appears that the variation in sediment loss with slope change is more dependent on the seepage velocity than on the total runoff rates. The importance of this conclusion is that soil erodibility may vary with slope

even for the same soil, as slope changes will affect seepage velocity. It may be erroneous to use runoff rate as a measure of the impact of slope on soil erodibility. It may be more appropriate to use the resulting changes in seepage velocity (due to slope changes) to measure the impact of slope on soil erodibility. Owoputi (1994) found a substantial decrease in runoff rates as the slope increases. Yet there is an increase in the rate of erosion as the slope increases. Thus for the results reported by Owoputi (1994) there is no correlation between the effect of slope on runoff rate and the effect of slope on the rate of sediment loss.

Huang and Laflen (1996) study the effects of seepage on erosion rates under both simulated rainfall and overland flow conditions. They find that for a clay loam soil, seepage conditions cause an increase in erosion. This finding contradicts the results of a study by Stolte *et al.* (1990), who conclude that the cohesion of clay soils is significant in reducing erosion rates. It is thought that clay soils may be more resistant to erosion due to larger aggregated material. However, often these aggregates have a lower bulk density and when the exfiltration gradient caused by seepage exceeds gravity and overcomes the cohesive forces holding the particles in together, they are easily eroded.

In general, where the effects of seepage have not been investigated and there is a positive correlation between slope gradient and erosion, the sediment loss is attributed to the effects of runoff rate.

### **3.3.3 Entrapped Air**

#### **3.3.3.1 Effects on Erosion**

During the infiltration process, the wetting front advances downward through the soil forcing the soil air phase deeper into the profile. Air entrapment occurs when this gas phase cannot find a route of escape and is trapped between the advancing wetting

front and an impermeable layer below such as the water table. As the gas phase is compressed, it applies a force upward onto the advancing wetting front thus slowing the infiltration rate and increasing the rate of overland flow. Thus, with an increase in the rate of overland flow, there is an increase in soil particle detachment as reflected in the increased erosion rates.

When entrapped air reaches a high enough pressure, the air is vented through the soil surface causing the soil particles to be popped up into the overland flow. Owoputi (1994) suggests that the escaping air can likely increase the amount of turbulence in the overland flow causing those particles entrained in the flow to remain suspended longer than they would under natural laminar flow conditions.

### **3.3.3.2 Examples of Erosion Impacts**

China (1985) reported a 26 % increase in sediment concentration and 66 % increase in sediment load due to air entrapment alone. Owoputi (1994) acknowledges that air entrapment may be more significant in laboratory experiments where a majority of erosion studies are conducted. However, the impact of air entrapment is not well understood under field conditions but is likely less significant because a larger number of natural escape routes may exist.

### **3.3.4 Surface Seals and Surface Crusts**

#### **3.3.4.1 Effects on Erosion**

A surface seal is defined as the initial phase or wetting phase in crust formation while crusting occurs in the drying phase (Bradford *et al.*, 1987). The development of a surface seal results from a breakdown of soil aggregates (Warrington *et al.*, 1989) on an exposed bare soil. This breakdown is a result of raindrop impact energy, rainwater chemistry and the initial infiltration gradient at the onset of rainfall that causes adsorption of fine soil particles to the surface of the soil (Huang and Laflen,

1996). The development of a surface crust is due to the drying of the surface layer of the soil mass. Surface seals and surface crusts have been studied based on hydrologic implications rather than on their contribution to the erosion process. Both surface seals and surface crusts reduce the infiltration rate, prevent the soil from reaching saturation and cause a reduction in seepage, which therefore increases runoff rates (Bradford *et al.*, 1987; Huang and Laflen, 1996). Due to the increase in the flow depth of runoff, there is expected to be an increase in soil erosion.

However, when the soil properties are considered in addition to the hydrologic implications, the surface crust causes an increase in the soil matric suction that then reduces the void ratio, increases the surface density and increases the soils resistance to erosion through an increase in soil shear strength (Watson and Laflen, 1986).

Most interrill erosion equations rely on the intensity of the rainfall rather than the relationship between the surface crust caused by the rainfall and the soil erodibility. However, as mentioned in Section 2.5.3 some researchers attempt to relate the interrill erosion process to soil strength. The ability to determine the relative importance of runoff or soil strength in the erosion process would likely indicate whether the runoff process would cause erosion or the surface crust would prevent it. However, at this point, the impact of soil characteristics on the soil erosion process is not well defined and there is a continued use of empirical constants that attempt to take into account these unknown interactions.

#### **3.3.4.2 Examples of Erosion Impacts**

A study by Shroeder (1987) investigated the erosion rates of reshaped coal mine spoils under naturally crusted and freshly, re-spread conditions. It is not surprising that due to reduced soil strength, spoil losses under wet conditions are 30% greater for the freshly, re-spread surfaces than for the crusted surfaces and 30 % less for the



freshly re-spread conditions than the crusted conditions when the conditions are initially dry. Shroeder (1987) attributes the 30 % increase in erosion of freshly re-spread, wet conditions to the ability of the overland flow to scour the spoil surface entraining a larger number of loose particles than would be possible from the sealed crusted spoil. This also indicates that any surface seal formed in the wet conditions is not as strong as the surface crust. However, once the surface crust is broken, depending on the moisture content of the loosely packed soil below, the soil erosion rate will either increase or decrease (Huang and Laflen, 1996). When rainfall is applied to completely dry plots, runoff is initiated sooner on the naturally crusted spoil surfaces due to the reduced infiltration rates while the wetting up of the freshly re-shaped spoil prevents the accumulation of excess surface water required to cause runoff.

Gilley (1977); however, finds greater sediment losses from crusted spoil surfaces than cultivated spoil. It is presumed that this discrepancy in results is due to the effect of the Sodium Absorption Ratio (SAR) (see Section 3.5.2 for further discussion). Higher SARs, in the range of 30 to 40 found in the study conducted by Gilley *et al.* (1977) would contribute to the differences in erosion rates compared to SAR values of between 4 and 20 reported by Shroeder (1987). In addition, semi-permeable surface crusts form readily in structurally unstable soils with 15 % to 20 % clay content and low organic matter (Warrington *et al.*, 1989). The constraints suggested by Warrington *et al.* (1989) are consistent with the material used by Gilley *et al.* (1977) having low organic carbon content characteristic of mine spoil.

### **3.4 Soil Physical Properties**

Physical characteristics such as soil texture, structure, permeability and combined compressive and shear strength act in combination with each other, chemical characteristics and the environment to influence soil detachment.

The interaction between the internal properties and external factors such as the air and soil water temperatures, the soil moisture content and water balance influence the erodibility of the soil. However, soils respond differently to, for example, identical rainfall kinetic energy or shear stress due to overland flow (Lal, 1990). Soil physical properties are amongst the more easily measured parameters though their combined contribution to erosion and soil erodibility is not understood.

### 3.4.1 Soil Texture, Structure and Strength

#### 3.4.1.1 Effects on Erosion

The distribution of particle sizes is what determines the soil texture. Table 3.1 shows the classification of soil particle sizes and Figure 3.3 provides definitions of the soil science classification that is often referred to in this investigation.

**Table 3.1 Sediment Classification**

SEDIMENT CLASSIFICATION	SEDIMENT SIZE RANGE (mm)
Boulders	> 200 mm
Cobbles	60 mm – 200 mm
Gravel	
Coarse	20 mm – 60 mm
Medium	6 mm – 20 mm
Fine	2 mm – 6 mm
Sand	
Coarse	0.6 mm – 2 mm
Medium	0.2 mm – 0.6 mm
Fine	0.06 mm – 0.2 mm
Silt	
Coarse	0.02 mm – 0.06 mm
Medium	0.006 mm – 0.02 mm
Fine	0.002 mm – 0.006 mm
Clay	< 0.002 mm

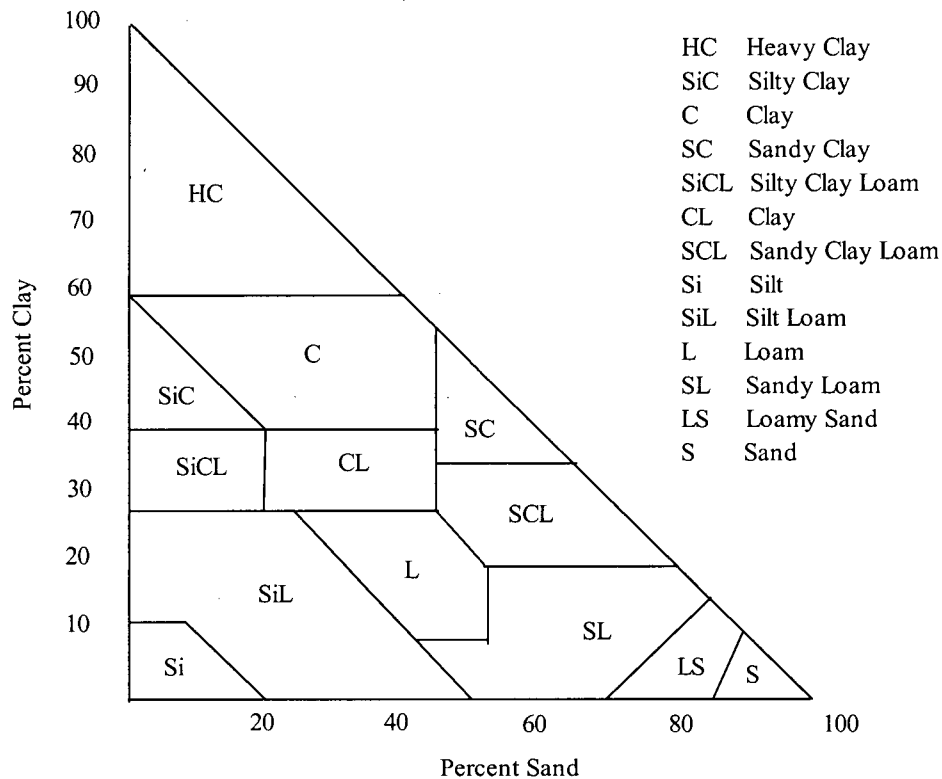


**Figure 3.3 Soil Texture Triangle (Ballard, 1999)**

Texture includes both primary (sand, silt and clay) and secondary (aggregate) particles and these affect the threshold force required to detach and entrain them. Greater forces are required to detach and entrain the larger primary particles. Often silt and clay sized material combine to form large heavy aggregates that, like larger primary particles, require greater forces to detach and entrain.

Soil structure refers to the arrangement of soil particles as they combine to create aggregates and each structure type responds differently to water. Soil aggregates are formed as clay particles combine into domains ( $\sim 5 \mu\text{m}$ ), domains and silt form micro-aggregates ( $5 \mu\text{m}$  to  $1 \text{ mm}$ ) and micro-aggregates and sand form aggregates ( $1 \text{ mm}$  to  $5 \text{ mm}$ ) (Lal, 1990). The susceptibility of the soil to erosion by water can be evaluated by the following characteristics (Lal, 1990):

- The binding of soil particles;
- The resistance of soil to dispersion by water;
- The aggregate diameter;
- The ability of the soil to accept and transmit water; and
- The percentage of water stable aggregates.

The binding of soil particles is increased by the presence of clay and organic material, which provide cohesion. A soil is cohesive if the particles adhere after wetting and subsequent drying and if significant force is then required to crumble the soil. Soils whose particles adhere when wet due to surface tension are not considered to possess cohesive characteristics and are said to be cohesionless (Craig, 1992).

Through cohesion, both organic and clay particles reduce the susceptibility of soil to dispersion to which sand sized particles are the most susceptible (Lal, 1990). The ability of the soil to accept and transmit water reduces runoff rates and as a result reduces soil erosion. These characteristics are largely dependent on the connectivity of micro-pores and the infiltration rate of rainfall into the soil. The resistance to erosion is also given by the stability of aggregates against scouring of water, through aggregate size distribution and aggregate stability indices.

Most sediment that erodes as primary particles has a density of  $2650 \text{ kg/m}^3$  while wet aggregates without sand material have a density of between  $1900 \text{ kg/m}^3$  and  $2100 \text{ kg/m}^3$  and wet aggregates with sand show densities ranging from  $2000 \text{ kg/m}^3$  to  $2650 \text{ kg/m}^3$ . Wet aggregates are more dense than dry aggregates due to the water filled pore spaces (Meyer, 1985).

Soil bulk density and shear strength are important factors in determining the resistance or susceptibility of soil to erosion (Lal, 1990). The soil bulk density

according to Craig (1992) is the ratio of the total mass to the total volume. In general, the higher the bulk density of the soil, the lower the porosity and therefore the lower the infiltration rate. During natural and artificial compaction, the bulk density of the soil is increased and beyond a certain threshold, it becomes more susceptible to water erosion due to increased overland flow velocities than loosely compacted soils (Lal, 1990). It should be noted that compaction changes the volume of air in the soil only. The volume of water remains the same. A trade-off exists however since, the higher the degree of compaction, the higher the shear strength of the soil (Craig, 1992) or ability of the soil ability to resist erosion.

The shear stress applied to soil particles by running water is the major cause of soil erosion through failure, the rolling and slipping of grains past one another (Lal, 1990). The resistance of the soil to this failure is called shear strength and in engineering terms, is defined by Coulomb's Law (from Craig, 1992).

$$\tau = c + \sigma \tan \phi \quad [3.1]$$

Where

- $\tau$  = shear strength
- $c$  = apparent cohesion of the soil
- $\sigma$  = normal stress
- $\tan \phi$  = coefficient of friction
- $\phi$  = angle of internal friction

Terzaghi (1925) reported the importance of pore water pressure on shear strength and Equation [3.2] was modified to Equation [3.3].

$$\tau = c' + \sigma' \tan \phi' \quad [3.2]$$

Where

$c'$  = effective cohesion of the soil (interparticle attraction effect)

$\sigma'$  = effective normal stress

$\tan \phi'$  = coefficient of friction

$\phi'$  = effective angle of internal friction

$$\sigma' = \sigma + \Psi \quad [3.3]$$

Where

$\sigma'$  = intergranular stress

$\sigma$  = total stress

$\Psi$  = pore water pressure

As the pore water pressure increases, the bulk density of the soil decreases and the susceptibility of the soil particles to the erosive shearing forces of flowing water increases. This is discussed in more detail with infiltration and seepage in Section 3.3.2.2.

The effects of internal changes in water content on soil strength are well understood from classical soil mechanics. As soil moisture increases, the soil strength decreases and when the soil loses moisture, the soil strength increases. As the pattern of hysteresis develops, and the soil undergoes many wetting and drying cycles, it is understood that there is a net gain in soil strength. However, the role of soil strength on the erosion process is again, not understood (Lal, 1990).

#### 3.4.1.2 Examples of Erosion Impacts

It is well established that texture plays a significant role in determining other properties of a soil and overburden material (Sheridan *et al.*, 2000b). From this line of reasoning and recognizing that determining texture is a relatively simple procedure, measuring other more difficult properties may not be required to

determine soil erodibility. However, under controlled experimentation, Olson and Wischmeier (1963) observe a 30-fold increase in erosion rates when only the soil properties are varied. As a result, no single soil property can be measured to establish soil erodibility and thus predict erosion rates. This conclusion is supported by Sheridan *et al.* (2000b) who, after analyzing the lack of correlation between erosion rates and media properties for varying slope gradients, indicate that “a single set of media properties for the estimation of erodibility does not exist” (Sheridan *et al.*, 2000b:276). However, many researchers have tried to determine a range of the most erodible texture classes.

Fine textured soils high in clay have low erodibilities because the particles can resist detachment and dispersion due to cohesion and the strength of chemical bonds (Meyer, 1985; Toy and Foster, 1998). However, once the clay sized particles are mobilized, they are easily transported and take longer to settle out of the flow. Coarse soils such as sands, though easily detached also have low erodibilities due to both the weight of each particle and the larger void spaces resulting in high infiltration rates and low runoff rates and volumes (Toy and Foster, 1998).

Farmer (1973) finds that soil detachment by flowing water is greatest in the medium to coarse sand size range (0.425 mm to 4.75 mm) and decreases at either smaller or large particle sizes. However Lal (1990) indicates that highly structured soils with a high percentage of 0.25 mm to 5 mm aggregates tend to be the most resistant to erosion. Medium textured soils such as silt loams have moderate erodibilities since they are moderately susceptible to particle detachment and dispersion and produce runoff at moderate rates (Toy and Foster, 1998). Soils high in silt sized particles are especially erodible since silt is easily detached but also crust easily producing high rates and large volumes of runoff (Toy and Foster, 1998). Lal (1990) reports that in general, particles (primary and secondary) of 0.1 mm diameter are the most easily eroded.

Foster and Meyer (1972a) indicate that soil particles detached by raindrop impact alone, are primarily aggregates with diameters between 0.002 mm to 5 mm and a majority greater than 0.5 mm. Meyer (1985) supports this finding, concluding that under simulated rainfall, poorly aggregated silt loams (a mixture of 50 % sand, 20 % silt and 30 % clay) are the most erodible. Rock fragments 5 mm in diameter or greater do not move due to raindrop splash or overland flow on slopes of any gradient or length (Toy and Foster, 1998).

Soil erosion is therefore related to flow shear stress and the soil critical shear stress. Values of soil critical shear stress reported in the literature are between approximately 0.96 Pa to 24 Pa (Foster and Meyer, 1972a). Singer *et al.* (1978) find the relationships shown in Table 3.2 between critical shear values and erodibility.

**Table 3.2 Soil Erodibility Based on Critical Shear Values**

CRITICAL SHEAR RANGE (Pa)	ERODIBILITY
0.0 – 2.0	Very Erodible
2.1 – 3.0	Fairly Erodible
3.1 – 9.0	Moderately Erodible
> 9.0	Less Erodible

Foster and Meyer (1972a) also report that the critical shear stress of agricultural soils is approximately 2.4 Pa, falling into the “Fairly Erodible” class as determined by Singer *et al.* (1978). However, knowing the exact values of critical shear stress may not be necessary as demonstrated in the following example. If overland flow concentrated in rills on 10 m long erosion plots approach a 1.2 cm hydraulic radius in the rill for a 6 % slope, with a 5 cm/hr runoff rate, the shear stress is approximately 7.7 Pa. As mentioned, values of critical shear stress for agricultural soils reported in the literature are approximately 2.4 Pa, approximately 3 times lower than the flow shear stress (Foster and Meyer, 1972a).



Ariathurai *et al.* (1978) find that the interface critical shear stress for saturated, remolded clay samples ranged between 1 and 3 Pa. For each unit increase in shear stress above critical, there is a corresponding linear increase in erosion rate. However, for samples with a higher critical shear stress, the increase in erosion rate as the shear stress is increased above a critical value is smaller than for those samples with a smaller critical shear stress. Thus, once erosion begins on samples with a higher critical shear stress, erosion proceeds at a slower rate than for those with a lower critical shear.

Watson and Laflen (1986) measure soil compressive strength and soil shear strength before and after rainfall to determine if these parameters could be used to estimate interrill erodibility. For the soil types under the slope gradients tested the soil compressive and shear strengths are reduced significantly after rainfall. However, the soil shear strength values are much lower than the compressive strength values after rainfall for all cases. As a result, it is concluded that shear strength after rainfall is a much better parameter for predicting interrill soil erosion. Soil strength measurements before rain are not very useful due to non-uniformities in surface conditions including clods, crusts and surface aggregates making measurements much more difficult to obtain. However, after rainfall, the soil structural conditions become more homogeneous (Watson and Laflen, 1986). In addition, Fan and Wu (2001) find that shear strength is an important parameter in interrill erosion since it affects the rate of erosion caused by splash. They conclude that whether the shear strength and cohesion or shear strength and median particle size are considered and substituted for erodibility, the physical mechanism of interrill erosion can be appropriately described for slopes between 10 % and 100 %.

Sheridan *et al.* (2000b) notes that the coal mine spoil most susceptible to rill erosion were the sandy spoils (50 % to 80 % sand), low in clay with low cohesion therefore

providing little resistance to erosion by overland flow. The most resistant to rill erosion are the sodic, dispersive overburden materials that form strong surface seals and resist detachment. The spoils that are the most susceptible to interrill erosion are the well-aggregated clay spoils (20 % to 60 % clay) due to the presence of low-density aggregates. Interrill erosion as explained in Section 3.8.1 is often limited by the transport capacity of the interrill flow at low slopes. Therefore under transport limiting conditions, the low density aggregates that make up these soils are carried more easily by the flow.

Evans *et al.* (1997) contrast the general properties of coal mine spoil and agricultural soil. They find that there is a high percentage (20 % to 45 %) of dispersed clay particles in eroded coal mine spoil samples whereas agricultural soils tend to be highly aggregated. Loch and Donnallan concur (1982b) finding little dispersed clay in the agricultural soils tested (<20 %). There is a distinct variation in both the texture and the percentage of dispersed clay in eroded sediment between the mine spoils and the agricultural soils demonstrated in these studies. Therefore, erosion parameters for mine spoils need to be measured prior to using an erosion prediction model and should not be estimated using agricultural soil data.

### **3.4.2 Bulk Density and Unit Weight**

#### **3.4.2.1 Effects of Erosion**

The bulk density of a soil is the ratio of the total mass to the total volume whereas the unit weight of a soil is the ratio of the total weight (a force) to the total volume (Craig, 1992). Foster and Martin (1969) conduct a study exploring the effect of unit weight and slope gradient on erosion under controlled rainfall-runoff conditions for a bare exposed soil of the following structural properties and grain size distribution (Tables 3.3 and 3.4).

**Table 3.3 Soil Characteristics**

SOIL CHARACTERISTICS	VALUE
Liquid Limit	49
Plasticity Index	18
Optimum Water Content	26%
Maximum Dry Unit Weight	91.5 lb/ft <sup>3</sup>

**Table 3.4 Grainsize Distribution**

U.S. STANDARD SIEVE OR PARTICLE DIAMETER	PERCENT FINER
No. 10	100
No. 20	98
No. 40	94
No. 100	79
No. 200	69
0.05 mm	62
0.005 mm	39
0.002 mm	34

The three slope gradients used in the experiment are 3H:1V (18.3°), 2H:1V (26.5°) and 1H:1V (45°). The specimens are compacted to four unit weights, 80 lb/ft<sup>3</sup>, 85 lb/ft<sup>3</sup>, 90 lb/ft<sup>3</sup>, and 95 lb/ft<sup>3</sup>.

### 3.4.2.2 Examples of Erosion Impacts

The results of the experiment are plotted in the paper published by Foster and Martin (1969) as the rate of erosion as a function of unit weight for each slope. The data show that for the lowest slope gradient (3H:1V), the erosion decreased with increasing unit weight and at the lowest unit weight (80 lb/ft<sup>3</sup>) and the lowest slope (3H:1V), the erosion rate is the highest. The combination of the high impact force of the raindrops and the greater depth of flow cause a high rate of erosion (see Section 3.7.1.2 for greater explanation). For the 2H:1V slope, the relationship between unit weight and erosion rate is parabolic, with the greatest erosion rates occurring between 85 lb/ft<sup>3</sup> and 90 lb/ft<sup>3</sup>. However, specimens tested at the 1H:1V slope show the highest erosion at the highest unit weight (95 lb/ft<sup>3</sup>), likely due to high runoff velocities. Erosion decreases linearly with decreasing unit weight.

When the rate of erosion is shown as a function of slope for each of the four unit weights tested, the results show the following. For a unit weight of  $80 \text{ lb/ft}^3$ , the rate of erosion is non-linear but decreases with increasing slope. For the  $85 \text{ lb/ft}^3$  unit weight, the shape of the graph is parabolic with the peak erosion rate between 2H:1V and 1H:1V and the lowest erosion rate at 1H:1V. The  $90 \text{ lb/ft}^3$  is again parabolic, though the shape of the parabola is not as steep as that of the  $85 \text{ lb/ft}^3$  scenario. The results of both the  $85 \text{ lb/ft}^3$  and  $90 \text{ lb/ft}^3$  scenarios indicate that there is a unique slope for a given unit weight for which a maximum erosion rate will occur since there is a slight variation in the peak location of these graphs indicating that it lies between 2H:1V and 1H:1V. Finally, for the  $95 \text{ lb/ft}^3$  there is a non-linear increase in erosion rate with an increase in slope gradient. Foster and Martin (1969) caution that since the results of their study are obtained under laboratory conditions, the results should not be used in field applications until they have been investigated under field conditions for the effects of scale, site dependence and other issues.

Many authors conclude that with an increase in slope, there is an increase in soil loss, which is not the case when the effects of unit weight are considered as indicated from the conclusions of the study by Foster and Martin (1969). However, many of the studies that suggest there is an increase in soil loss with an increase in slope test their hypothesis on gradients less than 4H:1V (25%) (Foster and Martin, 1969; Fan and Wu, 2001). However, the results of the study conducted by Foster and Martin (1969) are in agreement with a study conducted by Horton (1945) that indicates that erosion occurring on a slope increase to a maximum on a  $40^\circ$  (85 %) slope and then decrease.

Barfield *et al.*, (1988) hypothesize that increased soil density leads to decreased erosion. However, they also indicate that after conducting studies on tilled plots from surface mines in Illinois and Indiana, the relationship between bulk density and

erosion is likely soil dependent. Sheridan *et al.* (2000a) commonly find that soils and overburden materials behave dramatically differently to one another and likely soils and coal spoils do also.

### **3.5 Chemical and Mineralogical Properties**

The clay content, exchangeable cations and organic matter are the chemical constituents important in affecting the resistance of soil to erosion (Lal, 1990). Though it is recognized that these parameters will affect soil erosion rates, a majority of erosion research has focused on physical soil properties.

#### **3.5.1 Organic Material**

##### **3.5.1.1 Effects on Erosion**

Soils with higher degrees of organic matter content are generally less susceptible to erosion than those with low organic matter content. Organic polymers bind domains and microaggregates into aggregates stabilizing the soil particles and increasing their resistance to raindrop impact and surface runoff. Organic matter improves the soil nutrient conditions, promoting plant growth and other biological activity that then improve the soil aeration and infiltration capacity reducing runoff and soil erosion. Cultivated soils as well as mine waste generally have low organic carbon content making them more susceptible to erosion (Toy and Foster, 1998).

Soils with low organic content are more easily compacted than those with high organic material, therefore complicating the prediction of erosion rates as discussed in Section 3.4.2. Not only does the type of organic material have an effect on the erosion rates or the erodibility of the soil, the location of this material within the soil matrix is also important for structural stability, bulk density and permeability.

It should be noted however, that organic content may not always increase the resistance of the soil to the erosive action of flowing water. Water repellent soils containing high amounts of organic material may remain highly erodible due to the electrostatic repulsion between aggregates (Lal, 1990).

### **3.5.1.2 Examples of Erosion Impacts**

The introduction of organic molecules through the addition of, for example, manure or vegetation residue cement together domains and micro-aggregates into aggregates that resist the dispersive effects of raindrop impact (Lal, 1990)..

## **3.5.2 Clay Content and Exchangeable Cations**

### **3.5.2.1 Effects on Erosion**

Erosion of soils high in clay content is different from cohesionless sand material where the shear stress required to mobilize individual grains must exceed the effects of gravity only (Ariathurai *et al.*, 1978). The shear stress required to erode high clay soils must exceed the strength of the interparticle bonds. These are both the electric bonds, determined by the type of clay, that hold the clay domains together as well as the cement bonds that bind the clay domains and silt-sized particles. Once this critical shear stress for cohesive clay soils has been exceeded, the rate at which erosion takes place is then the factor of interest. Sample ranges of shear stress based on the erodibility of soil are provided in Table 3.2. The physical and chemical factors that affect the critical shear stress include: the type and amount of clay, the chemical composition of the pore and eroding fluids, the temperature, the presence of organic matter and the stress history.

The cation exchange capacity (CEC) of a soil is a measure of the type and amount of clay and is defined as the number of milliequivalents of exchangeable cations absorbed to the soil particles per 100 g of dry soil (Ariathurai and Arulanandan,

1978). Typical values based on soil texture according to Flanagan and Nearing, (1995) are shown in Table 3.5.

**Table 3.5 Ranges of CEC for various soil textures (Flanagan and Nearing, 1995)**

SOIL TEXTURE	CEC (meq/100g)
Sands	1 – 5
Fine Sandy Loams	5 – 10
Loams and Silt Loams	5 – 15
Clay loams	15 – 30
Clay	30 – 150

In addition to the CEC, the Sodium Absorption Ratio (SAR) is important in determining the interparticle attraction. The SAR is an equilibrium constant whereby the ratio of exchangeable sodium cations to the two most common exchangeable cations is expressed as shown in Equation [3.5]. Soils containing bivalent cations ( $\text{Ca}^{2+}$ ,  $\text{Mg}^{2+}$ ) on their exchange complex tend to be more stable than those with monovalent cations ( $\text{Na}^+$ ,  $\text{K}^+$ ) (Lal, 1990).

$$SAR = \frac{[\text{Na}^+]}{\sqrt{\frac{1}{2}([\text{Ca}^{2+}] + [\text{Mg}^{2+}])}} \quad [3.4]$$

The presence of  $\text{Na}^+$  on the exchange sites of the clay lattice, increase the soil dispersibility. Therefore, soils with high SAR values causing the particles to repel one another and promoting dispersion are particularly vulnerable to interrill and rill erosion (Ariathurai and Arulanandan, 1978). Soils with high SAR values experience dispersion when exposed to water resulting in reduced infiltration (Gilley *et al.*, 1977). Sodic soils also seal quickly causing the permeability to decrease, increasing runoff and the potential for erosion ((Toy and Foster, 1998).

### 3.5.2.2 Examples of Erosion Impacts

Low activity clays or soils where the clay fraction is composed of kaolinite and halloysite generally contain stable aggregates due to the hydrous oxides of iron and aluminum. They have an effective cation exchange capacity of 16 meq/100g or less (Lal, 1990). Since the oxides of iron and aluminum carry positive charges up to pH 7 and pH 9 respectively, they maintain strong aggregation of the permanently negative clay particles within the soil profile under normal soil conditions of approximately pH 6 (Lal, 1990) and the potentially acidic conditions of mine soils. In the event that the iron and aluminum oxides are inactivated due to saturation with organic anions, the dispersive potential of the clay aggregates increases. However, as indicated in Section 3.5.1, organic polymers contribute to aggregate stability and therefore there exists a balance between soil organic matter content and the nature and amount of clay minerals present in the soil profile.

Ariathurai *et al.* (1978) investigated the erosion rates of saturated cohesive soils under remolded, laboratory conditions. In particular, they investigated the magnitude of critical shear stress required to initiate erosion. A few tests on undisturbed samples showed non-linear relationships between erosion rate and shear stress and it was thought that this may be due to the effects of soil armouring. However, when the remolded samples were investigated, the increase in erosion rate per unit increase in shear stress above critical became progressively smaller for soils with larger critical shear stresses. Therefore, once erosion begins in soils of larger critical shear stresses, the erosion rate is slower than those with lower critical shear to start.

The types and concentrations of ions in the pore and eroding fluids have a significant effect on the erodibility of cohesive soils. In a low SAR samples, as the concentration of ions in the pore fluid is increased, dispersion increases, causing the



erosion rate to increase at low concentrations. However, at approximately 30 % ionic concentration of the pore fluid, the rate of erosion levels off indicating that the maximum flocculation has occurred and the structure of the soil has filled or exchanged as many of its binding sites as possible. Any addition in ions to the pore fluid increasing its concentration will not result in additional erosion (Ariathurai and Arulanandan, 1978). Thus increasing the value of the SAR caused a reduction in the erosion rate rapidly at first and then more gradually. However, the ultimate structure or the point at which the SAR no longer has an effect on the erosion rate was at a SAR value of 30.

Ariathurai *et al.* (1978) also investigated the interaction between the SAR and the CEC. They found that for high SAR samples (SAR = 30), erosion rates are especially high but decrease rapidly for CECs between 0 meq/100g and 10 meq/100g. For low SAR samples (SAR = 4), a small change in erosion rate with increase in CEC below 10 meq/100g is seen compared to the high SAR sample. However, above a CEC of 10 meq/100g, both the high and low SAR samples appear to show no change in erosion rate with increasing CEC. Thus, up to a CEC of 10 meq/100g the addition of clay will reduce the erosion rate in both high and low SAR samples, but will reduce the erosion rate more rapidly in the high SAR sample. Above a CEC of 10 meq/100g the addition of clay has very little effect on erosion rate.

The interaction between high SAR soils and organic matter promotes stability and strength in a soil. The effectiveness of the organic matter in forming stable aggregates depends on the flocculating ability of the pore fluid. Lal (1990) indicates that the optimum organic matter content at SAR 2 is approximately 4 %.

Warrington *et al.* (1989) added phosphogypsum, ( $\text{CaSO}_4 \cdot 2\text{H}_2\text{O}$ , PG) to soil plots to observe the effects on soil loss. PG spread over the soil surface has four major

implications on the erosion process. First, it increases the electrolyte concentration of the rain and runoff water, which prevents soil dispersion and crust formation and allows infiltration rates to remain high throughout a rainfall event. Second, it increases the rainfall penetration by reducing the volume and velocity of overland flow, reducing erosion. Third, it retains larger soil aggregates at the soil surface, maintaining surface roughness and reducing the velocity of overland flow, promoting infiltration and reducing erosion. Finally, since the PG causes clay particles to flocculate, surface clay particles combine into larger aggregates too heavy to be entrained and if any clay particles do become entrained in the flow, they are combined together into heavier aggregates that are immediately deposited. Since erosion by overland flow becomes the dominant mechanism as the slope angle increases, it is expected that the effectiveness of PG to reduce erosion is increased at greater slope angles.

Warrington *et al.* (1989) conclude that PG reduces soil loss dramatically and these effects are amplified with an increase in slope angle. At a 25 % slope, the soil loss from an untreated and treated plot is 6.7 kg/m<sup>2</sup> and 0.8 kg/m<sup>2</sup> respectively. Treatment with PG also reduces runoff between treated and untreated plots.

### **3.6 Soil Hydrologic Properties**

The effects of soil hydrologic properties on soil erosion have been discussed throughout this chapter.

Some of these topics include, climatic interactions with soil properties including, for example infiltration and seepage (Section 3.3), the changes in soil strength with soil water content (Section 3.4) and the effects of pore fluid ion concentration on soil erodibility (Section 3.5). Therefore, further detailed discussion of the interactions between soil and water will not be discussed.

### **3.7 Landscape**

The degree and length of slope and the slope shape affect the erosion rates in a given climatic area.

The slope angle will influence the volume, velocity and type of water flow as well as the impact of individual raindrops. The slope length influences the flow characteristics and the type of erosion (e.g. interrill or rill). Deposition of upslope sediment at various locations downslope is dependent on the slope shape. Smooth and regular slopes generate overland flow with more erosive potential than rough and irregular slopes with high water retention capabilities.

#### **3.7.1 Slope Gradient**

##### **3.7.1.1 Effects on Erosion**

The effect of slope gradient on water erosion in general has been studied extensively (Zingg, 1940; Horton, 1945; Foster and Meyer, 1972a; Warrington *et al.*, 1989; Rymshaw *et al.*, 1997; Sheridan *et al.*, 2000a). Soil erosion is shown by many researchers to increase with an increase in slope gradient (Warrington *et al.*, 1989; Grosh, 1994; Sheridan *et al.*, 2000a). However, since the upper limit of research in developed countries is a slope gradient of 20 % very little is known about erosion processes above this gradient (Grosh, 1994). Understanding and quantifying the erosion process at slopes below 20 % has been suitable for erosion applications in agricultural research, but as erosion theory is applied to other land uses including mining applications, understanding and quantifying the processes at steeper gradients is becoming necessary.

The literature indicates a greater amount of research surrounding quantifying the effects of slope gradient on interrill erosion rather than on rill erosion. However,

from the varied research, slope gradient is shown to have different magnitudes of effect on interrill and rill erosion rates. An increase in slope gradient will increase rill erosion more significantly than it will increase interrill erosion (Watson and Laflen, 1986; Toy and Foster, 1998). Foster and Meyer (1972a) propose the conceptual model shown in Figure 3.4 relating slope gradient to delivery rate for erosion on interrill areas.

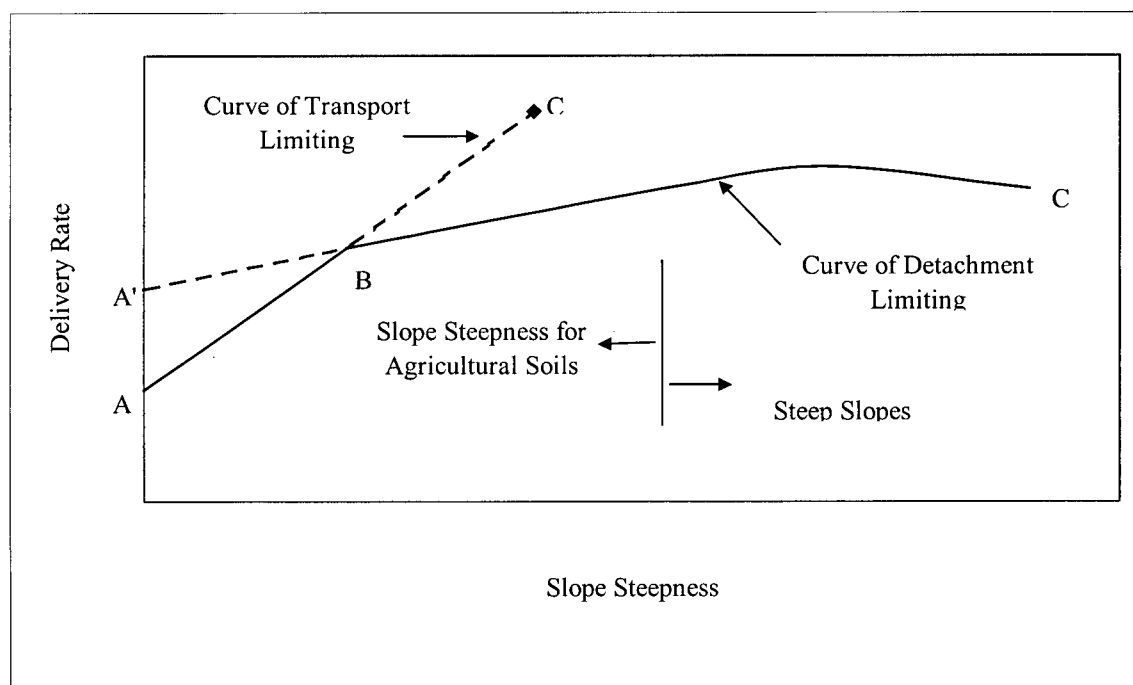


**Figure 3.4 Conceptual model showing the effect of slope gradient on delivery rate during interrill erosion (Foster and Meyer, 1972a)**

The A'BC curve in Figure 3.4 shows that for slopes less than or equal to approximately 4H:1V (25 %) have only a slight influence on the rate of detachment by raindrops. For slopes greater than 3H:1V and depending on the bulk density of the soil as discussed in Section 3.4.2, detachment rate by raindrop impact reaches a maximum and decreases with an increase in slope gradient (Foster and Meyer, 1972a). Any resulting increase in erosion beyond this critical slope gradient is due to the effects of rill erosion.

At low gradients, the transport capacity on interrill areas could be less than the availability of detached materials which is represented by curve ABC' in Figure 3.4. The transport capacity has a delivery rate greater than zero for a slope gradient of zero since even without a gradient, the flow has the capacity to transport some sediment. The lower of the two values for either curve A'BC or ABC' is the delivery rate  $D_l$  of particles detached on interrill areas to the rills. At lower slope gradients, the flow detaches larger particles than the flow has capacity to transport at those gradients and a segregation of particle sizes takes place. The curve in Figure 3.4 can shift and vary depending on the rainfall intensity, soil properties.

There are varied findings in regards to the effect of slope on runoff. Lal (1990) and Warrington *et al.* (1989) both report that under natural conditions and depending on soil texture, clay mineralogy and moisture regime, runoff decreases with increasing slope. If runoff decreases, then infiltration rate increases. Under rainfall conditions, increasing the infiltration rate means that the soil surface seal that forms during rainfall is not able to form. Preventing the surface seal from forming is likely caused by splash and sheet erosion. Additional reductions in runoff with increasing slope are caused by the decreased number of raindrop impacts per unit surface area, the decrease in the normal component of drop impact force and the reduction of the thin film of water that normally increases the compaction force of the raindrops (Warrington *et al.*, 1989). However under an agricultural regime (low slope gradients), it is concluded that runoff generally increases with increasing slope gradient (Lal, 1990).

#### **3.7.1.2 Examples of Erosion Impacts**

Erosion rates on interrill areas are much less sensitive to changes in slope gradient than erosion rates on rill areas. Erosion increases 50 % as slope gradient increases

from 2 % to 20 % and only increased 100 % when slopes increased from 2 % to 20 % (Lattanzi *et al.*, 1974; Meyer, 1985). It is expected that as slope gradient increase from 2 % to 20 % the combined effects of sheet and rill erosion would increase the erosion rate by a factor of 20 (Watson and Laflen, 1986).

Fan and Wu (2001) studied the effects of slope gradient (10 %, 25 %, 50 % and 100 %) on interrill erosion rates on six agricultural soils (ranging from loam to silty clay loam) in Taiwan under four rainfall intensities. They observe that when the slope gradient increases beyond approximately 20 %, the rate of interrill soil erosion reduces. This finding is consistent with the conceptual model proposed by Foster and Meyer (1972a). The reduction in the erosive power of the raindrops is attributed to the following. When the slope gradient is high, the area of the raindrop in contact with the soil surface is large, the normal force acting on the soil surface is low and therefore the erosion rate caused by splash is low. The force impacting on the soil surface increases with the increasing water depth up to 0.3 times the median drop diameter. Thus, while the slope is steep, the overland flow was thin and although the sheet flow velocity is high, the interrill erosion is low. Beyond a critical slope gradient, the interrill erosion rate decreases as the slope gradient increases further. These findings fit the conceptual model suggested by Foster and Meyer (1972a) outlined in Section 3.8.1.1 whereby at steeper slopes, detachment limits the sediment delivery resulting in a lower increase or possibly a decrease in soil loss with an increase in slope gradient (Fan and Wu, 2001)

Interrill erosion however, continues to be an effective erosion process in flat areas since soil detachment is dominated by raindrop impact (Warrington *et al.*, 1989). Below slopes of 10 % raindrop detachment is the main erosive agent while flow acts only to transport material and not cause additional erosion. Rill erosion at low slope angles therefore is insignificant (Meyer, 1985). Since rill erosion is a function of overland flow, the initiation of rills is attributed to a critical velocity of the overland

flow that increases dramatically as the slope angle increases. Sheridan *et al.*, (2000a) finds that rilling is observed at 20% slopes on 12 of the 16 rehabilitated coal mine spoils they tested, but is not active on the 5 % to 10 % slopes used in their erosion simulation.

When the erosion processes are compared on the rehabilitated coal mine soil and overburden plots, Sheridan *et al.*, (2000a) observes rilling to occur on the soil plots only and do not observe rilling on the overburden plots at any slope gradient. The implications of texture and other soil physical properties on erosion were discussed in the previous sections.

When observing the effects of rill erosion on coal mine spoil, Carroll *et al.* (2000) noted that rills occurring on steep slopes (approximately 30 %) tended to cut deeper rather than wider in spoil of low cohesive strength. The preferential erosion from the bottom of the rills resulted in a potential to form gullies if vegetation establishment is not successful.

### **3.7.2 Slope Length**

#### **3.7.2.1 Effects on Erosion**

There are two ways of defining slope length for analysis of erosion. The slope length can either be defined as the downslope distance from the slope crest to the point that deposition begins (Wischmeier and Smith, 1978) or the horizontal distance between the slope crest and toe of the slope (Zingg, 1940; Flanagan and Livingston, 1995).

#### **3.7.2.2 Examples of Erosion Impacts**

Zingg (1940), using limited data develops an empirical power law relationship to describe the relationship between erosion rates and horizontal slope length. He finds

that even for the large range in soil formation, infiltration rates and the varying intensities and amounts of rainfall, there is a small divergence in the exponential value. He shows that for an increased length in experimental plot, there is an increase in soil loss. The argument that increased length of slope may also reduce the amount of erosion was also presented. It is proposed that with an increase in slope length, there is an increase in retention storage reducing runoff, the key factor in erosion potential.

Zingg's (1940) major findings show that doubling the degree of slope, increases the amount of soil loss by 2.8 times. Doubling the horizontal slope length increases the soil loss by 3.03 times. Increasing the slope length decreases the runoff; however, increasing the slope gradient increases the runoff and the soil moisture content at the completion of the tests is inversely related to the total runoff.

Interrill erosion begins to occur with the onset of a rainfall event. Since one of the components of interrill erosion is splash where the particles are dislodged from their original location by raindrop impact and moved downslope, interrill erosion begins to occur as soon as the rainfall begins. Therefore, it is quite simple to measure the interrill erosion rate for a given rainfall event provided that the plot length is kept short. Short slope lengths ensure that rilling does not occur and that the erosion rates being measured during the experiment are those resulting from the interrill erosion process only. Several researchers have restricted the plot length to 0.75 m (Watson and Laflen, 1986; Fan and Wu, 2001) while Grosh and Jarrett (1994) chose slightly shorter plots (0.5 m long) to measure interrill erosion rates.

The shortest plot length reported in the literature for the combined measurement of rill and interrill erosion is 3.0 m (Sheridan *et al.*, 2000a; Loch *et al.*, 2001). Obtaining good estimates of rill and interrill erosion by allowing rills to develop requires a plot length between 4.6 m to 12 m (Meyer *et al.*, 1975; Loch *et al.*, 2001).



The 12 m plot length is also suitable for estimating rill erosion by overland flow (Loch *et al.*, 2001). It should be noted however, that under natural conditions, hillslope lengths rarely exceed 122 m; however, some have been reported to be as long as 305 m (Toy and Foster, 1998). Overland flow concentrates itself into rills long before 122 m.

### 3.7.3 Slope Shape

#### 3.7.3.1 Effects on Erosion

Slope shape affects erosion by determining the amount and velocity of overland flow. Slope shapes are described as being uniform, convex, concave or complex. Figure 3.5 shows the slope profiles of the various slope shapes.

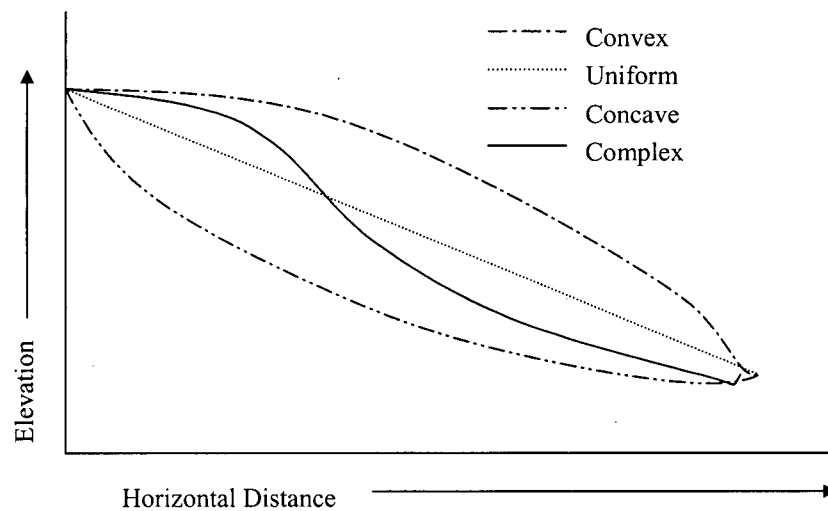


**Figure 3.5 Slope Shapes (Modified from Lal, 1990)**

#### 3.7.4 Examples of Erosion Impacts

Young and Onstad (1976) find that on convex slopes, the velocity of overland flow is increased, therefore increasing the detachment and transport capacity of the flow. However, on concave slopes, the velocity of overland flow is reduced at the flattened

toe thus causing deposition. Several studies have shown that erosion on convex slopes is about 5 times greater than that on uniform (Lal, 1990). On convex plots, erosion is not observed to occur at the upslope end, but as the flow gains velocity due to the convex shape, erosion is witnessed at the downslope end of the plots.

Young and Onstad (1976) conduct erosion studies on convex, uniform and concave slopes for various surface covers. Their results indicate that the erosion rates on the uniform and convex slopes are similar and approximately 20 t/ha greater than those on concave slopes.

Lal (1990) reports that for studies conducted on a tropical alfisol soils in 1972, 2.15 times as much soil is lost from the 12.5 m uniform plots of 10 % slope than from a 12.5 m long plot of 19.2 % concave slope. Also, 83 % more soil is lost from the 37.5 m plot of 9.3 % convex slope than from the 37.5 m plot of 13.4 % complex slope. Lal (1990) also shows that in a similar study conducted in 1973, that 54 % more soil is lost from a regular slope than the steeper concave slope. Also, 34 % more soil is lost from the convex slope than the complex slope.

The major conclusion from these studies is that the shape of the slope can be much more significant for the amount of erosion that occurs than the length or the gradient of the slope alone.

### **3.8 Land Use**

As mentioned previously, land use implies human interaction with the environment and often results in accelerated erosion rates.

Some land uses that have been identified as being particularly effective in accelerating erosion include deforestation, grazing, arable land abuse, intensified

cropping and faulty farming systems. The erosion of construction sites and mine waste areas are much more localized and though the severity of both situations has been realized, it has not been as readily recognized at a world wide scale.

### **3.8.1 Cover**

#### **3.8.1.1 Effects on Erosion**

Interrill erosion is most severe when raindrops reach terminal velocity before impacting the bare soil surface. Therefore, canopy and surface cover intercept raindrops reducing their erosive potential by the time they reach the soil surface. The most effective erosion control is the vegetation or rock cover that is in contact with the soil. This cover intercepts the raindrops at their final point before reaching the ground and allows the water to then percolate into the soil matrix. By intercepting falling raindrops, cover also reduces soil surface sealing caused by raindrop impact thus maintaining high soil infiltration rates and reducing the erosive effects of runoff (Meyer *et al.*, 1975).

Meyer *et al.* (1975) finds that after the interrill erosion quantities are subtracted from the total erosion losses, runoff from screen covered rills (used to simulate the effects of vegetative cover), is much less than from rills exposed to the direct impact of rainfall.

#### **3.8.1.2 Examples of Erosion Impacts**

The effects of vegetative cover are universal across all soil types. Carroll *et al.* (2000) indicate that any small differences in physical properties between soil and coal mine spoil, results in an even smaller effect on runoff and erosion. In addition, once vegetation is successfully established, there are few differences in the rates of erosion between slope gradients.

In waste cover design for mining applications, it has been concluded that the combination of a robust, well-graded, rip-rap cover with partial vegetation is the best cover (Williams, 2002a). The wide range of particle sizes in the rip rap combined with construction material will mimic the end result of weathering in nature. Natural processes tend to wash away a topsoil cover resulting in the loss of thousands of remediation dollars. A coarse cover on the other hand, will eventually break down into finer material. Therefore, using a well-graded material in combination with vegetation will ensure that small particles are not transported off-site, ending up in a sedimentation pond. This also minimizes the cost of large rip rap placement. Sheridan *et al.* (2000b) shows that rill erodibility is related to rock content by an exponential decay function. They indicate that at low levels of rock content, rill erodibility may be high or low, but at rock contents of about 30 % rill erodibility is low.

Owoputi *et al.* (1995) observes the erosion of a successfully vegetated mine waste rock cover after a rainfall event estimated to have a return period of over 100 years. They note that though the slopes range from 20 % to 70 % at this site, the rates of erosion are minimal in areas that are well vegetated. Williams (2002b) reports that in general, a 20% increase in vegetative cover reduces erosion of steep mining slopes in arid climates by 90%

During the early stages of rehabilitation when vegetation growth is slow, Carroll (2000) finds that ripping the surface of coal mine spoil to create surface roughness and promote infiltration will reduce runoff and erosion successfully until rill development occurs. The effects of ripping however are more predominant on the steeper slope gradients tested (30 %).

In agriculture, adding 0.5 t/ha, 2 t/ha and 8 t/ha straw mulch to a cultivated soil surface has reduced the impacts of interrill erosion by approximately 40%, 80% and

nearly 100 %, respectively, when compared with the effect of erosion on bare soil (Meyer, 1985).

The effects of vegetation establishment are not limited to the simple physical reduction in erosion. Vegetation growth also reduces the soluble salt concentrations at the surface of coal mine spoil material which reduces the risk of salt movement off-site (Carroll *et al.*, 2000).

### **3.8.2 Terraces**

#### **3.8.2.1 Effects on Erosion**

Terracing of agricultural land has been an effective means of controlling runoff and soil loss in many countries around the world. Applying this land alteration to surface mined lands and other mining waste piles is not new; however, in addition to providing stability and a trafficable surface, it also provides a means of controlling erosion. Terracing breaks up the long slopes of exposed earth, which are common features of the mining landscape.

Although vegetation provides an effective means of protection against runoff and erosion, its establishment is often difficult in areas disturbed by mining. The first year after mining often experiences the highest erosion rates and the ability of perennial vegetation to provide efficient control does not generally occur (Curtis, 1971). In addition, mining may be completed during a time of the year that vegetation establishment is not possible. As a result, terracing has been utilized to promote the establishment of vegetation and provide additional protection from high intensity rainfall. Terraces have been shown to not only reduce erosion, but also to improve soil moisture encouraging the successful, long-term growth of vegetation (Curtis, 1971).

### **3.8.2.2 Examples of Erosion Impacts**

Curtis (1971) investigates the effectiveness of terraces to regulate runoff and soil erosion on two surface mine overburden areas of shale and sandstone origin at 15 % slope. The results show that overall, there is a 65 % reduction in peak flow rates between the terraced and control plots. Terracing reduces the runoff on the shale plot by 65 % compared to an insignificant 6 % reduction in runoff seen on the sandstone plot.

In both cases, the concentration of suspended material and sediment yield is greater on the control plots than on those with terracing. However, difference in geologic material also contribute to the differences in erosion rates observed. The shale plots show considerably greater suspended sediment loads for both the control and terraced plots compared with the sandstone plots. The difference in erosion rates between the two materials occurs since shale weathers to smaller particle sizes than sandstone and therefore the erosive potential of the shale is greater (Curtis, 1971).

## **3.9 Summary**

Table 3.6 provides a summary of the findings of this chapter.

**Table 3.6 Summary of Factors Affecting the Erosion Process**

FACTOR	EFFECT ON EROSION	EXAMPLES OF EROSION IMPACT
<b>Climate</b>		
Rainfall Intensity	<ul style="list-style-type: none"> <li>Rainfall intensity rather than rainfall amount is the more dominant erosion process</li> </ul>	<ul style="list-style-type: none"> <li>Rainfall intensity exponent to describe interrill erosion in most erosion models is 2.0</li> </ul>
<b>Hydrology</b>		
Runoff	<ul style="list-style-type: none"> <li>Runoff in mining areas occurs as saturation overland flow and Hortonian overland flow</li> </ul>	<ul style="list-style-type: none"> <li>Overland flow velocities reported between 0.015 to 0.3 m/s</li> <li>Stream power of 0.1 W/m<sup>2</sup> for flow driven erosion</li> </ul>
Infiltration & Seepage	<ul style="list-style-type: none"> <li>Affected by the degree of soil compaction, ability of soil to develop a surface</li> <li>Exfiltration zones coincide with erosion points on hillslopes</li> </ul>	<ul style="list-style-type: none"> <li>Rates range between 2 and 2500 mm/hr</li> </ul>
Entrapped Air	<ul style="list-style-type: none"> <li>Creates a force upward that slows the infiltration rate</li> </ul>	<ul style="list-style-type: none"> <li>66% increase in sediment load caused by air entrapment alone</li> </ul>
Surface Seals & Surface Crusts	<ul style="list-style-type: none"> <li>Surface seal developed when the impact of raindrops seal the surface</li> <li>Surface crust occurs when the soil dries</li> </ul>	<ul style="list-style-type: none"> <li>Surface crusts form readily on structurally unstable soils with 15 % to 20 % clay and little organic matter</li> <li>Surface crust formation affected by SAR</li> </ul>
<b>Soil Physical Properties</b>		
Soil Texture	<ul style="list-style-type: none"> <li>Fine clays have low erodibilities due to cohesion and chemical bonds</li> <li>Coarse soils such as sands easily detached, but also less erodible due to large weight</li> <li>Soil shear stress determines how erodible sediments are</li> </ul>	<ul style="list-style-type: none"> <li>Many ranges in particle sizes determined to be the most erodible by researchers, therefore soil texture is not a dependable variable for determining soil erodibility</li> <li>Soil shear stress values range between 0.96 and 24 Pa</li> <li>Critical shear stress of agricultural soils is approximately 2.4 Pa</li> </ul>
Density & Unit Weight	<ul style="list-style-type: none"> <li>Trade off between runoff velocity and erosion rate</li> <li>There is a unique slope for a given unit weight for which a maximum erosion rate will occur</li> </ul>	<ul style="list-style-type: none"> <li>85 lb/ft<sup>3</sup> rate of erosion highest between slope gradients of 2H:1V and 1H:1V</li> </ul>

FACTOR	EFFECT ON EROSION	EXAMPLES OF EROSION IMPACT
<b>Soil Chemical &amp; Mineralogical Properties</b>		
Organic Matter	<ul style="list-style-type: none"> <li>• Soils with higher degrees of organic matter are less susceptible to erosion</li> </ul>	
Clay Content & Exchangeable Cations	<ul style="list-style-type: none"> <li>• CEC and SAR values affect erosion rates</li> </ul>	<ul style="list-style-type: none"> <li>• High SAR values (30) usually mean high erosion rates</li> <li>• Low SAR values (4) soils are less erodible</li> </ul>
<b>Landscape</b>		
Slope Gradient	<ul style="list-style-type: none"> <li>• Higher slope angles generally mean greater overland flow velocities and higher erosion</li> <li>• Rill erosion is attributed to critical flow velocities, and increases with increasing gradient</li> </ul>	<ul style="list-style-type: none"> <li>• Interrill erosion rates do not increase with an increase in slope gradient above approximately 25 %</li> <li>• Interrill erosion is effective on slopes with 0 % gradient since rainfall continues to dislodge material</li> <li>• Rilling is observed on coal mine spoil slopes greater than 20 %</li> <li>• Rilling does not occur on overburden plots at any slope angle</li> </ul>
Slope Length	<ul style="list-style-type: none"> <li>• Increased plot length can either increase or decrease the amount of erosion that takes place. Either an increase in slope length will provide additional available material for erosion or it will increase the surface area over which infiltration can take place reducing runoff volumes available for erosion</li> </ul>	<ul style="list-style-type: none"> <li>• For interrill erosion estimates, plots between 0.5 and 0.75 m are recommended to isolate and measure the erosion</li> <li>• For rill erosion estimates, plots between 3 and 12 m are sufficient to allow rills to develop</li> </ul>
Slope Shape	<ul style="list-style-type: none"> <li>• Convex slopes have been shown to produce the most erosion followed by uniform and then concave slopes</li> </ul>	<ul style="list-style-type: none"> <li>• Uniform plots can produce 200 % as much soil loss than concave plots</li> <li>• 83 % more soil is lost from a 37.5 m plot of convex shape than one of complex shape with similar slope</li> <li>• 54 % more soil lost from a regular slope than a steeper concave slope</li> </ul>



FACTOR	EFFECT ON EROSION	EXAMPLES OF EROSION IMPACT
Land Use		
Cover	<ul style="list-style-type: none"> <li>• Canopy and surface cover intercept raindrops before they contribute to interrill erosion</li> <li>• By intercepting raindrops, cover reduces surface sealing and maintains high infiltration rates, reducing the erosive potential of runoff</li> </ul>	<ul style="list-style-type: none"> <li>• Vegetative cover has a similar effect for all soil types</li> <li>• Rill erodibility is related to rock cover by an exponential decay function</li> <li>• A 20 % increase in vegetative cover will reduce erosion rates by 90 %</li> <li>• Ripping of coal mine spoil is an effective means of increasing surface roughness, promoting infiltration. Effects of ripping are the most notable at slope gradients &gt;30 %</li> <li>• Adding 8 t/ha of mulch to cultivated soils can reduce erosion by nearly 100 %</li> </ul>
Terraces	<ul style="list-style-type: none"> <li>• Effective means of controlling runoff and soil loss</li> </ul>	<ul style="list-style-type: none"> <li>• 65 % reduction in peak flow rates between terraced and un-terraced plots</li> </ul>

### CHAPTER 3 - LIST OF SYMBOLS

SYMBOL	DESCRIPTION
$\tau$	shear strength
$c$	apparent cohesion of the soil
$\sigma$	normal stress
$\tan \phi$	coefficient of friction
$\phi$	angle of internal friction
$c'$	effective cohesion of the soil (interparticle attraction effect)
$\sigma'$	effective normal stress
$\tan \phi'$	coefficient of friction
$\phi'$	effective angle of internal friction
$\sigma$	total stress
$\Psi$	pore water pressure

#### 4. EROSION MODELS

Models for predicting erosion rates have evolved from simple empirical equations to complex mechanistic numerical simulation packages. The techniques for erosion prediction and modeling have traditionally been developed for agriculture and forest industry purposes and as a result, calibration and validation of the available prediction models has taken place for these situations. Since the surface media, topography and management practices at mine sites are much different than in agricultural and forestry areas, questions have arisen as to the applicability of erosion models beyond their design settings (Sheridan *et al.*, 2000a).

There are two scenarios that arise when the mining industry uses erosion prediction technology. First, soil loss prediction models are used to design the slope of for example reshaped coal spoil to meet regulatory requirements while minimizing soil losses. Second landscape evolution models can be used to test the stability of these designs to determine where sediment will accumulate and where erosion features such as rills and depositional areas will develop (Evans *et al.*, 1991) over long time periods. The results of the landscape evolution models can then be used to redesign the piles under different configurations or to include drainage structures to minimize erosion. A survey of the erosion prediction models currently available is provided in this chapter in order to determine the most applicable models to evaluate erosion circumstances at mine waste sites.

Table 4.1 provides a summary of some of the distinguishing characteristics of the erosion models discussed in this chapter. Suggestions for the estimation and/or measurement of some of these input variables required to run the WEPP model are provided in Chapter 6.

## **4.1 Empirically Based Erosion Prediction Equations**

The research and development of equations to estimate soil loss from agriculture for the United States began as early as the 1930's. Although it was understood at that time that numerous spatially and temporally varying factors including soil physical properties and infiltration rates would contribute to soil loss on a hillslope, simplifying these complexities into statistical relationships between one or two parameters and soil loss was common practice. It was through these independent evaluations of contributing parameters that the Universal Soil Loss Equation (USLE) (Wischmeier and Smith, 1958) was first developed in the United States. The USLE has served as a starting point for erosion prediction, by estimating erosion rates on a mean annual basis.

Since empirical relationships are easier to use once data are available than process based models, they will likely continue to be widely used (Risse *et al.*, 1995). However, statistical models fail to account for deposition and do not always properly evaluate the erosive potential of a given area, as they report an absolute value of soil loss that over-estimates net erosion. In addition, the range of applicability of empirically based models is likely their greatest limitation unless considerable time and effort are taken in the derivation of model parameters for local conditions (Risse *et al.*, 1995). As a result, applying empirical equations to mining industry cases is not recommended for design purposes. These models however can provide average annual soil loss estimates for quick, conservative approximations. This section describes the USLE and its derivatives.

### **4.1.1 Universal Soil Loss Equation (USLE)**

The most widely accepted and applied erosion prediction model is the empirically based USLE (Wischmeier and Smith, 1958). Its popularity has been attributed to its

simple form and easy application procedure (El-Swaify and Fownes, 1989). The USLE is a multiplicative regression equation developed to predict long-term, average annual soil loss in runoff due to the effects of both interrill and rill erosion (Foster, 1982). It was originally designed to help soil conservationists develop farm management plans to maintain soil productivity and has been applied to sediment loss prediction from construction sites (Wischmeier and Smith, 1978). More recently, it has been used in estimating sediment yield for the design of reservoirs and the contribution made to non-point source pollution by erosion (Foster, 1982).

The statistical relationships developed using over 10,000 plot years of data on standard USLE plots (22.1 m long, 1.8 m wide, 9 % slope) for the continental United States have resulted in the development of the USLE as follows (Wischmeier and Smith, 1978)

$$A_{sl} = RKLSCP \quad [4.1]$$

Where

$A_{sl}$  = annual soil loss (t/ha)

$R$  = rainfall erosivity factor as an erosion index  $EI_{30}$  (MJ-mm/ha-hour)

Where

$E$  = total storm energy

$I_{30}$  = maximum 30-minute rainfall intensity

$K$  = soil erosivity factor (t-ha-hour/ha-MJ-mm)

$L$  = slope length factor

$S$  = slope gradient factor generally lumped with the length factor as the topographic factor LS

$C$  = cover and management factor which is determined by the crop rotation and the tillage system

$P$  = support practice factor which is determined by the mechanical control practices such as strip cropping and terracing and generally lumped with the C factor and discussed as the CP factor

The  $R$  factor quantifies the effect of raindrop impact and also provides information on the rate and amount of runoff associated with the rainfall. Using the iso-erodent map provided in the USLE Handbook (Wischmeier and Smith, 1978), values are selected for  $R$  based on the study location in the continental United States. The iso-erodent values link the rainfall erosivity through the product  $EI_{30}$  (total storm energy times the maximum 30-minute rainfall intensity). Since there is a direct relationship between soil loss and the  $EI_{30}$  factor, values between iso-erodents can be linearly interpolated for all locations in the United States. In order to incorporate the erosive forces of runoff from thaw, snowmelt or irrigation, an additional procedure is provided within the USLE Handbook (Wischmeier and Smith, 1978).

The soil erodibility factor  $K$ , is an experimentally determined factor for a particular soil. It indicates that different soils will erode at different rates depending on particle size distribution or texture and organic matter content as well as soil depth. The  $K$  factor is determined using the nomographs provided in the USLE Handbook (Wischmeier and Smith, 1978).

The slope length,  $L$ , and slope gradient,  $S$  are combined to account for the topographic effects on erosion. The  $LS$  factor is the ratio of soil loss from a unit area of a field in continuous fallow to that of a standard USLE plot of 22.1 m in length at a uniform 9 % slope under otherwise identical conditions. Continuous fallow is defined as land that has been tilled and kept free of vegetation for more than 2 years (Wischmeier and Smith, 1978).  $LS$  values are read from a graph provided in the USLE Handbook (Wischmeier and Smith, 1978) and are assumed to increase as the slope length and gradient increases and the runoff accumulates and accelerates downslope (Toy and Foster, 1998). The assumption is generally valid for areas where overland flow dominates such as slopes with exposed soil, but may not be appropriate for forested areas or areas dominated by dense vegetation (Toy and Foster, 1998). For complexly shaped hillslopes including convex, concave and

complex shapes,  $LS$  values can be computed by procedures outlined by Wischmeier and Smith (1978).

The cover and management factor  $C$ , is the ratio of soil loss from a field under cropped conditions to the corresponding loss from continuous fallow conditions. The cover and management factor is not only able to account for the ground area covered by vegetation that intercepts raindrops and reduces their erosive potential, it also incorporates the effects of crop canopy, residue mulch, incorporated residues, tillage and land use residuals.

Finally, the support practice factor  $P$ , represents the reduction in soil erosion due to the adoption of a soil conservation practice. Again, the factor is a ratio of the soil loss under practices such as contouring, strip-cropping or terracing to that with straight-row farming up and down the slope (Wischmeier and Smith, 1978).

Though the USLE was developed for use on agricultural soils, the Handbook lists provisions for applying the equation to construction sites. Under construction conditions and using periods of less than one year, Wischmeier and Smith (1978) report that the cropland estimation procedures can be used to provide acceptable estimates of erosion on construction sites. These estimates are acceptable because Hortonian overland flow is dominant on cropland areas and areas of exposed soil such as construction sites. The USLE however, has not been applied to areas with complete grass or tree cover where, saturation overland flow dominates.

The most prominent limitation of the USLE is that because it lacks a conceptual basis, it is not truly universal (Lal, 1990). It was developed under ecological conditions limited to the soil types and the environments east of the Rocky Mountains. Kirkby (1980) argues that since the variables of the USLE especially the  $K$  factor representing soil properties, are non-homogeneous, the factors cannot be

multiplied. Doing so results in the inability to accurately predict soil loss. Other, more specialized limitations of the USLE are that it:

- does not model gully, streambank or streambed erosion (Foster, 1982);
- does not apply to soils being eroded by mass wasting (Selby, 1993);
- is not intended to model soil erosion from single rainfall events (Wischmeier and Smith, 1978);
- does not model or estimate deposition (Wischmeier and Smith, 1978);
- performs best on medium textured soils (Wischmeier and Smith, 1978);
- is limited to slope length and gradients of less than 122 m and 18 %, respectively (Wischmeier and Smith, 1978); and
- has not been proven to work in tropical regions (Williams, 2002b).

Due to the wide variety of soil parameters that the USLE attempts to describe with the *K* factor, it performs well on soils from the corn belt of the United States (Wischmeier and Smith, 1978). Little validation of the accuracy of the USLE on soils outside the agricultural realm have been reported. Evans *et al.* (1991) conclude that in order for the USLE to be applied to open-cut spoil pile design, methods for adjusting the *K* factor to accommodate the competent sandstone and the fine fraction of overburden is amongst the future research needs. The response to the need for a more accurate procedure for estimating the erosion of disturbed soils such as those from mining and construction, resulted in the development of the Revised USLE (RUSLE) as described in the next section.

#### **4.1.2 Revised Universal Soil Loss Equation (RUSLE)**

The development of the RUSLE began in 1985 when it was recognized by erosion researchers that the original USLE needed to incorporate additional erosion research and technology developed after the USLE Handbook publication in 1978 (Renard *et al.*, 1994). The RUSLE retains the same basic structure as the USLE as shown in Equation [4.1] for calculating average annual soil loss and sediment yield from combined interrill and rill erosion (Toy and Foster, 1998). It is based on the same



data as the USLE (Renard *et al.*, 1994; Risse *et al.*, 1995; Brady and Weil, 1996) but the set of equations and algorithms used to calculate the individual factors have been changed significantly (Renard *et al.*, 1994). Refined values of  $R$ ,  $K$ ,  $L$ ,  $S$  and  $C$  and the identification of sub-factors allow more versatility in applying the RUSLE (El-Swaify and Fownes, 1989). However, perhaps the most significant change that resulted from the development of RUSLE is its computerization (Renard *et al.*, 1994). In 1992, the first computerized version of the RUSLE was released (Lafren *et al.*, 1997), followed by a Windows-based version in 1997. The Windows-based version assists the user with the selection of appropriate input factors and sub-factors (Risse *et al.*, 1995; Lafren *et al.*, 1997). The RUSLE is considered an improved USLE in that it recognizes the interrelationships between the parameters, to improve the accuracy of soil loss prediction (Toy and Foster, 1998).

Improvements to the USLE made in the RUSLE include the addition of  $R$  factor values for the Western United States and a more deterministic approach to estimating the  $R$  factor. These additions are the most significant changes to the USLE. Modifications to the  $K$  factor include providing an equation for estimating soil erodibility based on average particle diameter so that erosion from soils that do not fit within the original USLE soil nomograph can be estimated. In addition, the incorporation of rock fragments within the soil profile and on the soil surface can be modeled which requires a modification to the USLE  $C$  factor. Since erosion studies show that the value for the  $K$  factor is the highest in the early spring and lowest in the mid-fall or when the soil is frozen, the RUSLE is capable of varying  $K$  seasonally. Modification to the USLE  $LS$  factor to account for erosion due to the separate rill and interrill processes occurs through changes made to slopes greater than 9% (where rill erosion dominates) and slope lengths less than 4 m (where interrill erosion dominates). The values for the USLE  $LS$  factor for various ratios of rill to interrill erosion attempt to incorporate the effects of several soil conditions and make the choices easier and more consistent amongst users.  $LS$  values have been

separated into those applicable for rangeland or areas with consolidated soil under cover, row crop agriculture and moderately consolidated conditions, freshly prepared construction or other highly disturbed soil conditions or thawing soils where most of the erosion is caused by surface flow (Renard *et al.*, 1994). These modifications to account for highly disturbed soil conditions make the RUSLE more applicable to mine waste erosion prediction than the USLE. Finally, the USLE *C* and *P* factors have been separated into sub-factors to incorporate a wider range of conditions that result from cover, management and conservation practices. Some of these sub-factors include surface and sub surface residue levels, surface roughness canopy cover and soil moisture (Renard *et al.*, 1994).

The RUSLE is perhaps the only erosion model that has attempted to accurately predict soil loss from areas that have been affected by surface mining and reclamation activities. The RUSLE takes into account the soil, spoil and growth medium properties, landscape characteristics, vegetation, mulches, and percent rock cover as well as surface roughness due to mechanical equipment amongst other characteristics that are common in highly disturbed areas including construction sites, mine sites and reclaimed land (Toy and Foster, 1998).

Evans and Loch (1996) applied the RUSLE to two locations on the waste rock dump of the Ranger Uranium Mine in Australia. The cap and batter sites used in this study have differing compaction conditions and slope gradients that lead to differing erosion rates. They find that extreme caution must be taken in estimating the erosion parameters used in the RUSLE. However, the erosion rates predicted by the RUSLE reflected those measured from the runoff plots in their study.

Though the RUSLE appears to be the most applicable erosion prediction model for mined lands, several limitations of the model do exist that parallel those of the USLE and include the following (Toy and Foster, 1998):

- The RUSLE provides soil loss estimates rather than absolute soil loss data;
- The soil loss estimates are long term average rates rather than precipitation event specific estimates;
- The RUSLE has been developed for hillslope lengths between 11 m to 91 m. Hillslope lengths between 6 m and 11 m and between 91 m and 183 m will produce moderately accurate results with the poorest results for slope lengths between 183 m and 305 m. The RUSLE will not allow total slope lengths greater than 305 m;
- Gradient limits for which the RUSLE equation has been verified range between 0.2 % and 60 %; and
- The RUSLE does not produce watershed scale sediment yields.

Toy and Foster (1998) provide some example scenarios under which the RUSLE can be used including model set-up and model results.

#### **4.1.3 Modified Universal Soil Loss Equation (MUSLE)**

In order to modify the USLE to predict sediment yield from a watershed rather than the soil loss from a field-scale plot, the sediment delivery ratio (SDR) must be used (Williams, 1972). The SDR as defined in Section 2.1.3 as the sediment yield at any point along a channel divided by the sources of erosion above that point (Williams, 1972). Values of the sediment delivery ratio are not known for a majority of the watersheds within the United States and even fewer values are known for watersheds outside the United States (Williams, 1972; Lal, 1990). Replacing the rainfall erosivity factor of the USLE with a runoff-rate factor eliminates the need for the SDR since watershed characteristics influence runoff rates and SDRs similarly. Such watershed characteristics include stream slope and watershed shape. Williams (1972:244) indicates that "high stream slope produces high runoff rates and high delivery ratios."

The Modified Universal Soil Loss Equation (MUSLE) as developed by (Williams, 1972) therefore replaces the R factor in the USLE and is shown here in the metric version from Lal (1990) as

$$S_y = 9.05 (Vq_p)^{0.56} KLSCP \quad [4.2]$$

Where

$S_y$  = sediment yield (t)  
 $V$  = runoff volume ( $m^3$ )  
 $q_p$  = peak discharge rate ( $m^3/s$ )  
and all other variables are defined above.

Where the values for SDR are available, the American Society of Civil Engineers (1975) suggest taking the gross erosion rate provided by the USLE and multiplying it by an appropriate SDR factor to predict the sediment yield.

The most obvious limitation to the MUSLE is data availability in terms of both rainfall and runoff records. Where short-term runoff records exist for a watershed they can be extended to long-term rainfall records by applying an assumed rainfall-runoff relationship. However, in the event that rainfall records do not exist, determining a rainfall-runoff relationship or having runoff information is not likely.

Due to its empirical nature, application of the MUSLE to the mining industry is again not recommended. However, for a watershed within which mining practices may take place in the future, the MUSLE provides a simple method of sediment yield determination for pre- and post-mining impact comparison.

#### 4.1.4 Other USLE Modifications

Lal (1990) provides a discussion of several of the modifications to the USLE that allow the equation to be used under single storm conditions, on flatlands and rangelands and in tropical environments. Two of these modifications are.

The USLE-2D is designed to calculate the  $LS$  factor used in the USLE from a grid-based Digital Elevation Model (DEM). In two-dimensional overland flow, the resulting soil loss does not depend on the manually measured distance to the downslope end of the field, but rather on the area per unit contour length contributing to runoff. Therefore to increase the accuracy of the  $LS$  factor, the unit contributing area replaces the slope length in the USLE2D program.

The USLE-M is a modification of the USLE that allows the estimation of erosion rates on a single storm event basis. In this modification, the  $R$  (erosivity) factor is a product of the runoff rate  $Q_R$ , and the  $EI_{30}$  index. Due to the incorporation of runoff, the model is capable of predicting event erosion better than the USLE. Essentially, as the proportion of the rain that infiltrates into the soil increases, the efficiency of the USLE in predicting erosion decreases. The USLE continues to predict erosion based on rainfall though during infiltration, a reduced amount of runoff is being generated thus reducing the amount of erosion. However, by incorporating the runoff into the USLE  $R$  factor as is done in the USLE-M equation, the equation is effective in calculating erosion for each rainfall event where the infiltration rate varies over the event period. This modification to the USLE is incorporated into versions of the Agricultural Non Point Source Pollution (AGNPS) model discussed in Section 4.4.1.

## **4.2 Overview of Erosion Simulation Models**

The erosion simulation models described in the following sections are to some degree process-based models in that they require information to characterize the physical processes of erosion (Watson and Laflen, 1986). Simulation models typically have two components, a hydrologic simulation component and an erosion estimation component. Several of the models provide additional information such as

chemical migration and crop growth. The hydrologic component utilizes rainfall amount and duration as well as other influencing factors to compute runoff rates. The erosion component utilizes the output from the hydrologic component to determine sediment detachment and transport for the individual processes of interrill and rill erosion (Foster, 1982). These models can be classified as lumped or distributed parameter models based on their method of computation. They can also be run under a variety of circumstances such as cropland or rangeland conditions, field-scale plots or watersheds, single event or continuous simulation conditions.

Lumped models treat the modeling area such as a watershed or a hillslope as a homogeneous unit. As a result, the parameters selected are assumed to be valid for the entire area (Yulianti, 1996). A distributed parameter model divides the watershed or hillslope area into discrete cells or elements having individual topography, soil or land use characteristics, therefore requiring individual parameter estimates.

The distinction between cropland and rangeland is largely a function of the type of vegetation and the human interaction in the designated area. Croplands generally consist of one type of vegetation rotated at particular times of the year, or over several years. These may include row crops that have a distinct growth cycle including planting, harvesting and fallow periods and the soil is prepared through some form of tillage for the next cycle. Rangelands on the other hand, are generally open areas, often dominated by grasses and a variety of low shrub species and generally accommodate grazing animals.

The distinction between hillslopes and watersheds is a matter of scale. Hillslopes refer to single plots of land that together with other hillslopes and channels combine to form a watershed. Hillslopes may be complexly shaped, varying in length and

having a range of soil types and plant species. For lumped models, hillslopes or portions of the hillslope are generally the most convenient scale with which to work.

Single event and continuous simulation models provide erosion information either per rainfall event or over the long term incorporating many rainfall and seasonal changes. The output from these models can be useful in designing sedimentation ponds for the short and long term and planning management strategies into the future.

### **4.3 Physically Based Erosion Models**

WEPP, GUEST and EUROSEM are described below as steady state models indicating that they model change as a sequence of steady states. This approach avoids the need to solve partial differential equations in space and time, as is the approach in dynamic models. Instead, ordinary differential equations are used to describe spatial change (Rose, 1997). WEPP was chosen to be the most appropriate model for use in mining applications and therefore Chapter 5 provides a more detailed discussion of the model structure than the discussion provided in Section 4.3.1.

#### **4.3.1 Water Erosion Prediction Project (WEPP)**

The Water Erosion Prediction Project (WEPP) model is a distributed parameter, process-based, continuous simulation or event based erosion prediction model that was developed by the United States Department of Agriculture (USDA) to replace the USLE. The WEPP model has been designed to operate at scales of tens of meters for hillslope profiles and up to hundreds of meters for small watersheds. WEPP is a modular model, which includes components for weather generation, winter hydrology, irrigation, infiltration, overland flow hydraulics, water balance, plant growth and residue decomposition, soil disturbance by tillage, consolidation

and erosion and deposition. WEPP predicts soil loss and sediment deposition from overland flow on hillslopes, soil loss and sediment deposition from concentrated flow in small channels and sediment deposition in impoundments (Flanagan and Nearing, 1995).

The WEPP model has not been parameterized to model gully erosion, but has the capacity to model upland erosion through the separate processes of interrill and rill detachment and transport as well as channel erosion in watershed areas. The model has been validated under a range of land uses including cropland, rangeland and disturbed forest. The WEPP model has been applied in the mining context, though no published studies of such work have been noted (Laflen, 2002). Unlike many agricultural models including CREAMS and EPIC, WEPP does not have the capacity to model chemical migration.

On days when rainfall occurs, WEPP computes infiltration using a solution to the Green-Ampt Infiltration Equation for unsteady rainfall (Chu, 1978) and routes excess runoff downslope using the Kinematic Wave Equation (Flanagan and Livingston, 1995). From the surface runoff characteristics, WEPP computes the soil that is detached from the hillslope or watershed surface and deposited at the toe of the hillslope or delivered to the channels at the base of watershed slopes. The sediment detachment and transport relationships incorporated into the WEPP model are reported by Foster (1982) and Yalin (1963). In addition, WEPP uses crop growth routines adopted from the Erosion Productivity Impact Calculator (EPIC) and biomass decomposition routines from the RUSLE (Laflen *et al.*, 1997) to aid in determining erosion losses under different management regimes.

Though the WEPP model is a physically based model in its approach to the components in the erosion process, it does rely on empirical relationships to determine the erodibility of the soil. The equations supplied in the *WEPP User*



*Summary* (Flanagan and Livingston, 1995) for determining cropland and rangeland values of interrill erodibility  $K_i$ , rill erodibility  $K_r$  and critical shear stress of the soil  $\tau_{cr}$  are based on field studies to obtain the data required to develop the relationships. Since the erodibility parameters are affected by soil properties, they can vary widely among soils (Laflen, 1991). These parameters can also vary widely from year to year depending on the climate. Rather than adjusting these parameters based on the cropping and management factors as is conducted when using the USLE, WEPP internally adjusts these factors during its execution. It should be noted that there is no correlation between the three soil erodibility parameters used in WEPP and the USLE soil erodibility factor  $K$ . The USLE lumps together the interrill and rill erosion processes and therefore the soil erodibility factor  $K$  represents the susceptibility of the soil to both. WEPP however, separates erosion into the more fundamental processes of interrill and rill erosion yielding soil erodibility values that are very different and unrelated (Laflen, 1991).

#### **4.3.2 Griffith University Erosion System Template (GUEST)**

In the United States, extensive data for a variety of soils has been analyzed from annual average soil loss quantities using standardized runoff plots under natural rainfall to yield estimates of the soil erodibility factor,  $K$  used in the USLE. In other parts of the world, where such a database may not exist,  $K$  has to be determined from runoff plot data on a case-by-case basis prior to using the USLE for prediction (Loch, 1984). In Australia where the rainfall and stormflow data are highly variable and the occurrence of significant runoff events is low, producing a database of reliable values for the  $K$  factor based on natural rainfall would take a significant amount of time to complete (Loch, 1984; Yu *et al.*, 1997). Even with the use of simulated rainfall, the time required to estimate individual soil erodibilities seriously impedes the application of the equation. As a result, it was concluded that developing a model based on physical soil properties would, in the long term, be

more efficient in determining soil erodibility for a variety of soils with a less extensive period of experimentation (Yu *et al.*, 1997).

Based on this decision, the Griffith University Erosion System Template (GUEST) was developed (Misra and Rose, 1995). GUEST is a process-based model designed to determine soil erodibility for agricultural applications under Australian and South East Asian climate and soil conditions. The soil erodibility is then used in soil loss prediction.

The structure of GUEST model is best understood through the flowchart provided by Yu *et al.* (1997) as follows.

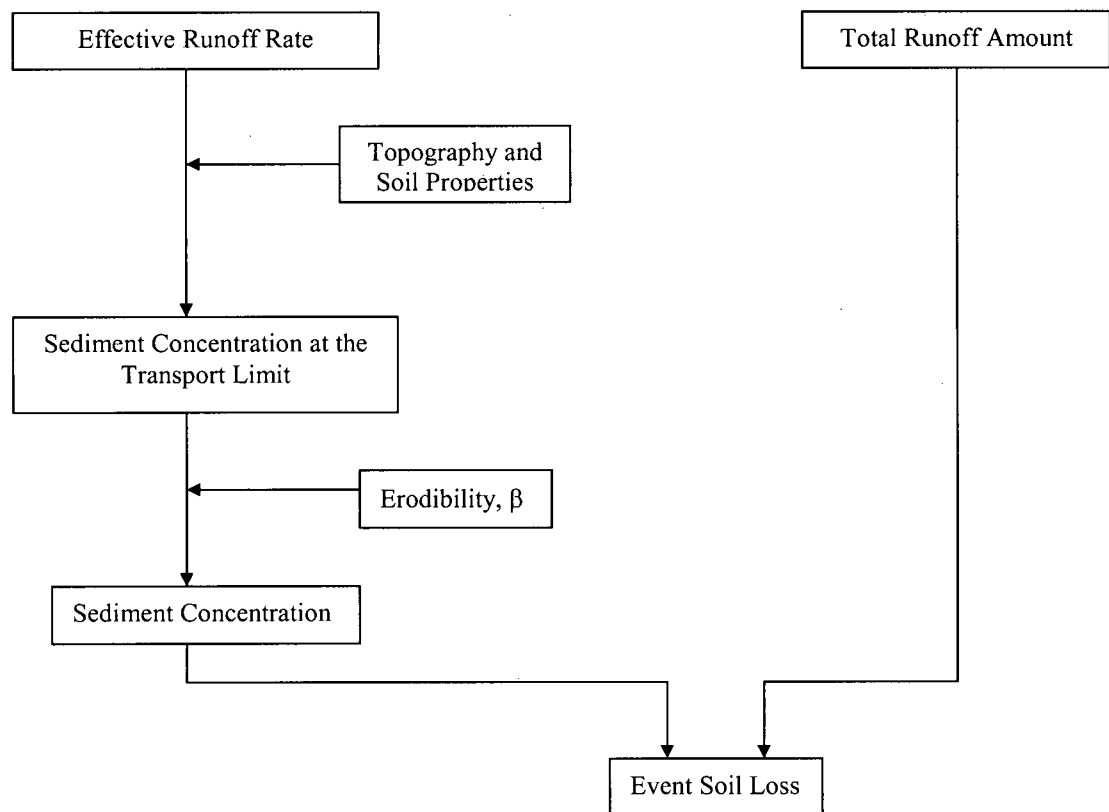


**Figure 4.1 Soil Erosion Prediction Using GUEST Technology (Yu *et al.*, 1997)**

GUEST is based on the notion of sediment concentration at the transport limit. However, the expression for the maximum sediment concentration is theoretically derived based on the concept of stream power,  $\Omega$ , rather than determined based on a sediment transport equation as in WEPP (Rose, 1997). Stream power is defined by Rose (1997:67) as the “working rate of mutual shear stresses between flowing water and the soil surface”.

The GUEST model divides the land area into sloping planar units and uses the following method for determining the amount of overland flow

$$R_e = P - I \quad [4.3]$$

Where

$R_e$  = rainfall excess (m/s)

$P$  = rainfall rate (m/s)

$I$  = infiltration rate (m/s)

From this, the runoff per unit area is given by

$$Q = \frac{q}{L} \quad [4.4]$$

Where

$Q$  = runoff rate per unit area (m/s)

$q$  = flux at a distance  $x$  from the top of a plane where  $q=0$   
( $m^3/m/s$ )

$L$  = plane length (m)

If the length of the plane is substantial and the runoff is assumed to vary with time, then changes in the runoff rate will lag behind the rainfall excess due to the time required for the flow to gather on the soil surface. Therefore, the rainfall excess cannot be measured directly and the following approximate analytical theory is used to determine the rainfall excess.

$$R_e = Q + K_p \left( \frac{dQ}{dt} \right) \quad [4.5]$$

Where

$K_p$  = coefficient depending on length, slope and roughness of the planar surface

$t$  = time (s)

and all other variables are defined above.

Since the runoff rate,  $Q$  can easily be measured, Equation [4.5] allows  $R_e$  to be calculated; once  $R$  is known,  $I$  can be calculated from Equation [4.3]

The GUEST model theory recognizes that all but the fine fraction of the sediment detached will return to the soil surface becoming available for rainfall re-detachment. The rate of rainfall detachment and re-detachment is taken into account by Equation [4.6], which shows that some portion of the original soil surface will be shielded from detachment by rainfall.

$$H = \frac{m_d}{M_d} \quad [4.6]$$

Where

$H$  = fractional shielding

$m_d$  = actual mass present per unit area of deposited layer  
(kg/m<sup>2</sup>)

$M_p$  = mass per unit area of deposited sediment (kg/m<sup>2</sup>)

The rate of rainfall re-detachment have been shown to be proportional to the rainfall rate.

The rate of entrainment and re-entrainment for sediment by overland flow relies on a similar theory. The primary reason for distinguishing between the processes of

detachment and re-detachment and entrainment and re-entrainment is that it takes more work to detach and entrain cohesive soil than that which has been previously detached or entrained.

Since the GUEST model again works based on a steady state assumption, the following form of the continuity equation is used.

$$W_r q = A v \quad [4.7]$$

Where

- $W_r$  = average rill spacing (m)
- $A$  = cross sectional area of the flow ( $m^2$ )
- $v$  = flow velocity (m/s)
- and all other variables are defined above.

The velocity is then determined using Manning's Equation

$$v = \frac{1}{n} R_h^{2/3} S^{1/2} \quad [4.8]$$

Where

- $n$  = Manning's roughness factor
- $R_h$  = hydraulic radius (m)
- $S$  = slope
- and all other variables are defined above.

Values of Manning's  $n$  for overland flow are approximately one order of magnitude higher than those used for channel flow because most of the vegetation and rock fragments protrude above the flow (Morgan *et al.*, 1998).

In areas where rills have not developed, planar geometry is used. However, when rilling occurs, the cross-sectional area of the flow is approximated according to the rill geometry (trapezoidal, triangular or rectangular). By numerically solving Equation [4.7], for water depth, at a given unit discharge and rill geometry, the hydraulic radius and flow velocity are then determined for use in evaluating stream power. Stream power is given by:

$$\Omega = \tau V \quad [4.9]$$

Where

$\tau$  = flow shear stress ( $\text{N/m}^2$ )  
and all other variables are defined above.

Since soil erosion on cultivated soils due to flow driven processes is known to occur when the stream power exceeds a critical value ( $\Omega_{cr} = 0.008 \text{ W/m}^2$ ), the results of Equation [4.9] will determine if erosion takes place (Yu and Rose, 1999). The excess stream power is then ( $\Omega - \Omega_{cr}$ ) and the fraction of the excess stream power,  $F_c$  (experimentally found to be approximately 0.1) maintains the sediment in suspension.

The sediment that returns to the soil surface does so at the deposition rate,  $\phi$ , which is important not only in determining sediment concentration at the transport limit, but also the soil erodibility parameter,  $\beta$ . Deposition rate,  $\phi$ , is defined as the mean particle settling velocity in water as follows:

$$\phi = \sum_{i=1}^1 v_s \quad [4.10]$$

Where

$v_s$  = settling velocity of a typical size class  
 $i$  = total number of size classes that the soil can arbitrarily be placed  
and all other variables are defined above.

Assuming equilibrium conditions and that the effective excess stream power is used to lift sediment against its immersed weight in water, the sediment concentration appears to be similar to the maximum transport capacity concentration used in the WEPP model.

For sheet flow the maximum sediment concentration,  $c_t$  ( $\text{kg/m}^3$ ) is given by Equation [4.11].

$$c_t = \frac{F_c \rho}{\sum v_f / i} \left( \frac{\sigma}{\sigma - \rho} \right) S_v \quad [4.11]$$

Where

$F_c$  = fraction of excess stream power  
 $\rho$  = density of water ( $\text{kg/m}^3$ )  
 $\sigma$  = sediment density ( $\text{kg/cm}^3$ )  
 and all other variables are defined above.

When erosion involves rectangular rills, Equation [4.12] is used.

$$c_t = \frac{F_c \rho}{\sum v_s / i} \left( \frac{\sigma}{\sigma - \rho} \right) \frac{\Omega}{gD} \left( \frac{W_b}{W_b + 2D} \right) \quad [4.12]$$

Where

$W_b$  = width of the rill (m)  
 $D$  = depth of flow (m)  
 $g$  = acceleration due to gravity ( $\text{m/s}^2$ )  
 and all other variables are defined above.

The shear stress acts uniformly around the wetted perimeter of the rill ( $W_b + 2D$ ) but entrainment takes place from the bottom of the rill. Thus  $W_b / (W_b + 2D)$  is the stream power responsible for re-entrainment which is the dominant process in order to achieve the sediment concentration at the transport limit,  $c_t$ .

Since some aggregates are not completely immersed in the flow due to their large diameters, the independent, but fully integrated program, GUDPRO provides GUEST with an effective soil deposition rate,  $\phi_e$ . This deposition rate represents the rate determined as if the aggregate were fully submerged. In addition, GUDPRO

provides GUEST with the fraction of the soil surface fully immersed in order to apply the soil deposition rate and the effective soil deposition rates appropriately.

The actual sediment concentration is related to the maximum concentration at the transport limit by Equation [4.13].

$$c = c_t^\beta \quad [4.13]$$

Where

$\beta$  = erodibility parameter  
 $c_t$  = sediment concentration at the transport limit (kg/m<sup>3</sup>)  
 $c$  = actual sediment concentration (kg/m<sup>3</sup>)  
 and all other variables are defined above.

There are two ways of calculating the soil erodibility parameter,  $\beta$ . Using the first method, the sediment concentration at the transport limit is calculated for each minute of runoff and then the average sediment concentration  $\bar{c}$ , for the event is determined by dividing the total soil loss by the total runoff. Then the erodibility parameter is calculated using

$$\bar{c} = \bar{c}_t^\beta \quad [4.14]$$

Or

$$\beta = \frac{\ln \bar{c}}{\ln \bar{c}_t} \quad [4.15]$$

Where

$\bar{c}_t$  = average sediment concentration at the transport limit  
 (kg/m<sup>3</sup>)  
 and all other variables are defined above.



The second method requires the calculation of the effective runoff rate,  $Q_e$  to calculate the sediment concentration in the flow based on a power law relationship rather than a simple time averaged method. The effective runoff rate is then used to calculate the sediment concentration at the transport limit and the soil erodibility parameter as follows

$$\beta_e = \frac{\ln \bar{c}}{\ln c_t(Q_e)} \quad [4.16]$$

Where

$\beta_e$  = effective soil erodibility  
and all other variables are defined above.

Most of the values of the erodibility parameter are calculated using the first method since collected tipping bucket runoff data allows for the determination of instantaneous runoff rates.

The original version of GUEST is developed to determine the soil erodibility parameter  $\beta$  using runoff rate data collected using a tipping bucket system and the data is then processed by the programs DATALOG and DATAMAN into 1-minute runoff rate data. Both DATALOG and DATAMAN are separately run programs that are fully integrated with the GUEST model. However, in situations where total runoff is collected using flumes rather than tipping buckets the runoff data cannot be processed by DATALOG and DATAMAN without significant manipulation. Also, at the time of GUEST development, the model did not predict soil loss since it was assumed that the average sediment concentration was measured and thus there was no need to predict it. As a result, the Griffith University Erosion Prediction System (GUEPS) model was written that does not rely on the DATALOG and DATAMAN programs while using the original GUEST technology explained previously to compute the sediment concentration at the transport limit.

The advantages of GUEPS include the following:

- It is able to predict the sediment loss as well as the soil erodibility parameter;
- It addresses the effects of surface contact cover; and
- The runoff rate data does not have to be supplied at the constant fixed interval of one-minute as was required previously.

Now, the runoff duration can vary for each data entry of runoff rate providing a more realistic use of the runoff data for long-term average rate of soil loss prediction.

The model assumes that erosion occurs by means of sheet or rill processes or a combination of both under the premise that the most erosion occurs in two or three large rainfall events a year (Morgan *et al.*, 1998). The major limitation of the model is that it does not consider gully erosion, landslides or tunnel erosion (Evans *et al.*, 1991).

#### **4.3.3 European Soil Erosion Model (EUROSEM)**

The complications of transferring the USLE to the European setting are similar to those encountered in Australia as indicated in Section 4.3.2. As a result, the European Soil Erosion Model (EUROSEM), a physically based model that considers erosion on a field sized area on an event based time scale was developed to take into account the unique conditions of Europe. Since the developers share the view that a majority of soil loss occurs during two or three major events per year an event based model is an appropriate time scale to begin model development.

The EUROSEM model is similar to both WEPP and GUEST in that it uses the concept of sediment concentration at the transport limit. Like WEPP, a sediment transport capacity relationship expressed as a solids discharge is used rather than a sediment transport capacity expressed as a sediment concentration as in GUEST.

The relationship used in EUROSEM was established by Govers (1987) rather than the relationship described by Yalin (1963) as used in the WEPP model. The power function described by Govers (1987) relating the sediment transport capacity to flow rate and slope is used in the EUROSEM model (see Equation [2.26]). Recognizing that the same hydraulic parameters that are used in sediment transport prediction in rivers are of fundamental importance to sediment transport prediction in overland flow, the equation developed (Govers, 1987) incorporates the principles of flow hydraulics.

The flow chart from Morgan *et al.* (1998) details the execution of the EUROSEM model as shown in Figure 4.2.

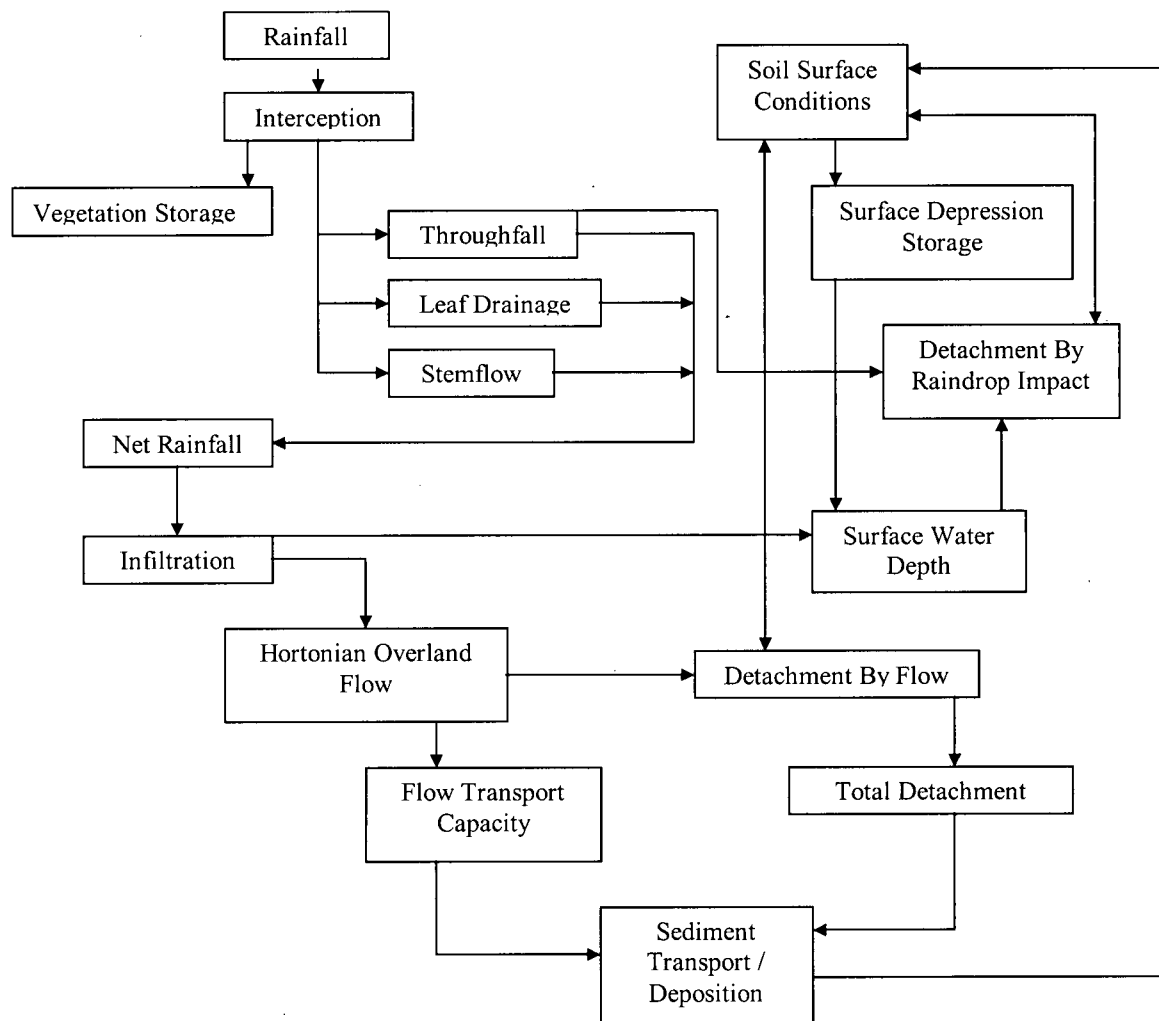


**Figure 4.2 EUROSEM Model Description (Morgan *et al.*, 1998)**

Like GUEST, EUROSEM simulates erosion for single events, over single slope segments. WEPP, GUEST and EUROSEM treat change as a series of steady states avoiding the need to solve partial differential equations in space and time for soil loss prediction. However, the EUROSEM model uses the KINEROS hydrologic model for overland flow that solves the continuity equation using a four-point implicit finite difference method.

$$\frac{\delta(AC)}{\delta t} + \frac{\delta(QC)}{\delta x} - e(x,t) = q_s(x,t) \quad [4.17]$$

Where

- $A$  = cross-sectional area of the flow ( $m^2$ )  
 $C$  = sediment concentration ( $kg/m^3$ )  
 $Q$  = discharge ( $m^3$ )  
 $e$  = net detachment rate ( $m^3/s/cm$ )  
 $q_s$  = external input/extraction of sediment per unit length of flow ( $m^3/s/cm$ )  
 $x$  = horizontal distance (m)  
 $t$  = time (s)  
 and all other variables are defined above.

The EUROSEM-KINEROS model combination simulates erosion by raindrop impact and saturation overland flow. However, the model does not simulate saturation excess runoff from perched aquifers which develop over a time scale greater than a single event. The model is effective at a hillslope or small watershed scale with time increments of one minute. EUROSEM is a distributed parameter erosion model linking homogeneous units or cells by a series of cascading planes and channels.

Rainfall is input into the model as a depth (mm) for each time step during a storm. The model can then calculate rainfall intensity (mm/hr), and rainfall volume ( $m^3$ ). The cumulative rainfall amount (m) received in a storm is also recorded. The following simple relationship determines the division of rainfall between that which is strikes the vegetation cover and that which falls directly on open ground or through the vegetation canopy

$$IC = R_d(COV) \quad [4.18]$$

Where

$IC$  = depth of rainfall intercepted by the vegetation (m)  
 $R_d$  = rainfall depth (m)  
 $COV$  = percentage cover over the vegetation

The infiltration process is modeled by the hydrologic component of EUROSEM, KINEROS. The infiltration equation used is the following:

$$f_c = K_s \frac{\exp(F/B)}{\exp(F/B) - 1} \quad [4.19]$$

Where

$f_c$  = infiltration capacity (cm/min)  
 $K_s$  = saturated hydraulic conductivity (cm/min)  
 $F$  = cumulative infiltration depth (cm)  
 $B$  = water deficit parameter of the soil

And

$$B = G(\theta_s - \theta_i) \quad [4.20]$$

Where

$\theta_s$  = maximum water content of the soil (cm<sup>3</sup>/cm<sup>3</sup>)  
 $\theta_i$  = initial water content of the soil (cm<sup>3</sup>/cm<sup>3</sup>)  
 $G$  = the effective net capillary drive

Infiltration is modeled through a single soil layer in three stages. At the onset of rainfall the infiltration rate is equal to the rainfall rate. Once the infiltration capacity has been reached which is equivalent to the time of ponding, the infiltration rate is then a function of the infiltration capacity as described by Equation [4.19]. Finally, once the rain drops below the infiltration capacity, the infiltration is modeled based on the percentage of ground covered by water. This is determined based on the roughness of the soil surface.

EUROSEM takes into account the effects of rock fragments and vegetation cover on infiltration. Rock fragments on the surface help preserve soil structure and protect the soil from erosion while promoting infiltration. Rock fragments imbedded in the

soil surface however, create a surface seal that reduces infiltration rates, promoting runoff and soil erosion. The percentage of vegetation cover is also used to determine the infiltration capacity since vegetation will modify the saturated hydraulic conductivity of bare soil.

The soil surface roughness determines the volume and the velocity with which overland flow moves over the soil surface thus affecting erosion rates. The Manning's Equation (see Equation [4.4]) is used in EUROSEM to describe the mean velocity of shallow overland flow due to its ability to take into account the soil surface roughness and the increased roughness due to vegetation and rock fragments.

Surface runoff occurs when the rainfall rate exceeds the infiltration capacity and the depression storage is satisfied. Surface runoff is routed over the soil surface using the Kinematic Wave Equation developed for interrill or rill flow. This equation is used in other models such as WEPP since it has been shown to be a valid approximation for most overland flow cases (Flanagan and Nearing, 1995). Solving the Kinematic Wave Equation requires the use of a four-point implicit finite difference grid. The upslope boundary conditions at  $x=0$  and  $t=0$  is either zero or equal to the depth of runoff from an upslope contributing plane.

EUROSEM models detachment by raindrop impact and overland flow. Soil detachment by raindrop impact is calculated using the following equation:

$$DET = k(KE)e^{-bh} \quad [4.21]$$

Where

$DET$  = soil detachment by raindrop impact ( $\text{g/m}^2$ )

$k$  = an index of detachability ( $\text{g/J}$ )

$KE$  = kinetic energy of the rainfall ( $\text{J/m}^2$ )

$b$  = constant

$h$  = depth of the surface water layer ( $\text{mm}$ )

The soil detachability values are provided by the model developers and are based on soil texture. A working value of 2.0 is adopted for the exponent  $b$  since insufficient experimental evidence exists to define the relationship between  $b$  and the soil texture, though the relationship is believed to exist (Morgan *et al.*, 1998). Equation [4.21] shows that as the water depth increases, the soil detachment by raindrop impact decreases exponentially.

Soil detachment by runoff assumes that the two opposing processes of erosion and deposition determine the sediment transport capacity concentration of the flow. Thus, the ability of flowing water to erode additional material is a function of the energy expended by the flow and independent of the amount of material it is carrying. The EUROSEM model developers conclude however, that the detachment of particles by overland flow and the initiation of particle movement caused by grain shear velocity and turbulence within the flow support this theory. The general equation for soil particle detachment by flow and the deposition during flow is shown in Equation [4.22].

$$DF = \beta w v_s (T_C - C) \quad [4.22]$$

Where

- $DF$  = net detachment rate of flow ( $\text{m}^3/\text{s}/\text{cm}$ )
- $w$  = width (cm)
- $v_s$  = settling velocity (m/s)
- $T_C$  = transport capacity of the flow
- and all other variables are defined above.

The cohesion that is present in most soils and reduces the rate that soil is separated from the soil mass is accounted for by  $\beta$  in Equation [4.22]. When detachment is occurring ( $DF$  is positive or  $T_C$  is greater than  $C$ ),  $\beta$  is less than 1.0.



$$\beta = 0.79e^{-0.85J} \quad [4.23]$$

Where

$J$  = cohesion measured under saturated conditions (kPa)  
and all other variables are defined above.

For values of  $J$  less than 1.0,  $\beta$  is assumed to be 0.335; however, when  $J$  is greater than 1.0,  $\beta$  is reduced exponentially.

The transport capacity of rill flow is modeled as a function of stream power while the transport capacity of interrill flow is modeled as a function of modified stream power. In rills when particles range in size from 50  $\mu\text{m}$  to 150  $\mu\text{m}$  the transport capacity is expressed as shown in Equation [4.24] where the streampower is a function of flow velocity and slope only.

$$T_C = c(\Omega - \Omega_{cr})^\eta \quad [4.24]$$

Where

$\Omega$  = unit stream power (cm/s)

$\Omega_{cr}$  = critical unit stream power (0.4 cm/s)

$c$  and  $\eta$  = experimentally derived coefficients depending on particle size

and all other variables are defined above.

The relationships used to describe  $c$  and  $\eta$  are based on the median grain size of the soil material. The relationships are limited to particle sizes between silt and coarse sand, slopes from 1 % to 12 % and discharges from 2  $\text{cm}^3/\text{cm/s}$  to 100  $\text{cm}^3/\text{cm/s}$  and sediment concentrations of 0.32. The sediment concentration of 0.32 is noted to be the upper limit beyond which any increase in stream power does not increase the amount of sediment in the flow (Morgan *et al.*, 1998). The authors also suggest that the equation will not be valid for low stream power as indicated by the critical value of 0.4 cm/s.

Like rill transport capacity, the interrill transport capacity relationship used by EUROSEM is based on a relationship fitted to particle sizes between 33  $\mu$  and 390  $\mu$ , described as:

$$T_C = \frac{b}{\rho_s q} \left( (\omega_e - \omega_{cr})^{0.7/n} - 1 \right)^n \quad [4.25]$$

Where

- $n = 5$
- $\omega_e$  = effective stream power (cm/s)
- $\omega_{cr}$  = critical stream power (cm/s)
- $b$  = a function of median particle size  
and all other variables are defined above.

The modified or effective stream power  $\omega$ , and the critical stream power  $\omega_c$ , are based on the work of Bagnold (1966) where

$$\omega_e = \frac{\Omega^{1.5}}{h^{2/3}} \quad [4.26]$$

$$\omega_c = \frac{(0.5 v_{*c}^2)^{3/2}}{h^{2/3}} \quad [4.27]$$

And

$$v_{*c} = \sqrt{Y_c (\rho_s - 1) g d_{50}} \quad [4.28]$$

Where

- $Y_c$  = modified Shield's critical shear velocity based on particle Reynold's number
- $v_{*c}$  = critical flow velocity (m/s)  
and all other variables are defined above.

Finally in order to calculate the rate of erosion per unit length of flow  $e$ , (introduced in Equation 4.17), the solution to the Kinematic Wave Equation for  $Q$ ,  $A$ ,  $u$  and  $C$  at

each finite difference node plus the upstream condition of  $C$  ( $C_{i=0}$ ) allows explicit solution of the sediment continuity equation (Equation [4.16]).

#### **4.4 Other Erosion Simulation Models**

The trend in erosion modeling has evolved from simply determining sediment detachment rates. The main purpose of describing the erosion process in agricultural settings is to determine the fate of nutrients such as nitrogen and phosphorus as well as pesticides while estimating soil productivity. Therefore, many of the agriculture simulation models have erosion modules, often based on the empirically derived equations of the USLE, MUSLE and RUSLE, which provide the means of evaluating non-point source pollution. Models such as WEPP, GUEST and EUROSEM with erosion and deposition estimation as the primary output and based on fundamental physical principles are preferable for mining erosion prediction. However an overview of some of the erosion prediction models available are provided in Sections 4.4.1 through 4.4.12.

##### **4.4.1 Agricultural Nonpoint Source Pollution (AGNPS)**

AGNPS was originally developed as a distributed parameter model for event based cases for fields of up to 20,000 ha (Young *et al.*, 1987). The runoff simulations are based on the Soil Conservation Service Curve Number method and the sediment components of simulated erosion using both the USLE and sediment transport analysis based on Bagnold's Equation (Bagnold, 1966).

##### **4.4.2 Areal Non-Point Source Watershed Environment Response Simulation (ANSWERS)**

The original ANSWERS (Beasley *et al.*, 1980) model was developed as an event-based, distributed parameter, planning model to evaluate the effects of Best Management Practices (BMPs) on surface runoff and sediment loss from agricultural

watersheds of up to 10,000 ha in size (Yulianti, 1996; Bhuyan *et al.*, 2002). BMPs included conservation tillage, ponds, grass waterways and tile drainage systems (Beasley *et al.*, 1980). The original ANSWERS model simulated runoff, as overland flow, subsurface flow and channel flow. The infiltration component was based on Holtan's Equation (1961). The sediment yield component consisted of separate routines for soil detachment by raindrop impact and overland flow, based on work by Meyer and Wischmeier (1969). The sediment transport was based on the modified Yalin Equation (Yalin, 1963; Evans *et al.*, 1991). In the late 1980's, the model was modified, incorporating capabilities to model nitrogen and phosphorus transport (Bouraoui and Dillaha, 1996).

The current version, ANSWERS-2000 (Bouraoui and Dillaha, 1996), is a continuous simulation model containing nutrient sub-models and improved soil moisture and plant growth components. This continuous simulation version relies on the Green-Ampt infiltration equation to aid in runoff prediction, but maintains the original sediment yield and sediment transport relationships. The major feature of this model now is its ability to simulate the transformations and interactions between the nitrogen pools.

ANSWERS is classified as a topographic evolution model by Evans *et al.* (1991) and is thought appropriate for predicting soil erosion from rehabilitated slopes. Topographic evolution models provide information on the long-term morphological development of a surface subject to erosion processes. Since it is possible to map the variation in soil erosion, sedimentation and runoff patterns with time, ANSWERS provides information regarding where drainage problem areas may occur (including rills and gullies) indicating locations where control measures may be necessary (Evans *et al.*, 1991). This feature is attractive to the mining industry when meeting regulatory requirements for erosion control is required for permitting. Evidence from the literature suggests that the ANSWERS model provides estimates of erosion

on mine soil with about the same accuracy as it does for agricultural soils (Sheridan *et al.*, 2000a).

#### **4.4.3 Chemicals, Runoff and Erosion from Agricultural Management Systems (CREAMS)**

The CREAMS model (Knisel, 1980) is a lumped, process-based model developed by the USDA for the prediction of runoff, erosion and chemical transport in field-sized plots (Laflen, 1994). It can operate on an event basis, utilizing breakpoint precipitation data, or it can be run under short-term continuous simulation conditions (2 – 50 yrs) (Knisel, 1980).

The three components of the CREAMS model (hydrology, erosion and chemical migration) utilize the following methods for developing the information required of each. Depending on the time scale, the hydrology component simulates runoff by either utilizing daily rainfall data and the modified Soil Conservation Service (SCS) Curve Number (CN) Method or by using hourly breakpoint data and the Green-Ampt Infiltration Equation (Knisel, 1980). The erosion component can simulate erosion and sediment yield. The erosion estimates are based on elements of the USLE equation (Knisel, 1980) and the estimate of transport capacity is based on the Yalin equation (Yalin, 1963). Using the daily flows generated in the hydrology component and the soil loss from the erosion component, the chemical component simulates the transformation and movement of nutrients and pesticides (Yulianti, 1996). The nutrient component uses enrichment ratios to estimation the proportion of nitrogen and phosphorus that is transported by the sediment and the pesticide component incorporates interception, degradation and transport by runoff as well as adsorption, desorption and degradation in the soil (Knisel, 1980). The major limitations of the CREAMS model include the model complexity and large data requirements as well as its reliance on the modified USLE relationships and parameters.

Several of the equations developed for the CREAMS model have been used in other runoff and erosion models including the Simulator for Water Resources in Rural Basins (SWRRB) and WEPP. As a result, when choosing an erosion simulation model to be used in mine waste erosion prediction, the complexity of the CREAMS model as well as its redundancy make some of the other models more suitable.

#### **4.4.4 Erosion Productivity Impact Calculator (EPIC)**

Predicting impacts of erosion on soil productivity requires not only the ability to predict soil erosion rates and the associated changes in soil quality, but also the crop response to soil quality (El-Swaify and Fownes, 1989). The erosion and soil productivity relationships determined by EPIC, are designed to represent all situations in the entire United States (Bhuyan *et al.*, 2002). The EPIC model can be interfaced with economic models to quantify the costs of soil erosion and benefits of soil erosion research and control in the United States (Meinardus *et al.*, 1996).

The EPIC model can estimate erosion caused by water as well as erosion caused by wind (Yulianti, 1996). It was originally designed to run on an event basis for watersheds of approximately one hectare (Yulianti, 1996; Favis-Mortlock, 1998). As a lumped model, EPIC assumes that the watershed or area being modeled is a homogeneous unit in topography and soil (Favis-Mortlock, 1998). Though the EPIC model is a lumped model, it is a complex, comprehensive model that requires large amounts of data to run (El-Swaify and Fownes, 1989). It consists of physical and chemical process based components including nutrient cycling and pesticide migration and can now be run on a continuous basis, simulating the erosion process at a daily time step. Surface runoff is predicted using the SCS Curve Number Method and soil loss and sedimentation due to sheet and rill erosion are estimated using a choice of the USLE, the MUSLE or several other empirical models (Bhuyan *et al.*, 2002).

#### **4.4.5 Kinematic Runoff and Erosion Model (KINEROS)**

The KINEROS model (Smith *et al.*, 1995) is an event-based, distributed parameter model describing the processes of interception, infiltration, surface runoff and as optional features, upland erosion and sediment transport from small agricultural and urban watersheds (approximately 760 ha). Using finite difference techniques, the partial differential equations for channel flow, overland flow, erosion and sediment transport are solved while accommodating the spatial variation in rainfall, infiltration, runoff and erosion parameters. Since the EUROSEM model is linked to the KINEROS model, much of the theory used in the KINEROS model has been described in Section 4.3.3. Since there are many sediment transport relationships available in the literature and most have been developed and tested for streams and flumes rather than overland flow conditions, several sediment transport relationships have been provided to the user in the KINEROS model package. The difference between the KINEROS model and most erosion models is that the KINEROS model allows soil and sediment to be characterized by up to five particle size classes rather than a single median particle size. Finally sediment routing through detention structures is another feature provided in the KINEROS model (Smith *et al.*, 1995).

Since the KINEROS hydrologic model has been successfully linked to the EUROSEM soil erosion model, it is recommended that soil erosion modeling on an event basis for the mining industry be conducted using the EUROSEM model.

#### **4.4.6 Kentucky Erosion Model (KYERMO)**

The KYERMO model (Hirschi and Barfield, 1988) is a physically based, event oriented erosion prediction model developed as a research tool to isolate the aspects of the rainfall/runoff/erosion process. It was developed specifically to aid in erosion prediction on steep slopes given that knowledge of the rill pattern and density can be used to set up the model.

KYERMO is based on four components: a runoff generation component, a runoff routing component, a sediment generation component and a sediment routing component. The runoff generation component consists of a surface storage calculation routine, an infiltration routine and a runoff calculation routine. The surface storage is determined based on the plot slope and the random roughness. The infiltration routine is based on an extension of the Green-Ampt Mein Larson model, which includes a two-layered soil system rather than the single layered system upon which the model was originally developed. Rather than allowing runoff to occur once the surface storage is filled, the KYERMO model allows surface runoff to occur while the surface storage is filling.

The runoff routing component of the flow within each rill is calculated on a smaller time step than the model itself to maintain stability. This routine calls an additional routine that does the actual flow routing using the Kinematic Wave Equation based on a four-point implicit finite difference method. The quantities calculated from the Kinematic Wave Equation are then passed on to another routine that calculates the depth of flow within the rills (Hirschi and Barfield, 1988).

Once the flow conditions have been established, the sediment generation component determines sediment availability based on raindrop detachment, rill flow detachment, rill wall sloughing, and change of the rill channel cross section caused by detachment (Hirschi and Barfield, 1988). Finally the sediment routing component calculates transport and deposition for both interrill and rill flow. Two different sediment transport equations are provided. One is based on a modification to the Yalin (1963) Equation which is essentially a shear excess equation. The other is based on distributing the sediment transport among particle sizes.



Many of the features of the KYERMO model are also available in the other erosion prediction models such as WEPP. Since KYERMO was developed for a localized area, the WEPP model is a more suitable choice for erosion prediction due to its versatility.

#### **4.4.7 Limburg Soil Erosion Model (LISEM)**

The LISEM model was originally developed for the Province of Limburg in the Netherlands. It is a physically based, distributed parameter, runoff and erosion model that simulates hydrology and sediment transport during and immediately after a single rainfall event in a small catchment (10 – 300 ha) (Jetten, n.d.). The model incorporates rainfall, interception, surface storage in micro-depressions, infiltration, vertical movement of water in the soil, overland flow, channel flow (in man-made ditches), detachment by rainfall and throughfall, transport capacity and detachment by overland flow. The impact on hydrological and soil erosion processes of compaction due to tractor wheels and surface sealing has recently been added to the models' capabilities. In addition, the fate of nitrogen and phosphorus, multiple sediment classes for erosion and deposition as well as the incision and formation of gullies have also been incorporated.

LISEM uses breakpoint data to describe each storm event and then routes water using a four point finite difference solution of the Kinematic Wave Equation over each grid cell. Routing takes place after infiltration has been taken into account and there are five choices of infiltration models available in LISEM. The choice of the infiltration model depends on data availability and the experience of the user. However, each infiltration model provides a different outcome and re-calibration is recommended when a different infiltration model is used. Erosion modeling is identical to the detachment equations used in EUROSEM (Morgan *et al.*, 1998). Like many erosion models, the transport capacity concentration is assumed to be a balance between the continuous erosion process and deposition (Foster, 1982).

LISEM is a suitable choice for mine waste sites undergoing gully erosion due to the ability of the model to account for such severe processes.

#### **4.4.8 Modeling Within-Storm Sediment Dynamics (MWISED)**

The MWISED project is currently under development by a research team comprising six countries in Europe. The project mandate is to develop a fully dynamic model able to take into account the changes that happen in the landscape within an individual event as required to simulate the effects of a major erosive storm. This model could then be used as a stand-alone conservation tool or incorporated into continuous simulation modeling tools. Predicting where ephemeral gullies will form in the landscape within an individual event is a priority research area of within-storm modeling of erosion to be achieved by MWISED (European Commission, 2001).

The project developers conclude that models such as WEPP, GUEST and CREAMS depend on assumptions of steady-state conditions within a storm. In reality, these conditions are only achieved for very short periods. EUROSEM, with the use of the KINEROS, a dynamic hydrologic model, is very similar to the structure of MWISED; however, it does not incorporate the formation of ephemeral gullies. In addition, only a few models simulate rill erosion separately from interrill erosion (e.g. EUROSEM and WEPP); however, these models require the user to specify whether rills will occur and the frequency of rill occurrence in the landscape. The MWISED model should be able to determine rill generation and development determining the associated extent of erosion. Since some models can now be linked with Geographic Information Systems (GIS) and Digital Terrain Models (DTMs), it may be possible to determining where in the landscape these features occur (European Commission, 2001).

Due to the early stages of model development and apparent research purpose that the MWISED project provides, it does not provide any additional features for mining industry applications. As a result, the models that are currently available, namely EUROSEM and WEPP will provide acceptable results for the estimation of erosion of mine waste.

#### **4.4.9 Productivity Index (PI)**

Like EPIC, PI (Pearce *et al.*, 1986) has been used to estimate the relative productivity of different soils (El-Swaify and Fownes, 1989). The model is simple and logical, requires modest amounts of data and can easily accommodate additional input variables. The permissible soil losses and long-term erosion productivity impacts can be utilized in conservation planning.

#### **4.4.10 RillGrow 1 and 2**

RillGrow 1 and 2 are research models that attempt to determine the pattern of rill initiation and development on initially unrilled surfaces without user specification of rill spacing and width (Favis-Mortlock, 2002). RillGrow 1 uses initial data on micro-topography and the preferential paths of overland flow are then developed, causing erosion and a more defined pathway for subsequent flow. This positive feedback loop then generates the pattern for rill development at a local scale. RillGrow 2 uses the same information on micro-topography to determine the initiation of rills on unrilled surfaces, but also contains simple routines for developing flow and sediment transport characteristics.

In combination with one of the models recommended for the use in erosion prediction of mine waste sites, RillGrow 1 and RillGrow 2 will be beneficial in that the user will not have to specify the spacing and depth of rills prior to modeling. However, until

such time as the models are interfaced, RillGrow1 and RillGrow 2 do not demonstrate any practical use in the mine waste erosion prediction.

#### **4.4.11 Water and Tillage Erosion Model (WATEM)**

WATEM is an extended version of the USLE2D with the additional capacity to model deposition and tillage processes (Katholieke Universiteit Leuven, 2002). It is similar to the more sophisticated computer packages such as WEPP and EUROSEM in that it focuses on the spatial rather than the temporal distribution of erosion parameters. WATEM is a distributed parameter model that relies on an adapted version of the RUSLE since parameter values are readily available for the United States. The main difference between WATEM and many other erosion models particularly the RUSLE upon which it is based, is that it incorporates the effects of the direct movement of soil by tillage on soil erosion on agricultural land. The tillage component incorporates the intensity of the tillage process for different implements.

Like many of the models described in this section, the WATEM model was designed for application on agricultural land. As a result, the WEPP and EUROSEM models to which the WATEM model has been likened are superior choices in erosion prediction of mine waste material.

### **4.5 Summary**

Table 4.1 provides a summary of the models currently available for water erosion prediction. Column provides the model name as an acronym. Columns 2, 3 and 4 indicate whether each model computes runoff, is a distributed parameter or lumped model or can be run under continuous simulation and/or event based conditions. Column 5 provides a rating, which determines the applicability of the model to the mining industry. The rating system ranges from 1 to 7. The WEPP model is the

only highly recommended model receiving a rating of 1. Those models that received a rating of 2 have features that are unique or features that are considered desirable. For example, LISEM can model the gully erosion processes that may be advantageous to severely eroded mining cases. GUEST and EUROSEM are versatile physically based models, but can only be used in event mode. The RUSLE model received a rating of 3, since although it is still part of the USLE family of models, it does have some provisions built into it for the mining industry in particular. Those models with a rating of 4 have features that can be found in other more robust models. A rating of 5 indicates that the model should not be used due to a large number of limitations and a rating of 6 was given to those models that were not reviewed.

**Table 4.1 Erosion Model Summary**

MODEL	RUNOFF	DISTRIBUTED /LUMPED	CONTINUOUS /EVENT	MINE WASTE EROSION PREDICTION RATING*
ACTMO	Y	D	C	6
AGNPS	Y	D	C	4
ANSWERS	Y	D	C	2
ARM/HSP	Y	D	C	6
CREAMS	Y	L	C/E	4
EPIC	Y	L	C/E	5
EUROSEM	Y	D	E	2
GWLF	Y	D	C	6
GUEST	Y	D	E	2
HSP	Y	D	C	6
KINEROS	Y	D	E	4
KYERMO	Y	D	E	4
LANDRUN	Y	D	C/E	6
LISEM	Y	D	E	2
MWISED	Y	D	E	4
MUSLE	N/A	N/A	N/A	5
PRMS	Y	D	C	6
PI	N/A	N/A	N/A	5
PROPRIL	Y	D	E	6
RILLGROW 1 & 2	N/A	L	N/A	5
RUSLE	N/A	N/A	N/A	3
SEDEC	N	D/L	C	6
SEDIMOT	Y	D	E	6
SOILEC	N	D/L	C	6
SWMM	Y	D	C/E	6
USLE	N/A	N/A	N/A	5
RUNOFF	Y	D	E	6
WATEM	Y	D	E	4
WEPP	Y	D	C/E	1

1 - Highly Recommended

2 - Recommended

3 - Recommended for quick, conservative estimates

4 - Features available are available in other more highly recommended models

5 - Not Recommended

6 - Not Reviewed

## CHAPTER 4 – LIST OF SYMBOLS

	SYMBOL	DESCRIPTION
	$A_{sl}$	annual soil loss
	$R$	rainfall erosivity factor as an erosion index $EI_{30}$
	$E$	total storm energy
	$I_{30}$	maximum 30-minute rainfall intensity
	$K$	soil erosivity factor
	$LS$	topographic factor
	$CP$	cover, management and support practices factor
	$S_y$	sediment yield
	$V$	runoff volume
	$q_p$	peak discharge rate
	$R_e$	rainfall excess
	$P$	rainfall rate
	$I$	infiltration rate
	$Q$	runoff rate per unit area
	$q$	flux at a distance $x$ from the top of a
plane		
	$L$	plane length
	$K_p$	coefficient depending on length, slope and roughness of the planar surface
	$t$	time
	$H$	fractional shielding
	$m_d$	actual mass present per unit area of deposited layer
	$M_p$	mass per unit area of deposited
sediment		
	$W_r$	average rill spacing
	$A$	cross sectional area of the flow
	$v$	flow velocity
	$n$	Manning's roughness factor
	$R_h$	hydraulic radius
	$S$	slope
	$\tau$	flow shear stress
	$\Omega$	stream power in rill areas

$\Omega_{cr}$	critical stream power in rill areas
$\beta$	soil erodibility parameter
$\phi$	deposition rate
$v_s$	settling velocity of a typical size class
$i$	total number of size classes that the soil can arbitrarily be placed
$c_t$	sediment concentration at the transport limit
$F_c$	fraction of excess stream power
$\rho$	density of water
$\sigma$	sediment density
$c_t$	sediment concentration at the transport limit
$W_b$	width of the rill
$D$	depth of flow
$g$	acceleration due to gravity
$\beta$	erodibility parameter
$c$	actual sediment concentration
$\bar{c}_t$	average sediment concentration at the transport limit
$Q_e$	effective runoff rate
$\beta_e$	effective soil erodibility
$A$	cross-sectional area of the flow
$C$	sediment concentration
$e$	net detachment rate
$q_s$	external input/extraction of sediment per unit length of flow
$x$	horizontal distance
$t$	time
$IC$	depth of rainfall intercepted by the vegetation
$R_d$	rainfall depth
$COV$	percentage cover over the vegetation
$f_c$	infiltration capacity
$K_s$	saturated Hydraulic Conductivity
$F$	cumulative infiltration depth
$B$	soil water deficit
$\theta_s$	maximum water content of the soil
$\theta_l$	initial water content of the soil
$G$	the effective net capillary drive
$DET$	soil detachment by raindrop impact
$k$	an index of detachability



$KE$	kinetic energy of the rainfall
$b, c$ and $\eta$	constant
$h$	water depth
$DF$	net detachment rate of flow
$w$	width
$T_C$	transport capacity of the flow
$J$	cohesion measured under saturated conditions
$\omega_\varepsilon$	unit stream power in interrill areas
$\omega_{cr}$	critical unit stream power in interrill areas
$Y_c$	modified Shield's critical shear velocity based on particle Reynold's number
$v^*_c$	critical flow velocity

## **5. WATER EROSION PREDICITON PROJECT MODEL: OVERVIEW**

The WEPP model is considered to be one of the most appropriate erosion prediction tools for the mining industry. It has been advertised as a robust model, suitable for estimating runoff, soil loss and sediment yield under continuous simulation conditions and on an event basis for a variety of erosion applications. Predicting erosion under continuous simulation conditions is important for long-term mine operation as well as for closure and post-closure estimates of soil loss from mine waste slopes. The erosion may be predicted on bare, mine waste or closure cover conditions. Current erosion theory recognizes that most erosion takes place during two or three significant storm events per year (Morgan *et al.*, 1998). As a result, event based erosion prediction also provided by the WEPP model, will be important for day-to-day mine erosion control. The following chapter provides a description of the WEPP model including its advantages and limitations especially related to mining applications. Chapter 6 provides the details for determining WEPP input parameters outlining key issues for setting up an erosion monitoring and prediction program both in the field and the laboratory. Chapter 6 also provides the results of a sensitivity analysis using the WEPP model for a mine site in South East Asia.

### **5.1 Background**

The United States Department of Agriculture, Agricultural Research Service (USDA-ARS) initiated the planning and development of the WEPP model in 1985 (Lane *et al.*, 1989). The project team consulted specialists in a number of disciplines in efforts to develop an erosion prediction tool that would be applicable to a range of erosion environments (Laflen and Schertz, 1990). Such environments include farmlands, rangelands, disturbed forests and urbanized areas as well as construction sites (Laflen *et al.*, 1997; Yu *et al.*, 2000). It was intended that the WEPP Hillslope model would replace the widely used and heavily relied upon USLE and the RUSLE

(Yu *et al.*, 2000) by offering “a new generation of water erosion prediction technology” (Nearing *et al.*, 1989:1587).

During the development of the WEPP model, it became clear that there are two degrees of complexity at which erosion modeling takes place. The Hillslope version of WEPP released in 1989 is designed to model single field-scale plots (Lane *et al.*, 1989). The Watershed version of the WEPP model, released in 1995, links hillslope profiles to channels and impoundments allowing for more complexity when analyzing small watershed situations (Flanagan and Nearing, 1995). It is important to note that the Watershed version is interfaced with the Hillslope version to calculate runoff, erosion and deposition and the Hillslope version provides the interface for displaying spatial erosion results.

Between 1989 and 1995 rigorous testing and validation of the model took place, largely for agricultural and forestry applications in the United States (Laflen *et al.*, 1997). According to the literature, limited international validation of the WEPP Hillslope model has taken place with some testing conducted in Australia and Europe (Nearing *et al.*, 1998; Yu *et al.*, 2000). Since 1995, there have been several re-releases for both the Hillslope and Watershed versions of the WEPP model.

The new technology as developed for WEPP aims to provide a more fundamentally driven, process-based approach to erosion prediction by calculating erosion from the mechanisms of detachment and transport (Laflen *et al.*, 1997). The WEPP model is capable of predicting soil loss along and sediment yield and deposition at the toe of complexly shaped hillslopes (Nearing *et al.*, 1990), providing sediment size information as well as spatially and temporally based distributions of erosion (Tiwari *et al.*, 2000). Sediment yield and deposition rates can be calculated under both continuous simulation conditions at a daily time step or event based conditions (Nearing and Nicks, 1998). These capabilities are not available for the USLE or the

RUSLE which provide at best, an annual, average, net soil loss (Nearing and Nicks, 1998).

## **5.2 Scope and Application**

It is expected that the current users of the USLE and the RUSLE will use the WEPP model. Such user groups include conservation project planners, resource managers and engineers as well as farmers (Lane *et al.*, 1989; Laflen *et al.*, 1997). WEPP has been developed for use primarily in the agriculture and forestry industries. Calibration and validation has taken place in these contexts resulting in suggested ranges of input parameters that apply to both industries. The WEPP model was not developed for use in the mining industry and as a result, there are no published validations of the model in this context. However, several consultants have used the model for erosion estimates in ongoing projects primarily related to coal mining (Laflen, 2002).

The WEPP technology attempts to answer such questions as, what is the probability that a contractor can complete a construction job with no erosive events? Or, what are the probabilities that a sedimentation pond will fill with sediment in a given period of time? The answers to questions of this nature have become increasingly more sought after when realizing that onsite sediment deposition and sediment delivery offsite may be more relevant to mining regulatory agencies and project managers than simply soil particle detachment (Laflen *et al.*, 1997).

## **5.3 Model Structure**

The Hillslope and Watershed versions of the WEPP model incorporate several modules for modeling the erosion process. A flow chart linking the modules is provided in Figure 5.1 to aid in the discussion that follows.

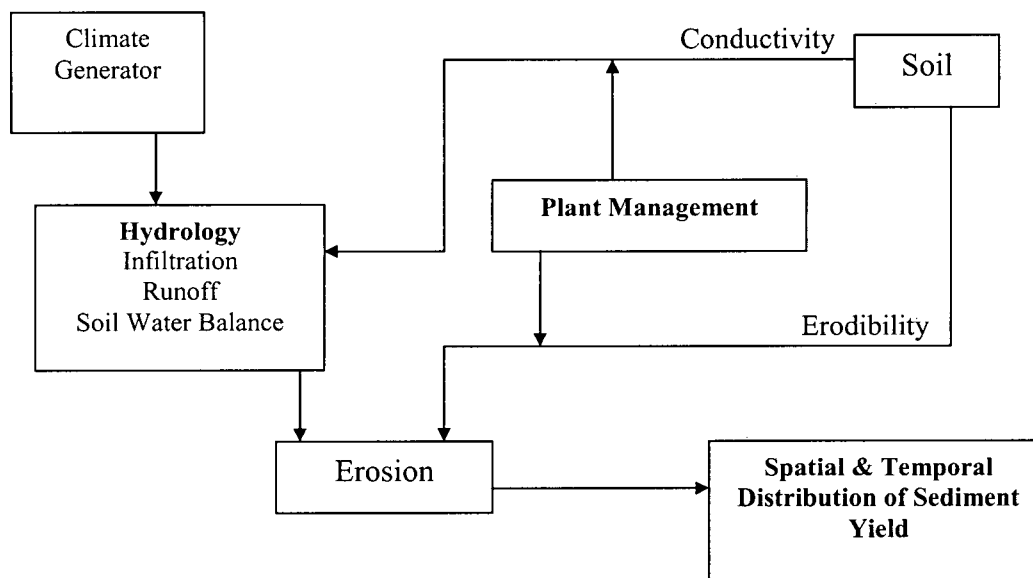


**Figure 5.1 WEPP Model Structure (Modified from Flanagan and Nearing, 1995)**

A detailed description of the modules of the WEPP model can be found in the *WEPP Technical Documentation* (Flanagan and Nearing, 1995). A summary of the input files including appropriate ranges of input parameters is provided in the *WEPP User Summary* (Flanagan and Livingston, 1995). The Hillslope version rather than the Watershed version of the WEPP model was determined in this work to be the most appropriate for modeling mining scenarios. The engineered slopes of mine waste sites are generally uniform, comprising uncomplicated topography and the Hillslope version of the WEPP model introduces the least complexity when defining the problem. As a result, some of the key elements of each of the WEPP Hillslope version modules are outlined below with particular emphasis on applying the model to mining erosion situations.

### 5.3.1 Climate Generation

The driving force behind the water erosion process is the climatic conditions. There are two climate data file formats recognized by the WEPP model and each is adopted depending on data availability. The first technique involves the use of a stochastic weather generation program called CLIGEN that is initiated by, but run separately from WEPP (Baffaut *et al.*, 1995). CLIGEN uses data acquired from weather stations in the United States to randomly generate representative climate data for either long-term continuous simulations or single storm events. The second technique requires the user to generate a breakpoint data file that can be read by WEPP and used in subsequent calculations. The breakpoint data file option is generally used when the project climatic conditions are outside the CLIGEN database.

CLIGEN was developed to be used with the WEPP model, but is based on the principles of the climate generators found in EPIC (Williams, 1995) and the Simulator for Water Resources in Rural Basins (SWRRB) (Arnold and Williams, 1995). However, CLIGEN also contains algorithms to estimate rainfall intensity distributions, which are not included in many other climate models (Flanagan and Nearing, 1995). Historical daily, hourly and 15-minute data were obtained from the National Climate Data Center for the United States. After data compilations were complete, 7000 climate stations had data for precipitation or precipitation and temperature for a minimum 25-year record. Of these 7000 stations, 1200 stations with both precipitation and maximum and minimum temperature were selected for statistical parameterization based on a one-degree latitude by one-degree longitude grid over the entire country (Flanagan and Nearing, 1995). Data such as solar radiation and dew point temperature were then calculated for each of the stations to complete the database. Data were also compiled for Alaska, Hawaii, the US Pacific Islands and Puerto Rico (Flanagan and Nearing, 1995).

Using monthly statistical parameters such as mean, standard deviation and skew coefficient of, for example, precipitation amount, CLIGEN will generate a daily sequence of simulated, representative, weather for as many years as desired by the user. CLIGEN also has the capacity to generate weather data for a single event based on user defined storm amount, storm duration and maximum intensity. Under continuous simulation or event based conditions the CLIGEN output file then contains values for the following parameters (Baffaut *et al.*, 1995):

- precipitation amount;
- storm duration;
- peak storm intensity;
- time to peak intensity;
- maximum and minimum temperature;
- wind speed and direction;
- solar radiation;
- relative humidity; and
- dew point temperature.

Under continuous simulation conditions, the storm data from the CLIGEN output file is then disaggregated by WEPP into simple single-peak storms that can be used by the infiltration and runoff modules of the WEPP model (Lane *et al.*, 1989). However, when the single storm option is chosen, the single-peak storm is used directly by the infiltration and runoff components of the model without further manipulation.

Since the CLIGEN program requires access to extensive statistical climate information in order to generate the climate files used by WEPP, it works well for mine sites located in areas like the United States where the period of record is long and relatively complete. Problems generating climate files useful to WEPP for mine sites located in other areas of the world, particularly in developing countries, can

potentially be overcome by the second technique whereby breakpoint precipitation data are used (Zeleeke *et al.*, 1995).

A file representing breakpoint data contains two columns. The cumulative time from the beginning of the storm is in the first column and the average rainfall intensity over the time interval between successive times is in the second column (Flanagan and Livingston, 1995). Though this method uses actual data collected from a weather station, it has conventionally been generated by hand, a laborious and often error prone process. Unlike CLIGEN, which can generate climate files for any desired length of time, breakpoint data files are limited in that the model simulation cannot exceed the period represented by the data file. This method is often used for single-event modeling or short-term modeling when the data to construct the climate files are available.

In order to overcome the laborious nature of developing breakpoint precipitation files, a program called Breakpoint Climate Data Generator (BPCDG) has been developed (Zeleeke *et al.*, 1995). BPCDG automates the process of creating breakpoint data files in the format recognized by WEPP from standard rain gauge data and other daily weather data sets of any meteorological station (Zeleeke *et al.*, 1995). As long as the mine site for which the WEPP model simulation is being developed has a reliable weather station, developing climate files for the WEPP model can be undertaken.

### **5.3.2 Winter Hydrology**

The key aspects of winter hydrology are the flow of heat into and out of the soil surface that in turn affects the changes in frost and thaw depths as well as snow accumulation and melting. The heat flux is determined based on information provided in the climate file including solar radiation, temperature and wind speed as well as information available from the management file including residue cover and



plant cover. The degree of plant cover may provide insulation and can contribute to snow accumulation and melting (Flanagan and Nearing, 1995). Soil freezing and thawing will affect the soil physical properties such as hydraulic conductivity, erodibility and soil water holding capacities.

During the continuous simulation, which is based on a daily time step, the winter hydrology module will be called if one of the following conditions occurs (Flanagan and Nearing, 1995):

- a snow pack already exists;
- a soil frost layer already exists; and
- a daily temperature is less than 0 °C.

In the continuous simulation mode, the winter hydrology module requires values on an hourly basis; however, the WEPP climate file generated by CLIGEN provides data on a daily basis. Therefore, a similar disaggregation process that is undertaken to generate the daily climate data from monthly statistical values in CLIGEN occurs, in order to provide precipitation, temperature, solar radiation and wind speed and direction for the winter processes.

The ability of the WEPP model to evaluate erosion considering a frost layer is important to conditions in many mine sites in both Canada and parts of the United States. At several mine sites, it is advantageous to keep the tailings frozen year round to reduce the influx of oxygen, thus limiting Acid Rock Drainage (ARD) production. WEPP can therefore be used to provide estimates of erosion rates of the overlying cover material while also indicating whether the underlying tailings or waste rock remain frozen.

### 5.3.3 Hydraulics of Overland Flow

Runoff, flow shear stress and flow transport capacity are each affected by soil roughness, plant cover and residue cover including rock fragments. Rougher soil surfaces or hillslopes with vegetative cover increase the soil surface resistance to flow which decreases runoff rates and flow shear stress acting on the soil while also decreasing sediment transport capacity of the flow. Thus, the friction coefficients for cropland and rangeland, rill and interrill areas are calculated in the Hydraulics of Overland Flow module. These values affect the runoff amounts used in the Hillslope Surface Hydrology module and the subsequent erosion rates calculated by the Hillslope Erosion module.

The Darcy-Weisbach friction factor for uniform flow conditions is the underlying equation used in the WEPP model to describe overland flow characteristics. Separate estimates are made for the rill and interrill areas for both cropland and rangeland conditions. In rills, the flow shear stress is partitioned into that which acts on the soil to cause detachment and that acts on exposed residue and other surface cover and does not cause detachment. If plant cover exists in a rill area, a portion of the flow shear stress will act directly on the soil to cause detachment. Therefore the total friction coefficient for rills in cropland and rangeland areas will be affected friction caused by rill surface roughness, rill surface residue, living plants and random roughness. In interrill areas, the friction factor includes factors for interrill surface roughness induced by tillage operations, surface residue cover, standing plant material and gravel and cobbles.

The total friction factor for an area is then an area weighted average of friction factors for rill and interrill areas. The total equivalent friction factor is used for overland flow routing as described in the Hillslope Surface Hydrology module in Section 5.3.4.

#### 5.3.4 Hillslope Surface Hydrology

From climate data inputs as well as antecedent moisture conditions calculated for the previous day, the Hillslope Surface Hydrology module provides the Hillslope Erosion module with the duration of rainfall excess, the rainfall intensity during the period of rainfall excess, the runoff volume and the peak discharge rate (Flanagan and Nearing, 1995). Next, the Hillslope Surface Hydrology module provides the quantity of water which infiltrates into the soil to the Water Balance and Percolation module and the Plant Growth and Residue Decomposition and Management module which can then be used to update the infiltration, runoff routing and soil erosion parameters. The Hillslope Surface Hydrology module therefore calculates the following in the order listed:

- infiltration;
- rainfall excess;
- depression storage; and
- peak discharge.

On days when rainfall occurs, infiltration is partitioned into that which enters the soil profile and that which is available for runoff as Hortonian excess (Lane *et al.*, 1989). In the WEPP model, dynamic infiltration-runoff modeling for overland flow is accomplished by using an infiltration equation that computes the infiltration rate as it varies with time from an unsteady rainfall input. This equation incorporates a routing function that transforms rainfall excess into flow depth on a flow surface (Flanagan and Nearing, 1995).

The Green-Ampt infiltration equation is widely used for modeling one-dimensional vertical flow of water into a homogeneous soil of uniform antecedent moisture content under ponded conditions (Risse *et al.*, 1993). However, scientists have often modified this equation to apply it to specific situations. One such modification is the cumulative infiltration calculation used in the WEPP model where a solution to the

Green-Ampt-Mein-Larson infiltration equation for unsteady, intermittent rainfall with multiple times of ponding as developed by Chu (1978). Here, up until ponding occurs, the rate of infiltration equals that of the precipitation rate; however, after ponding develops, the infiltration rate follows an exponential decrease until a constant or final infiltration rate is reached (Risse *et al.*, 1993). The infiltration rate for each time increment is calculated using Equation [5.1]

$$f = K_e \left( 1 + \frac{N_s}{F} \right) \quad [5.1]$$

Where

- $f$  = infiltration rate (m/s)
- $K_e$  = effective hydraulic conductivity (m/s)
- $N_s$  = effective matric potential (m)
- $F$  = cumulative infiltration depth (m)

The effective matric potential is given by

$$N_s = (\phi_e - \Theta_i) \Psi \quad [5.2]$$

Where

- $\phi_e$  = effective porosity (m/m)
- $\Theta_i$  = initial water content (m/m)
- $\Psi$  = average capillary potential across the wetting front (m)

Therefore, there are four internally adjusted soil parameters that drive the infiltration component of the WEPP model. These are the effective soil porosity, the initial water content, the capillary potential across the wetting front and the effective hydraulic conductivity. Porosity is defined as the void spaces between the soil particles and depends on bulk density (Craig, 1992). The effective porosity, calculated on a daily basis is determined to be the difference between the total porosity (with a correction for entrapped air) and the initial water content (Flanagan

and Nearing, 1995). The initial water content is obtained from the WEPP moisture balance. The importance of the wetting front is the capillary potential across the interface between the “dry” and “wet” soil and is based on soil properties. The effective hydraulic conductivity is the only user-defined parameter and is the most important parameter in WEPP erosion modeling due to the large effect it has on infiltration. Risse *et al.* (1993) report that sensitivity analyses of the Green-Ampt infiltration model show that the parameters most sensitive to infiltration and runoff amounts are the porosity and hydraulic conductivity while the capillary potential across the wetting front is less sensitive.

When the rainfall rate is greater than the infiltration rate, rainfall excess can occur; however, rainfall excess is not translated into runoff until the volume is adjusted for saturated soil conditions and depression storage (Flanagan and Nearing, 1995). Once rainfall excess is occurring, the overland flow is routed as broad uniform sheet flow in the interrill areas and concentrated flow in rills. Flow is partitioned based on the results of unsteady flow calculations and routed down the hillslope. The routing function of the dynamic infiltration-runoff model for overland flow transforms the time-intensity distribution of rainfall into the time-intensity distribution of runoff (the hydrograph) using a shallow water equation in the form of the Kinematic Wave Equation (Flanagan and Nearing, 1995). Separate methods are used depending on whether the WEPP model is run in the continuous simulation or the event based mode. Under continuous simulation conditions, peak discharge is approximated based on the Kinematic Wave Equation. However, when a single storm simulation is used, a semi-analytical solution to the Kinematic Wave Equation is used to compute the runoff hydrograph (Lane *et al.*, 1989).

### **5.3.5 Water Balance and Percolation**

The Water Balance module of the WEPP model provides estimates of water content in the soil profile and evapotranspiration losses (Flanagan and Nearing, 1995).

Taking inputs from the climate generator, infiltration information from the Hillslope Surface Hydrology module and above ground biomass amounts from the Plant Growth module, percolation and evapotranspiration are estimated at a 24-hour time step coincident with that of the climate generator.

The continuous water balance maintained by the Water Balance and Percolation module of the WEPP Hillslope model on a daily basis is provided by the following equation:

$$\Theta = \Theta_{in} + (P - I_{in}) + I_{in} - S - Q - ET - D - Q_d \quad [5.3]$$

Where:

- $\Theta$  = soil water content in the root zone in any given day (m)
- $\Theta_{in}$  = initial soil water in the root zone (m)
- $P$  = cumulative precipitation (m)
- $I_{in}$  = precipitation interception by vegetation (m)
- $S$  = snow water content (m) (+ for snowmelt, - for snow accumulation)
- $Q$  = cumulative amount of surface runoff (m)
- $ET$  = cumulative amount of evapotranspiration (m)
- $D$  = cumulative amount of percolation loss (m)
- $Q_d$  = subsurface lateral flow or flow to drain tiles (m)

This equation uses hydrologic processes such as infiltration, runoff routing, soil evaporation, plant transpiration, snowmelt and seepage linked through other modules of the model to maintain a continuous water balance.

The infiltration process as modeled by the WEPP Hillslope Surface Hydrology module is linked to the evapotranspiration and percolation in the Water Balance and Percolation module. Infiltration is added to the water content in the upper soil layer and routed through to the lower soil layers while being subjected to either evapotranspiration or percolation. The soil moisture in the upper soil layer is used as the initial conditions for infiltration in the Green-Ampt infiltration equation. Any

water that percolates through and into the layers below the root zone is considered to be lost from the model.

Using calculated values of the Leaf Area Index (LAI), root depth, total plant biomass and residue cover from the Plant Cover module and the Residue Decomposition and Management module as described in the following sections, the evapotranspiration calculations can be made for the Water Balance and Percolation module. This can then be related to the water stress factor that determines the amount of daily plant growth thus altering such parameters as evapotranspiration and affecting other modules of the model.

#### **5.3.6 Subsurface Hydrology**

Subsurface water and subsurface flow are important components of the erosion process since both affect the magnitude of runoff generated from rainfall events and provide the moisture required for plant growth and residue decomposition. The Subsurface Hydrology module of the WEPP model is concerned with the soil water in the root zone since as explained in the Water Balance and Percolation module Section above, any water that percolates below the active root zone is considered to be lost from the model.

The Subsurface Hydrology module of the WEPP model moves water in the root zone as either subsurface lateral flow or subsurface drainage. Subsurface lateral flow has been shown to be a significant contributor to surface runoff production in hillslope hydrology theory (Dunne and Black, 1970) and its contribution is described by two processes. First, in forested areas where the surface soil layer has a high hydraulic conductivity and is bounded by a lower impermeable layer, the storm water yield is dominated by subsurface lateral flow. When the flow daylights, it creates return flow that is added to any existing Hortonian overland flow or saturation overland flow increasing runoff amounts and therefore erosion quantities. Since the WEPP

model has been developed for application in forested regions, it simulates the subsurface flow response in this way (Flanagan and Nearing, 1995).

The Green-Ampt effective hydraulic conductivity links the Hillslope Surface Hydrology module of the WEPP model to the Subsurface Hydrology module. Infiltration through the unsaturated zone as well as the percolation theory incorporated in the Water Balance and Percolation module contributes to the rise in the water table and the likelihood of the second surface runoff process, saturation overland flow. Therefore the effects that water table fluctuations have on erosion and runoff are also taken into account (Flanagan and Nearing, 1995).

In mine waste, the location of the water table and the resulting exfiltration zone will be important in determining where erosion takes place. Though WEPP does provide the amount of seepage that occurs on a daily basis, the location of the seepage face is not available from WEPP output. This information can be generated using a seepage analysis program independent of the WEPP model and the combination of the seepage analysis results and the WEPP erosion results can then be used for design and remediation purposes.

Mine waste piles particularly those composed of tailings have been observed to exhibit saturation overland flow, subsurface return flow and Hortonian overland flow. Saturation overland flow occurs in poorly drained fine grained material, subsurface return flow is visible in seepage zones located at the toe of lifts and Hortonian overland flow occurs where compaction has occurred or in fine grained material that does not allow adequate infiltration rates under storm conditions. Therefore, the WEPP model is capable of simulating all types of runoff generation and is appropriate in modeling both surface and subsurface flow in mining situations for the use of erosion estimation.



### 5.3.7 Soils

The Soil module of the WEPP model computes soil properties based on the impact of tillage operations. Tillage acts to decrease the soil bulk density, increase the soil porosity, change the soil roughness and ridge height, destroy rills, increase infiltration parameters and change the erodibility parameters. The consolidation of the soil due to raindrop impact as well as natural consolidation under its own weight, which occur after tillage is also simulated.

The Soil module of the WEPP model is linked to many of the other modules since like the Hillslope Surface Hydrology module, the Soil module is a major factor in soil detachment. The soil variables that influence the hydrology portion of the erosion process are random roughness, ridge height, bulk density and effective hydraulic conductivity. The soil detachment parameters that are significant in the estimation of the erosion process are the interrill erodibility, rill erodibility and critical shear stress.

The angularity of the soil particles is significant in determining the angle of repose of tailings and waste rock slopes. Fresh waste rock and tailings typically have higher angles of repose than those of their weathered counterparts. Since WEPP was designed for use with agriculture and forestry soil types, the WEPP model does not allow the user to input an internal friction angle as an associated input parameter. Therefore, the angularity of the soil material is not taken into account when determining the soil erodibility characteristics. It is postulated that soil particle angularity will contribute to reducing erosion rates at mine sites since the freshly mechanically ground tailings and waste rock fragments will have a greater ability to "lock" together resisting erosion during the initial stages of mining. The weathering and chemical breakdown of the tailings and waste rock as they seek equilibrium conditions with the surrounding environment will increase the erosion rates over the

long-term. However, depending on the environment and the mine life, the closure process of covering the material will likely be taking place at this point.

#### **5.3.8 Plant Growth**

This module of the WEPP model is designed to accommodate cropland and rangeland plant growth and the influence of this growth on hydrology and erosion processes (Flanagan and Nearing, 1995). The above and below ground biomass production in cropland situations and plant growth for rangeland applications is computed through the Cropland Plant Growth Model and the Rangeland Plant Growth Model respectively. Potential plant growth is based on daily heat accumulation and actual plant growth is then reduced if water and temperature stresses are encountered.

Both plant growth models used in WEPP predict the development of above and below ground biomass for cropland and rangeland plants to be used in the Water Balance and Percolation module and the Hillslope Erosion module. The Water Balance and Percolation module determines the amount of water that can be used by plants and balances the extraction of water from the soil layers (Lane *et al.*, 1989). Since the interrill soil detachment calculated by the Hillslope Erosion module is influenced by the impact of raindrops, the Plant Growth module of the WEPP model provides information on the canopy cover and height. Canopy characteristics influence the amount of precipitation interception affecting the rate of interrill erosion (Lane *et al.*, 1989). In addition, the amount of leaf residue remaining after harvest and the amount of leaf litter associated with seasonal changes are then used by the Residue Decomposition and Management module again influencing soil erosion caused by rainfall and runoff.

The Cropland Plant Growth Model takes into account such activities as crop yield, root growth, LAI and the influence of perennial crops while also accounting for

Cropland Management Options. Such options include hay harvesting and the application of herbicides to name a few.

The Rangeland Plant Growth Model has a slightly different focus since the plant growth is not cyclical like that of cropping systems. Here the initiation of plant growth both above and below ground is based on the potential growth curve. The growth curve attempts to explain the growth of plant communities based on growing season, water stress and plant characteristics such as height, projected plant area and canopy cover. The Rangeland Management Options available include whether plant or no plant growth occurs, grazing, burning and the application of herbicides.

The Plant Growth module of the WEPP model is valuable in assessing erosion rates that may occur on closure covers themselves rather than on bare exposed tailings or waste rock. Therefore, WEPP provides the capacity to assess the success of a closure cover system in sustaining plants to reduce erosion rates beyond mine closure.

#### **5.3.9 Residue Decomposition and Management**

The simulation of plant residue and decomposition for croplands and rangelands as carried out by this module are called by separate sub-routines within WEPP (Flanagan and Nearing, 1995). The plant and residue management options such as tillage, shredding, burning or removing residue will influence the decomposition and the erosion processes.

The WEPP cropland residue and decomposition sub-routine for example is designed for agricultural applications and is based on a "decomposition day" approach similar to a growing degree-day used in many plant growth models (Lane *et al.*, 1989). Using the residue from the previous three crop harvests, WEPP will calculate the

decomposition rate recognizing that each vegetation type has an optimal rate affected by moisture and temperature.

The rangeland residue and decomposition calculations, however, are based on the antecedent rainfall, average daily temperature and the carbon to nitrogen ratio in the vegetation in order to determine the decomposition rates. Currently, the rangeland option of WEPP does not support mechanical practices such as tillage (Flanagan and Nearing, 1995).

The affect that residue and decomposition have on the erosion of mine waste material is important when establishing a successful cover system. Since the tailings or waste rock are devoid of organic material, the residue and decomposition will be important in sustaining vegetation by introducing important organics.

#### **5.3.10 Hillslope Erosion**

The Hillslope Erosion module represents the culmination of all of the other modules of the WEPP model through, in particular, outputs from the Hillslope Surface Hydrology module, the Hydraulics of Overland Flow module and the Soil module. Each provides values required for estimating erosion and deposition on a hillslope.

Interrill detachment and transport (through sediment routing) by raindrop impact as well as rill detachment, transport and deposition by concentrated flowing water are the processes represented by the WEPP Hillslope Erosion module (Lane *et al.*, 1989; Laflen *et al.*, 1997). Like many process-based erosion models, the WEPP model uses a steady state, conservation of mass equation (Equation [5.4], introduced by Foster and Meyer (1972a) as the basic equation for estimating the changes in sediment load in rill flow with distance downslope (Flanagan and Nearing, 1995)

$$\frac{d(G)}{dx} = D_r + D_i \quad [5.4]$$

Where

- $G$  = sediment load (kg/s/m)
- $x$  = distance downslope (m)
- $D_r$  = rill erosion rate (kg/s/m<sup>2</sup>)
- $D_i$  = interrill sediment delivery rate to the rills (kg/s/m<sup>2</sup>)

For erosion computations for each individual storm, the time period used is the effective duration of runoff computed in the Surface Hillslope Surface Hydrology module of the WEPP model (Laflen, 1994). Estimates of  $dG/dx$  are made at a minimum of 100 points along the hillslope profile and a running total of the sum of all detachment and deposition at each point from each storm is used to obtain monthly annual and average annual value for the simulation (Laflen, 1994).

The WEPP model uses separate equations to describe the rate of soil erosion between and within rills. However, WEPP calculates erosion in the rill and interrill areas on a per rill area basis (Tiwari *et al.*, 2000) and therefore the sediment load is the soil loss per unit rill area. The erosion in the interrill area is assumed to be independent of distance, which suggests that erosion in interrill areas occurs at a constant rate down the slope (Tiwari *et al.*, 2000). The sediment delivery from interrill areas to rills is modeled as a function of rainfall intensity, residue cover, canopy cover and interrill soil erodibility as well as runoff rate (Laflen, 1994) and is given by:

$$D_i = K_i I^2 q C G_r \left( \frac{R_s}{W} \right) S_f \quad [5.5]$$

Where

- $K_i$  = interrill erodibility (kgs/m<sup>4</sup>)
- $I$  = rainfall intensity occurring in the period of rainfall excess (m/s)

$$\begin{aligned}
 q &= \text{flux (kg/m}^3\text{/m)} \\
 C &= \text{effect of canopy cover} \\
 G_r &= \text{effect of ground cover} \\
 R_s &= \text{rill spacing (m)} \\
 W &= \text{rill width (m)} \\
 S_f &= \text{interrill slope adjustment factor}
 \end{aligned}$$

$C$  is a function of the fraction of the soil surface area covered by canopy and the height of the canopy.  $G_r$  is a function of the fraction of the interrill area covered by surface litter, residue and rocks. The  $S_f$  is a function of the interrill slope. The processes of detachment, transport and deposition on interrill areas are lumped together in Equation [5.13] (Laflen, 1991) which is a more complex version of the relationship of interrill erosion as shown in Equation [2.5].

The eroded material from the interrill area delivered to the concentrated flow channels of the rills is either transported downslope or deposited within the rill itself (Risse *et al.*, 1995). Since, as explained in Section 2.4.1, transport of sediment by interrill flow is negligible, sediment routing is used to deliver interrill material to rills within the WEPP model.

Rill erosion is a function of many factors including slope and surface roughness and is dependant on soil rill erodibility, hydraulic shear stress, surface cover, below ground residue, consolidation and the ratio of sediment load to transport capacity (Nearing *et al.*, 1990). Flowing water in rills has the ability to both transport sediment and detach additional material as it moves through the rill network. When the rill flow becomes laden with sediment due to either sediment supplied from the interrill areas or sediment detached in the rill channel itself, the rill flow will lose some of its ability to detach additional soil and transport sediment. This relationship between detachment capacity and transport capacity determines whether erosion or deposition occurs.

The detachment capacity of flowing water in rills is considered to occur when the hydraulic shear stress of the flow (i.e. the force exerted by the flow on the bed and banks) exceeds the critical shear stress of the soil (i.e. the resistance of soil to detachment). This relationship is expressed by Equation 5.6 (Laflen, 1994).

$$D_C = K_r (\tau - \tau_{cr}) \quad [5.6]$$

Where

$$\begin{aligned} D_C &= \text{detachment capacity of rill flow (kg/m}^2\text{/m)} \\ K_r &= \text{rill erodibility (kg/s/m}^4\text{)} \\ \tau &= \text{hydraulic shear (kgm/s}^2\text{)} \\ \tau_{cr} &= \text{critical hydraulic shear for rill detachment can occur (kgm/s}^2\text{)} \end{aligned}$$

The maximum detachment capacity is the rate of rill detachment that occurs when there is no sediment in the flowing water (Laflen, 1991). As the sediment load in the flow increases, the rill detachment rate decreases.

Rill hydraulics are used to calculate shear stresses and a simplified transport equation based on the Yalin transport equation is used in WEPP to compute transport capacity ( $T_c$ ) or the upper limit of sediment transport in rill flow (Laflen, 1991). Modifications to the Yalin sediment transport equation attempt to take into account the shallow nature of rill flow and the impact that raindrops can have on the sediment erosion rates.

$$T_C = K_T \tau^{2/3} \quad [5.7]$$

Where

$$\begin{aligned} T_C &= \text{transport capacity} \\ K_T &= \text{transport coefficient} \\ &\text{and all other variables are defined above.} \end{aligned}$$

Although there may be sufficient flow shear stress to detach material within rills, transport of material through the rill network can only occur when the sediment transport capacity is greater than the sediment load as expressed in Equation [5.8]

$$D_r = D_C \left( 1 - \frac{G}{T_C} \right) \quad [5.8]$$

Where all variables are defined above.

Thus, as the flow fills with sediment,  $G$  approaches  $T_C$  and the rill detachment rate decreases. The transport capacity of the flow is used to calculate the rill contribution to the sediment continuity equation. Rill erosion in the WEPP model is assumed to be positive for detachment and negative for deposition (Tiwari *et al.*, 2000). The equation used by WEPP to predict deposition is Equation [5.9]

$$D_e = \left( \left( \frac{\beta(V_{eff})}{q} \right) (T_C - G) \right) \quad [5.9]$$

Where

- $D_e$  = rill deposition rate (kg/s/m<sup>2</sup>)
- $\beta$  = rainfall induced turbulence factor (0.5)
- $V_{eff}$  = an effective particle fall velocity (m/s)
- and all other variables are defined above.

One of the strengths of WEPP is its ability to estimate both rill detachment and deposition allowing comprehensive evaluation of both on site and off site effects of erosion.

Rill spacing, width and shape are important factors in estimating erosion with WEPP. Rangeland rill spacing is recommended to be between 0.5 m and 5 m (Laflen, 1994). Rill width is estimated based on factors such as topographic and flow characteristics, and rill shape is always rectangular (Laflen, 1994).



### **5.3.11 Irrigation**

Since erosion is caused by the application of water to a hillslope or watershed, WEPP is able to identify the amount that rainfall, snowmelt or irrigation contribute to the erosion process (Flanagan and Nearing, 1995). Several irrigation system options are available for modeling with WEPP including sprinkler irrigation and furrow irrigation that can be applied individually or in combination. The infiltration and hydraulics of furrow irrigation are provided in the *WEPP User Manual* (Flanagan and Nearing, 1995) including options for scheduling irrigation events to minimize erosion. The topic of irrigation induced erosion is not included in this thesis since it is likely not going to be of major concern in mining applications.

## **5.4 Limitations of the WEPP Model**

As with any modeling software package, the limitations are a major factor in determining the model applicability. Of the available erosion prediction models, the limitations of the WEPP model are not significant in applying it to mining situations, however, it is important to keep these limitations in mind when setting up and analyzing the results of any WEPP simulation.

Several limitations exist in defining the problem within the WEPP model interface itself. The length of the hillslope profile that is recommended in the *WEPP User Summary* restricts the horizontal distance from the slope crest to the toe to between 50 m and 100 m in length (Flanagan and Nearing, 1995). However, the length of the hillslope profile that can be modeled with WEPP will depend on the complexity of the topography (Lane *et al.*, 1989). Though many mining slopes exceed the maximum slope length recommended by the WEPP model developers, the topography is usually limited to single or multiple raises of uniform slope shape.

The slope length is significant for two reasons. First, the width of any rill channel is based on the flow out of an Overland Flow Element (OFE), the homogeneous soil and plant area of a hillslope. The channel width increases starting at the top of the OFE and for long slopes consisting of one OFE, the channels will become wider at the top and remain wider than they would exist in nature for a large proportion of the hillslope. This channel widening would result in lower runoff depths, causing lower internally adjusted shear stress values during the simulation and therefore underestimate soil erosion rates.

Second, in the hillslope erosion module of the WEPP model, there is assumed to be no change in soil erodibility or shear stress with soil depth. This assumption is usually correct for most storms and most slopes. The model allows erosion to proceed downward without any change in soil properties. For long slopes, this could result in very high erosion rates as compared with what happens in nature. In nature, usually (but not always), the rill channel bottom reaches a layer that is virtually non-erodible and erosion is reduced.

In order to detect either this underestimation or overestimation of erosion prediction due to excessive slope length, it is suggested that the model be run at different slope lengths and the erosion and runoff rates be compared to known data. Discontinuities can be detected whereby the erosion rates dramatically increase or decrease as the slope length is progressively increased. WEPP Technical Support advises that due to the relatively simple nature of mining slopes, slope lengths of up to 300 m can be used without complications. However, as slope lengths of simple topography approach 3000 m, the ability of the WEPP model to mimic nature is seriously compromised. Successful application of the WEPP model to agricultural slopes of 600 ft (183 m) have been reported (Laflen, 2002); however, the slope gradient of these slopes are much shallower than those encountered in mining situations.

In addition to slope length restrictions, the WEPP model does not allow the user to input negative slopes. Though negative slope gradients do occur in nature and are particularly useful in mining environments to collect and route seepage and runoff water, their effect on erosion cannot be adequately determined. In the event that a negative slope is used on for example a bench between raises, either each raise can be modeled individually neglecting the negatively sloped benches between them or multiple raises can be modeled using flat benches.

Perhaps one of the most important limitations of the WEPP model erosion estimation is that the user is required to input the rill spacing. It is not possible with WEPP to predict the locations that rills will develop on a previously un-rilled surface.

Though the interrill and rill erosion processes are known to be the beginning stages of the more severe gully erosion process, WEPP has not been parameterized to model classical gully erosion (Lane *et al.*, 1989). Several mine sites report active gully erosion taking place. However, by reducing the interrill and rill erosion processes, the initiation of gully erosion can also be reduced. Alternatively, the LISEM model discussed in Section 4.4.7 is a possible alternative to modeling gully initiation and advancement.

The other erosion processes that the WEPP model does not predict include stream bank sloughing, tillage erosion or mass wasting (Laflen *et al.*, 1997). Ephemeral gullies are treated like channels and modeled through the Watershed version, channel hydrology module. The WEPP model computes rill and interrill erosion due to overland flow and irrigation and its applications are therefore limited to these areas (Lane *et al.*, 1989). Areas dominated by partial area response hydrology and subsurface flow causing tunnel and pipe erosion, are not within the scope of the model (Lane *et al.*, 1989).

Finally, the major limitation in the WEPP model technology is its reliance on empirical relationships. Though the model is marketed as being one of the first erosion prediction tools based on fundamental physical concepts, these physically based relationships predominantly exist between the modules themselves (Owoputi, 1994). Within the modules, empirical relationships particularly with respect to the soil erodibility parameters, still exist resulting in unexplained model uncertainty.

## CHAPTER 5 - LIST OF SYMBOLS

SYMBOL	DESCRIPTION
$f$	infiltration rate
$K_e$	effective hydraulic conductivity
$N_s$	effective matric potential
$F$	cumulative infiltration depth
$\phi_e$	effective porosity
$\Theta_i$	initial water content
$\Psi$	average capillary potential across the wetting front
$\Theta$	soil water content in the root zone in any given day
$\Theta_{in}$	initial soil water in the root zone
$P$	cumulative precipitation
$I_{in}$	precipitation interception by vegetation
$S$	snow water content (+ for snowmelt, - for snow accumulation)
$Q$	cumulative amount of surface runoff
$ET$	cumulative amount of evapotranspiration
$D$	cumulative amount of percolation loss
$Q_d$	subsurface lateral flow or flow to drain tiles
$G$	sediment load
$x$	distance downslope
$D_r$	rill erosion rate
$D_i$	interrill sediment delivery rate to the rills
$K_i$	interrill erodibility
$I$	rainfall intensity occurring in the period of rainfall excess
$q$	flux
$C$	effect of canopy cover
$G_r$	effect of ground cover
$R_s$	rill spacing
$W$	rill width
$S_f$	interrill slope adjustment factor
$D_C$	detachment capacity of rill flow
$K_r$	rill erodibility

$\tau$	hydraulic shear
$\tau_{cr}$	critical hydraulic shear for rill detachment
$K_T$	transport coefficient
$T_C$	transport capacity
$D_e$	rill deposition rate
$\beta$	rainfall induced turbulence factor (0.5)
$V_{eff}$	an effective particle fall velocity

## **6. WATER EROSION PREDICTION PROJECT MODEL: APPLICATION**

Prior to the use of any erosion prediction tool, the estimation of input parameters is required. In many models, the developers provide a range of suggested input parameters based on previous regression analyses. However, in the case of the WEPP model, the ranges of input parameters suggested for the soil erodibility factors were established based on analysis of agricultural soils. In the case of non-agricultural soils, the erodibility parameters suggested by the model developers may not be suitable for the media being tested. The necessary laboratory and field experimentation to determine the erodibility from soil loss data as well as for calibration and validation of the WEPP model are described in the following sections. Next the results of an example sensitivity analysis of the WEPP model under tropical mining conditions are evaluated.

### **6.1 WEPP Required Parameters**

The soil properties and the climatic conditions are the main variables required to apply an erosion prediction model. Of particular importance for the WEPP model is the determination of the soil erodibility and infiltration parameters. The soil erodibility is described by three factors: the interrill erodibility ( $K_i$ ), the rill erodibility ( $K_r$ ) and the soil critical shear stress ( $\tau_{cr}$ ). The infiltration rate is governed by the user defined effective hydraulic conductivity ( $K_e$ ).

### **6.2 Field vs. Laboratory Evaluation**

Using long-term field plots to estimate values of soil loss and soil erodibility is time consuming and expensive (Sheridan *et al.*, 2000b). As a result, researchers have relied on laboratory rainfall simulators with soil plot boxes and tilting flumes for more rapid estimation.

Some researchers have expressed concerns regarding applying laboratory simulator results to field erosion behavior. The differences in results are attributed to the limited size and scale of laboratory plots, the effects of plot boundary conditions, the preparation of soil including aggregate size, soil depth, drainage and initial moisture content and the difference in simulated rainfall characteristics from those of natural rainfall (Bradford and Huang, 1993). Though it was indicated earlier that rainfall characteristics are very well known parameters that are easy to estimate from natural rainfall, it can be difficult to replicate them under laboratory conditions (Lal, 1990; Laflen and Roose, 1998). The simulation of soil conditions for erosion research is more difficult than the simulation of rainfall. Maintaining the natural structural characteristics of soil during the transfer from the field to the laboratory is likely to be the greatest challenge. Usually, a large quantity of soil is required for erosion studies and the soil can be used only once without appreciably changing its physical condition (Bubenzer and Meyer, 1965). However, the laboratory provides a controlled environment under which the factors that influence the soil erosion process can be studied and there are significant cost and time savings associated with these experiments.

### **6.3 Setting Up a Field Study**

The success of a field study is based on the care with which the test apparatus is set up, the data are collected and the plot site is maintained. There have been many reported failures of erosion studies due to the inappropriate design of the test apparatus resulting in the materials being washed away by large rainfall events, intermittent data collection due to various mechanical and personnel reasons and the runoff and soil loss being improperly isolated.

Setting up a runoff plot using natural rainfall is the cheapest and simplest method of data collection, but the reliability of rainfall can make this difficult. In areas where



rainfall is predictable, the use of a natural runoff plot is the most desirable. Under conditions where data collection for the important rainfall events may be missed, the use of rainfall simulators is a viable alternative.

At mine sites, the waste material is the control material and additional test plots are likely to be used to estimate the effectiveness of alternate cover materials. Evaluation of the response of possible covers compared with bare, exposed mine waste as well as the approximation of erosion and runoff rates at the top and bottom of a slope are important field results. They are necessary for meeting regulatory requirements during operation and at closure

Natural runoff and erosion plots of 100 m<sup>2</sup> have been suggested as an appropriate size for estimating runoff and erosion rates while minimizing border effects (Sheng, 1989; Hudson, 1993). Border materials should be chosen to confine runoff to the area being studied and inserted deep enough to avoid leakage underneath. Common construction materials include bricks, sandbags, earth banks, timber plants or strips of metal (Sheng, 1989). When plots are built on the lower end of slopes, a drain constructed at the upslope end of the plot will divert runoff from higher ground, isolating the effects of runoff to the plot area. In addition, plots should not share common boundaries and a buffer strip should be left between plots to ensure that any damage that occurs affects only one plot.

For large plots of the size recommended above where erosion and runoff rates are expected to be high, collecting and measuring the runoff and sediment presents an additional problem. Several options for collection systems, storage tanks and divisors used for splitting the runoff are discussed by Hudson (1993). No single system can be recommended for the mining industry. Each system is highly dependant on climate and Sheng (1989) cautions that when deciding on an appropriate system, economics should not be the deciding factor.

It is necessary to collect and analyze data from every runoff producing rain. Rainfall amount and intensity, runoff and sediment yield are the most important factors. Determining the onset of runoff and the peak runoff rate cannot be completed without the use of automatic data recorders. Erosion theory is based on the notion that detached particles primarily move as bedload, which is collected in the bottom of the collection tanks and troughs. This sediment is weighed, sampled and oven dried to determine the dry weight contents. Information about suspended loads is usually omitted from data collection without much loss in accuracy (Sheng, 1989).

The relative success of the USLE is that it has been developed and refined based on 10,000 plot years of data (Wischmeier and Smith, 1978). Laflen (1998) suggests that though an experimental length of between four and six years will not capture all of the variation in climate, it will provide a sufficient range to establish average erosion rates.

#### **6.4 Laboratory Experimentation**

Laboratory experimentation as explained above is a convenient way to estimate soil erodibility parameters under controlled conditions. Laboratory experiments also produce results within a shorter time period than field experiments, making their convenience critical in short term erosion studies.

The most common method of determining soil erodibility in the laboratory is to use soil loss pans (or plot boxes) and/or flumes under simulated rainfall (Bradford and Huang, 1993). Plot boxes may range in size from 0.5 m to 0.75 m in length for interrill erosion studies (Watson and (Laflen *et al.*, 1997) and flumes can be up to 30 m in length for studies of gully erosion (Thornton, 1999).

Several rainfall simulators have been designed to mimic natural rainfall conditions taking into account drop size distribution, kinetic energy and momentum as well as terminal velocity. An appropriate rainfall simulator design will be dependent on the rainfall properties being replicated.

## **6.5 Parameter Estimation**

The following sections describe the methods of determining the input parameters for use in the WEPP model.

### **6.5.1 Interrill Erodibility ( $K_i$ )**

Estimating interrill erodibility,  $K_i$ , requires the use of rainfall simulators and soil plot boxes with an apparatus for collecting soil splash and soil detached and transported by thin sheet overland flow. These boxes are therefore restricted to short lengths of approximately 0.5 m to 0.75 m (Watson and Laflen, 1986; Grosh, 1994; Fan and Wu, 2001) to ensure that rilling does not occur. These plot boxes are often fitted with collection systems or deflectors to ensure that the splashed material does not leave the plot box. In the initial stages of rainfall simulation, the sediment concentration in runoff can be significantly higher than during the latter stages as the loose material is washed from the plot. As a result, the initial samples are often omitted from the dataset in order to isolate the sediment detached by rainfall impact alone. The interrill erodibility parameter is then defined based on plot gradient and the delivery rate of sediment per unit area, which is estimated from runoff rate and sediment concentration.

The range of interrill erodibility values reported by Sheridan *et al.* (2000a) for a variety of spoil and overburden materials at coal mine sites in Australia fall within the ranges provided by the model developers of the WEPP model. Therefore, though there is uncertainty as to whether the erodibility of coal mine spoil is similar to that

of agricultural soils, the variability within the interrill erodibilities is similar (Sheridan *et al.*, 2000a).

#### **6.5.2 Rill Erodibility ( $K_r$ )**

Flumes provide a simple means of estimating the rill erodibility of soils (Sheridan *et al.*, 2000b). Flumes can range in length and provide the ability to isolate the effects of overland flow while controlling the slope angle, a feature not available from natural runoff plot experiments. At pre-determined times during the experiment, measurements of flow depth and width are taken and runoff samples are collected to determine sediment concentration.

The rill erodibilities determined by Sheridan *et al.* (2000a) for several spoil and overburden materials at mine sites throughout Australia fall within the ranges provided in the WEPP documentation for agricultural soils. However, the mean value of rill erodibility for the mining spoils as determined by Sheridan *et al.* (2000a) was higher than the values for rill erodibility published in the *WEPP User Summary* (Flanagan and Livingston, 1995). This finding indicates that the mine site media tested in their study are more susceptible to rill erosion than those agricultural soils published in the WEPP compendium (Sheridan *et al.*, (2000a)

Also, results of the study by Sheridan *et al.* (2000b) indicate that the values of rill erodibility coefficients of coal mine spoil vary by approximately 290 times. The magnitudes of these variations indicate that the estimation of appropriate erodibility parameters is important in successful erosion prediction modeling. Using those erodibilities supplied by the WEPP model developers for agricultural soils are likely not reflective of the properties of materials encountered in mining.

### 6.5.3 Critical Shear Stress ( $\tau_c$ )

Critical shear stress is a function of the flow depth and gradient at the point being considered. Since the critical shear is the shear which must be overcome for the initiation of rilling, critical shear and rill erodibility are often measured together.

Flow shear stress is plotted against the detachment rates (determined from sediment concentrations) within the rill flow and the intercept of this linear plot is taken to be the critical shear value. The inverse of the slope of the line gives the value for the rill erodibility factor,  $K_r$  (Laflen, 2002). In well-graded material, it is common to see an initially high rate of erosion in the flume studies due to rapid erosion of the fine material and the gradual bed armoring due to the flow. Samples taken after this initially high rate of erosion are therefore used.

Sheridan *et al.* (2000a) compare the measured values of critical shear stress for the coal mine spoil and overburden material tested in their study with the range of values provided in the *WEPP User Summary* (Flanagan and Livingston, 1995). The range of values they determine are significantly higher than the critical shear stresses provided by the WEPP model developers. Sheridan *et al.* (2000b) conclude that the high critical shear stress values they found are consistent with the sealing and hardsetting nature of the spoils and overburdens tested.

### 6.5.4 Effective Hydraulic Conductivity Parameter ( $K_e$ )

The effective hydraulic conductivity parameter requires the estimation of the soil infiltration rate. Infiltration rates are often measured using small, horizontal plot boxes under simulated rainfall. The bottoms of these boxes are often made of wire mesh to promote the free flow of air and water through the base of the boxes as the wetting front propagates through the soil sample. The free flow of air is important to ensure that air entrapment and water ponding do not occur, both of which may alter

the infiltration and soil erosion rates (Owoputi, 1994). Soil may be compacted to the desired density using a variety of methods. In the field, the ring infiltrometer method has been reported as a successful means of determining infiltration rate slopes.

For any individual soil, the Green-Ampt effective hydraulic conductivity parameter ( $K_e$ ) is estimated by fitting calculated Green-Ampt infiltration curves for various effective hydraulic conductivities to measured infiltration rates. The steady state infiltration rate or the final infiltration rate represented by the tail end of the graph which is more important in fitting the curve than are the initial infiltration rates.

## **6.6 Sensitivity Analysis Using the WEPP Model**

Expected errors in model prediction due to errors in the model parameters are a measure of the uncertainty of the model results. Ultimately, sensitivity analyses are used to rank model parameters based on their overall contribution to errors in model prediction (Tiscareno-Lopez *et al.*, 1993). A sensitivity analysis using the Hillslope version of the WEPP model was conducted for a tropical mine site in South East Asia using climate and mine waste characteristics typical of a oxide/sulphide mine in this area. The name of the mine has been omitted from the following analysis to maintain anonymity and the results of the analysis have been discussed generally in order to be applicable to any mine site in the area. The Hillslope version of the WEPP model was chosen since it is assumed that no permanent channel features would be present on the tailings or waste rock pile slopes.

This analysis was compared with and supplemented by sensitivity analyses of agricultural sites reported in the literature to demonstrate the common findings when using the WEPP model in practice. However, no sensitivity analyses, calibrations or validations of the WEPP model have been undertaken for such severe tropical conditions using tailings or waste rock material. Therefore, the results of this

analysis are intended to provide an indication of the most sensitive parameters for the WEPP model under tropical mining conditions. Until calibration and validation of the WEPP model has been undertaken at a mine site in this region, the results of this analysis provide only relative predictions and the absolute values for runoff, soil loss and sediment yield can not be used for any further purpose.

#### **6.6.1 Site Background**

The tropical conditions of South East Asia are the conditions used for this analysis. This area was chosen due to its intense climatic conditions and the number of oxide/sulphide mines currently operating. Since efforts to quantify the amount of erosion facing mine waste sites in this area involves the use of erosion prediction tools such as the WEPP model, a sensitivity analysis was conducted with parameter values derived from the climate and soil conditions at a typical oxide/sulphide mine in the area. It is intended that the relative sensitivity of the WEPP input parameters be referred to when future erosion prediction estimations are conducted in tropical mining settings.

#### **6.6.2 WEPP Model Input Parameters: Estimation of Suitable Ranges**

The following outlines the parameter estimation method used to determine ranges of values appropriate when running the WEPP model for a generic oxide/sulphide mining case. A summary table of the baseline WEPP input parameters and their upper and lower bounds are provided in Appendix I.

##### **6.6.2.1 Structural Characteristics**

The baseline tailings or waste rock pile design is shown in Figure 6.1. It consists of multiple 4 m vertical lifts with side slopes of 3H:1V and separated by horizontal 8 m wide benches.

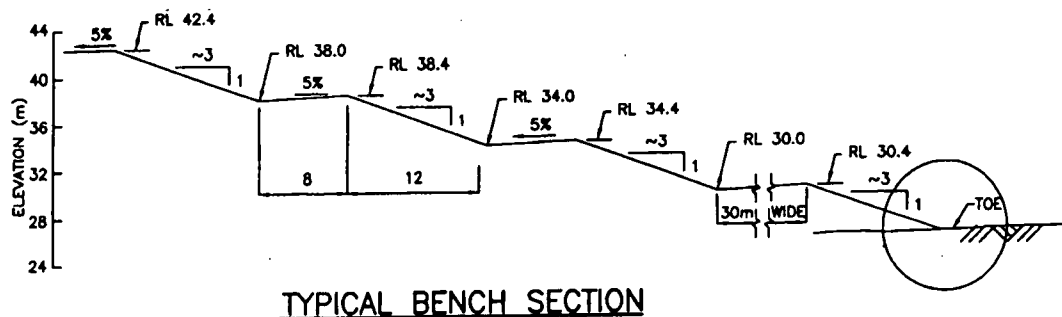


**Figure 6.1 Baseline Tailings or Waste Rock Pile Design**

In the proposed design shown in Figure 6.1 above, the 8 m wide benches are built with a negative 5 % slope to promote seepage and runoff collection at the toe of each lift while routing this drainage via longitudinal bench drains to the emergency spillways, leading off the pile. As mentioned in Section 5.4, WEPP does not have the capability to model zero or negative slope angles and therefore, these slopes are input as close to zero slope as the model will allow (0.0000001%).

The baseline slope configuration was entered into the model to match the dimensions shown in Figure 6.1 with a width of 10 m. In order to assess the response of runoff and soil loss characteristics, variations in this hillslope configuration as well as variations to a hypothetical dam configuration were developed. For the remainder of this sensitivity analysis discussion, a hillslope profile is assumed to be a 4 m high vertical lift whereas a dam is assumed to be a 40 m high vertical lift, each representing possible mining configurations. However, it should be noted that both configurations used here are hypothetical and modeled to compare the effects of slope length on erosion rates.

Hillslope and dam configurations were modeled under single lift and multiple lift conditions. Figure 6.2 shows the single and multiple lift configurations of a uniform slope shape for a hillslope profile of a tailings or waste rock dump.



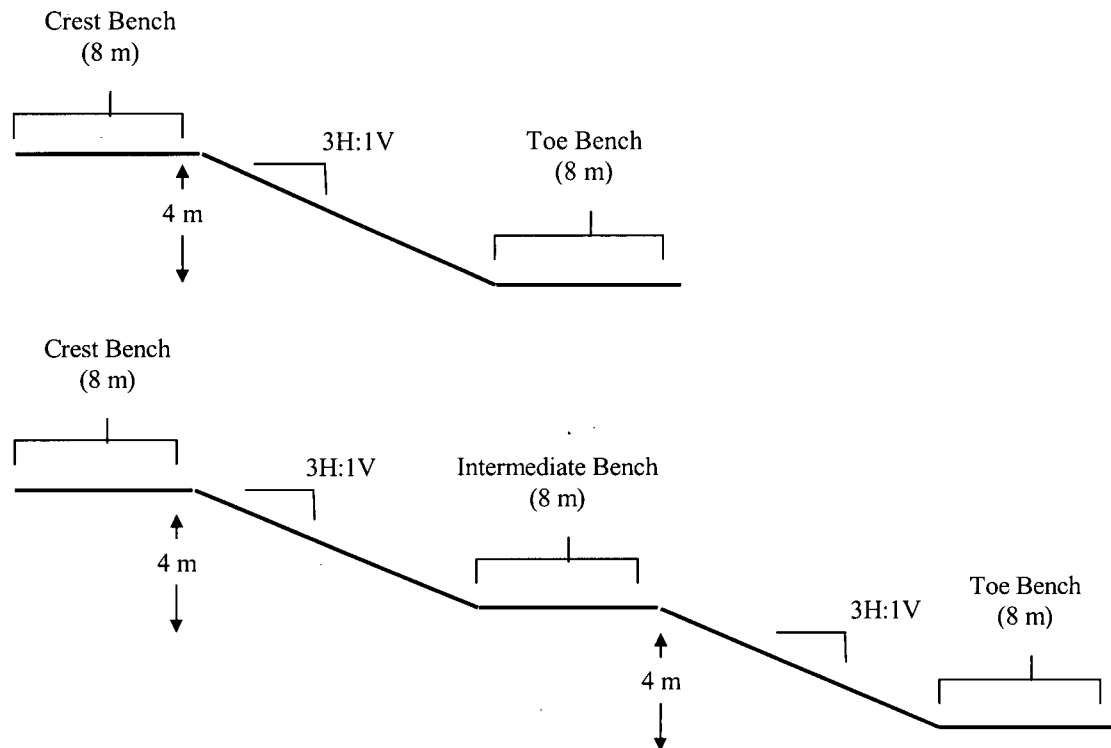


**Figure 6.2 Single and Multiple Lift Configurations of Uniform Slope**

A single lift condition consists of crest and toe benches as well as one 4 m high lift or one 40 m high lift for the hillslope or the dam configuration respectively. Multiple lift conditions include the crest and toe benches for two 4 m high lifts or two 40 m high lifts for the hillslope or the dam configurations respectively as well as an intermediate bench. Multiple lifts were limited to two lifts since the WEPP slope profile only allows the input of 9 points to describe the slope profile. Under uniform slope profile conditions as shown in Figure 6.2 it would be possible to enter in more than two lifts; however when concave and convex slope profiles are being modeled, the 9 point limit used to describe the profile restricts the non-uniform configurations to two lifts. Therefore in order to make valid comparisons of runoff and erosion quantities between slope shapes for multiple lift scenarios, a maximum of two lifts were modeled.

Modifying the slope shape from uniform to concave or convex shapes required preserving the height of the lift as well as the total horizontal distance from the crest of the slope to the toe of the slope in order to make runoff and soil loss comparisons. Uniform slope profiles were first developed using the WEPP model. From those templates, concave and convex profiles were then developed, by dividing the slope profile into three equal segments. For the concave profiles, the crest segment was determined to be steeper than the uniform slope shape being used as a template, the middle section had an equivalent slope gradient to that of the uniform slope and the toe segment had a lower gradient than that of the template. Figure 6.3 shows the concave slope configuration based on the 3H:1V slope profile indicating that the middle segment retained the 3H:1V gradient while the crest segment was steeper and the toe segment shallower than the uniform slope template.

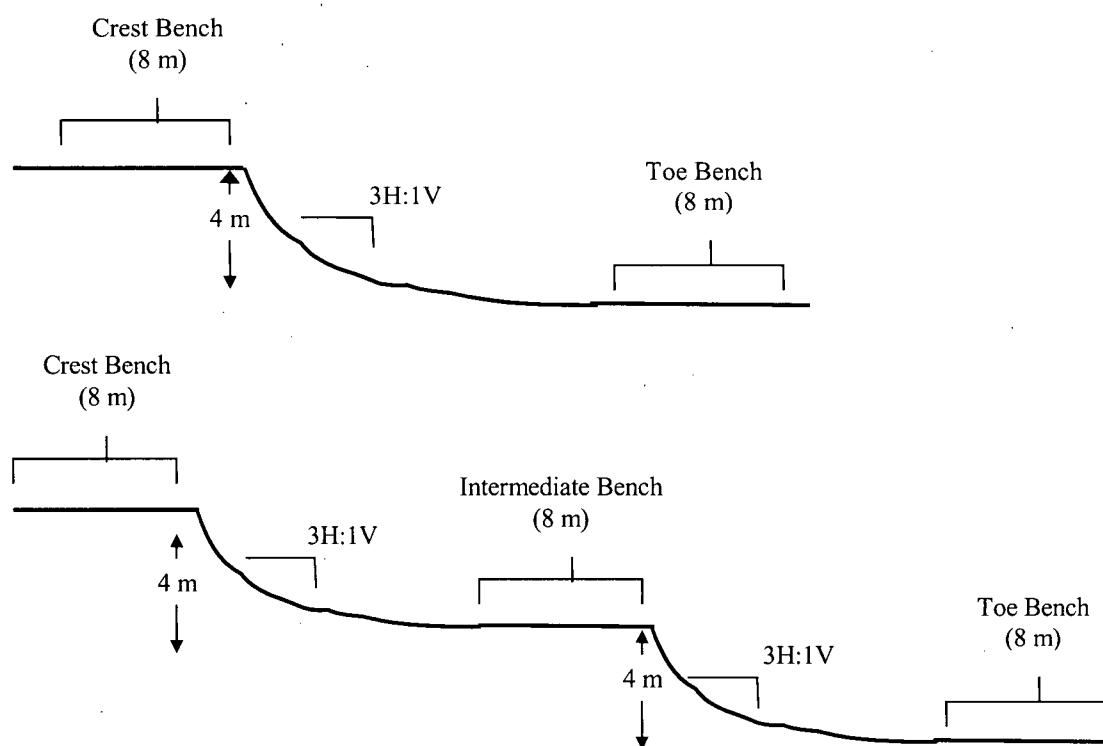


### Figure 6.3 Concave Slope Configuration

Table 6.1 shows how the uniform slopes were modified into concave configurations.

**Table 6.1 Uniform Slope Profile to Concave Slope Profile**

UNIFORM SLOPE GRADIENT	CREST CONCAVE SLOPE GRADIENT	MIDDLE CONCAVE SLOPE GRADIENT	TOE CONCAVE SLOPE GRADIENT
3H:1V	2H:1V	3H:1V	4H:1V
4H:1V	2.5H:1V	4H:1V	5.5H:1V
5H:1V	4H:1V	5H:1V	5.5H:1V

A similar procedure was conducted for the convex slope profile; however, in this case, the crest slope gradient was shallower and the toe segment steeper than the middle section.

In addition to investigating the variations in the slope gradient, the length of the crest, intermediate and toe benches were varied to determine how these contribute to erosion quantities under the climatic conditions being modeled. Table 6.2 shows the variations in structural characteristics that were investigated during the WEPP sensitivity analysis. It should be noted that a 10 m width was maintained for all slope configurations.

**Table 6.2 Structural Characteristics Varied in the WEPP Sensitivity Analysis**

SLOPE CONFIGURATION	SLOPE SHAPE	SLOPE GRADIENT (H:V)	BENCH LENGTH (m)	PROFILE WIDTH (m)
Dam	Uniform	2:1, 3:1, 4:1, 5:1, 6:1	1, 10, 20	10
	Concave	3:1, 4:1, 5:1	1, 10, 20	10
Hillslope	Uniform	2:1, 3:1, 4:1, 5:1, 6:1	1, 4, 8, 16	10
	Concave	3:1, 4:1, 5:1	1, 4, 8, 16	10

Slope angles represent the middle 1/3 of the slope profile

#### 6.6.2.2 Climate Parameters

Assuming that many of the mine sites in South East Asia do not have sufficient climate data to randomly generate a representative long-term climate file using CLIGEN for use in WEPP continuous simulation modeling, alternative climate data

must be used. The United States Forest Service provides the ability to modify existing climate parameters for any climate station in its database through an online climate generator (United States Forest Service, 2002) for use with WEPP. In addition to the stations available for the continental United States, stations including the Pacific Islands, Puerto Rico and the US Virgin Islands are also available. From the Pacific Islands database, Pohnpei Island, part of the Caroline Islands archipelago of Micronesia was chosen since its location (latitude, longitude), elevation and annual rainfall could mimic the severe mountainous rainfall often encountered in South East Asia. Figure 6.4 shows the location of Pohnpei Island and Table 6.3 provides its geographic characteristics.

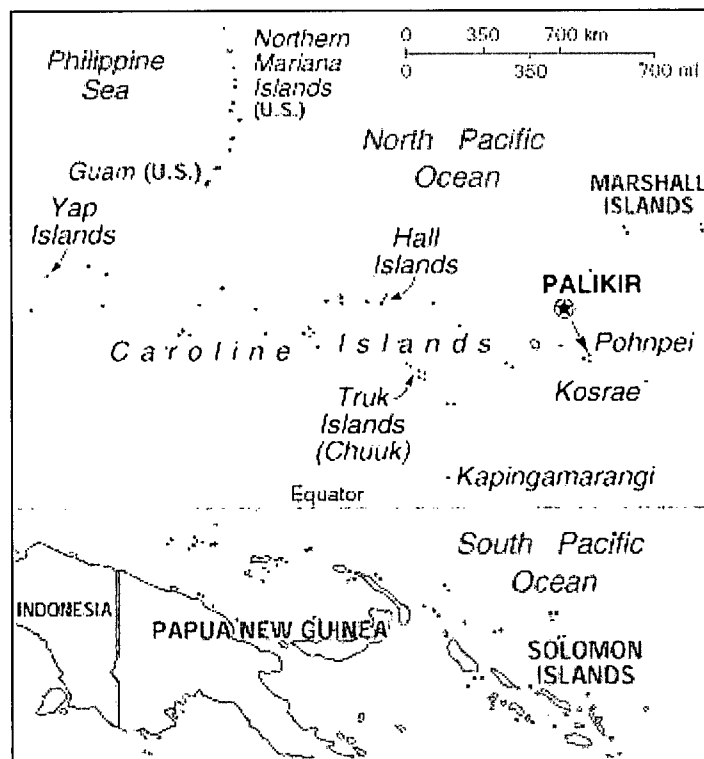


**Figure 6.4 Location of Pohnpei Island (Graphic Maps, 2001)**

**Table 6.3 Pohnpei Island Characteristics**

CHARACTERISTIC	POHNPEI ISLAND
Latitude	6.97°N
Longitude	158.22°E
Elevation	36 m
Annual Rainfall	4799.1 mm
Years of Record	40

Table 6.4 shows how the Pohnpei climate was modified in the United States Forest Service climate modifier to generate a more severe long-term simulation climate file.

**Table 6.4 Climate Parameters for Pohnpei Island and South East Asia**

MONTH	MEAN MAXIMUM TEMPERATURE (°C)		MEAN MINIMUM TEMPERATURE (°C)		MEAN PRECIPITATION (mm)		NUMBER OF WET DAYS	
	POHNPEI	SEA*	POHNPEI	SEA*	POHNPEI	SEA*	POHNPEI	SEA*
January	30.2	37.4	24.1	21.3	305.37	695.75	21.9	23.5
February	30.3	37.5	24.1	21.5	262.86	585.25	19.5	23.5
March	30.5	38.6	24.1	21.5	358.79	493.50	22.8	24.3
April	30.6	37.1	23.9	20.6	446.23	683.75	24.4	25
May	30.8	37.3	23.8	21.1	489.17	629.5	27.1	22.5
June	30.8	36.6	23.4	20.3	435.52	564.25	27.2	25.75
July	30.9	35.4	22.8	20.3	453.34	345.25	27.0	20
August	31.2	37.8	22.7	17.7	416.07	281.00	26.4	23.5
September	31.2	39.6	22.7	18.0	415.89	405.75	24.1	22.5
October	31.2	39.4	22.7	19.0	408.75	499.75	25.1	23.75
November	31.1	39.5	23.0	21.6	414.17	506.50	24.7	22.75
December	30.6	37.9	23.8	21.5	392.93	572.15	25.0	24.75
ANNUAL					4799.1	6261.4	295.3	281.8

\* South East Asia

Since the major advantage of the WEPP model is its ability to predict continuous simulation and event-based erosion quantities, the event-based option within CLIGEN was also explored. The event-based option requires the user to input the total storm rainfall amount, the storm duration, the maximum storm intensity and the duration of the peak rainfall intensity. Four 15-minute peak intensities were modeled using the WEPP model for comparison purposes only. Though the return period of these events is not known since their location has not been specified, the storm provides event information that could be used in the sensitivity analysis.

### 6.6.2.3 Soil Parameters

All soil parameters required by WEPP were determined using typical sand sized tailings or waste rock characteristics and the equations provided in the *WEPP User Summary* (Flanagan and Nearing, 2000). WEPP Technical Support provided additional formulae where they were required (Laflen, 2002). The following section describes the input variable values required by the Soil Database Editor dialogue box within the WEPP model user interface.

#### Soil Texture

The Soil Texture box requires the input of the soil texture class from the Soil Texture Triangle (see Figure 3.3) (Ballard, 1999). This symbol is for information purposes only and no calculations within the model are based on this.

#### Albedo

Albedo refers to the proportion of the incoming radiation that is reflected by a surface back to the atmosphere (Ahrens, 1991) and is used to estimate the net radiation reaching the soil surface for moisture balance requirements. The soil albedo is entered as the value for bare dry soil and adjusted internally based on soil moisture, vegetation and residue cover during WEPP simulations. Values for albedo can range from 0 to 100 % with fresh snow having an albedo of 0.9 to 0.95 indicating that it reflects 90 % to 95 % of the incoming solar radiation. The *WEPP User Summary* provides Equation [6.1] for estimating soil albedo (Flanagan and Livingston, 1995).

$$SOALB = \frac{0.6}{e^{(0.4 * ORGMAT)}} \quad [6.1]$$

Where

$SOALB$  = soil albedo  
 $ORGMAT$  = quantity of organic matter in the soil sample (%)

The above equation yields an albedo of 0.6 for soils without organic matter, the baseline condition used in the analysis since mine waste is generally void of organics.

#### Initial Saturation

The initial saturation as defined by the *WEPP User Summary* as being the fraction of the porosity filled by water at the beginning of the simulation (Flanagan and Livingston, 1995). Initial saturation can range from 0 to 100%, however, it is recommended that a value of 70% be used which corresponds to approximately 33 kPa (field capacity) for most soils (Flanagan and Livingston, 1995). As a result, 70 % initial saturation was used as a baseline value for the analysis.

#### Empirical Soil Parameters

Each of the empirical soil parameters can be calculated based on cropland or rangeland conditions. Cropland rather than rangeland conditions were chosen when making calculations since tailings or waste rock pile sides themselves more closely represent bared tilled agricultural soil than grassed rangeland conditions. In addition calculation of the empirical soil parameters is dependant on the percentage of sand sized material in the soil. For cropland soils with greater than 30 % sand, the equations for interrill erodibility, rill erodibility and critical shear stress are based on the fraction of Very Fine Sand (*VFS*) whereas soils containing less than 30 % sand are based on the fraction of clay in the sample. The equations suggested for cropland soils with greater than 30 % sand were used for soil erodibility factors since the grainsize distribution being modeled here indicates a composition of approximately 90 % sand.

Interrill Erodibility ( $K_i$ ) reflects the susceptibility of the soil to detachment by raindrop impact and shallow overland flow (Flanagan and Livingston, 1995). The empirical equation for determining interrill erodibility as suggested in the *WEPP User Summary* is Equation [6.2] as follows

$$K_I = 2728000 + 192100(VFS) \quad [6.2]$$

Where

$$\begin{aligned} VFS &= \text{quantity of Very Fine Sand in the soil sample} \\ &= 5 + (\text{SIV } 40 + \text{SIV } 100) / (\text{SIV } 10) + 0.5 * \text{SILT} \end{aligned}$$

And

SIV = United States standard sieve size

The *WEPP User Summary* follows (Flanagan and Livingston, 1995) indicates that if the *VFS* component of a sample exceeds 40 %, then 40 % should be used. Forty percent *VFS* was used to determine the upper bound of interrill erodibility for use in this analysis.

Rill erodibility reflects the susceptibility of the soil to shear detachment by water flowing in rills. Equation [6.3] is provided in the *WEPP User Summary* as follows (Flanagan and Livingston, 1995).

$$K_R = 0.00197 + 0.00030(VFS) + 0.3863e^{(-1.84*ORGMAT)} \quad [6.3]$$

Where

all variables previously defined

The critical shear is a threshold value under which rill detachment does not occur. Again the cropland rather than the rangeland option was chosen since the waste material used here has greater than 30 % sand and Equation [6.4] was therefore used



$$\tau_{cr} = 2.67 + 0.65(CLAY - 0.058)(VFS) \quad [6.4]$$

Where

$CLAY$  = quantity of clay in the soil sample (%)  
all variables previously defined

#### Effective Hydraulic Conductivity

The effective hydraulic conductivity,  $K_e$ , is the final soil user input parameter that is important for determining the infiltration using the Green-Ampt Infiltration model. This parameter is not equivalent to the soil's saturated hydraulic conductivity, but is related to it. The hydrologic soil group of the waste material being used here is group B according to the *WEPP User Summary*. Therefore, Equation [6.5] was used to calculate the effective hydraulic conductivity.

$$K_e = 1.17 + 0.072(SAND) \quad [6.5]$$

Where

$SAND$  = quantity of sand in the soil sample (%)

Flanagan and Livingston (1995) provide ranges of  $K_i$ ,  $K_r$ ,  $\tau_{cr}$  and  $K_e$  for soils of varying textures to be used as comparison when calculating these parameters. Though the range of  $K_e$  values has been determined from a database of agricultural soils, the values calculated for the waste material being used here fall within the range provided by the authors of the WEPP model.

#### Grainsize Distribution

The WEPP Soil Database Editor window allows for 8 different soil layers to be input into the model to a maximum depth of 1.7 m. In modeling the tailings pile used here, the full 1.7 m was incorporated; however, due to the relative uniformity of the material, a single soil layer was entered. The soil characteristics are shown in Table 6.5.

**Table 6.5 WEPP Soil Layer Characteristics**

LAYER NUMBER	DEPTH (mm)	SAND (%)	CLAY (%)	ORGANIC (%)	CEC (meq/100mm Soil)	Rock (%)
1	1700	90	10	0	2	0

The soil input parameters for WEPP require the input of % sand, % clay, % organics and % rock fragments. The WEPP model considers

$$\%SAND = (100 - \%CLAY) \quad [6.6]$$

$$\%CLAY = (100 - \%SAND) \quad [6.7]$$

The % clay is used to estimate soil parameters such as bulk density, porosity, water retention and effective hydraulic conductivity.

During the sensitivity analysis the sand percentage was varied between 70 % sand (30 % clay) and 100 % sand for comparison purposes only. WEPP does not support a grainsize distribution of 100 % sand; therefore during the 100 % sand simulations, a very small percentage of clay was entered (0.0001 %) to avoid any model failures.

A rock fragment percentage was kept at 0 % under baseline conditions and the baseline Cation Exchange Capacity (CEC) was determined from the range of values supplied in *WEPP User Summary* as 2 meq/100 g of soil (Flanagan and Livingston, 1995). The CEC is used in calculating the effective hydraulic conductivity of the soil. For the purpose of this analysis, % rock and the CEC were kept constant.

#### **6.6.2.4 Management**

The management factors were set to reflect the operating conditions at any waste pile. The details of these conditions are provided in Appendix I. Some notable settings are described here. Since the WEPP model has been developed for

agriculture, an initial plant must be chosen in the Management dialogue box. The initial plant is the name of the previous crop grown in the area and options exist to indicate the amount of fertilization that took place. Since vegetation has never existed on bare exposed mine waste piles, this condition is accomplished by setting the initial plant to “Bluegrass”, the Initial Residue Cropping Setting to “fallow” and the number of days since the last tillage and harvest to 10 years prior. In addition, the rill width type was set to temporary allowing the rills to migrate and form randomly as would be expected on an untilled slope. The spacing between rills was set to 0.5 m typical of rill networks.

### **6.6.3 Results of Sensitivity Analysis**

The following sections highlight the key results of the sensitivity analysis. Several analyses were conducted to investigate the runoff amount and erosive potential of the waste pile configuration itself as well as the effects of climate and soil parameters. It should be noted that when the sensitivity of the structural characteristics are being investigated (Section 6.6.3.1), many slope gradients, lengths and bench lengths were used for comparison. However, when the effects of climate and soil properties are analyzed, only the single raise, uniform, 3H:1V hillslope profile with 8 m wide benches is used and compared to the concave hillslope equivalent (Sections 6.6.3.2 and 6.6.3.3). In addition, the sensitivity to runoff and soil loss are reported since in most instances, the computed values for sediment yield differ from those of soil loss by a factor of 10, the conversion between the units used to report soil loss and those used to report sediment yield. The similarity between soil loss and sediment yield results from the severity of the climate in this South East Asian scenario.

#### **6.6.3.1 Sensitivity to Structural Characteristics**

Section 6.6.2.1 and Figure 6.1 provide the details of the structural characteristics used to test the sensitivity analysis. While holding all remaining parameters

constant, several variations to the slope profile were investigated to determine the sensitivity of the slope shape, gradient, length and bench lengths as well as whether multiple raises would contribute significant increases in runoff and soil loss under 100 year continuous simulation conditions.

#### 6.6.3.1.1 Slope Shape

The general conclusion that slope shape has an effect on the average annual runoff from a hillslope and the average annual soil loss was explored using three slope shapes with the WEPP model. The difference in the average annual runoff generated by each of the slope shapes was negligible because the surface area over which the runoff flows is approximately equivalent for all slope shapes. Where differences were observed, the uniform slope shape produced slightly more runoff than the concave and convex shapes due to the slightly smaller surface area and resulting lower infiltration.

In general, the convex slope produced the highest soil loss, followed by the uniform and concave slope shapes. Figure 6.5 shows the difference in soil loss for the slope shapes tested.

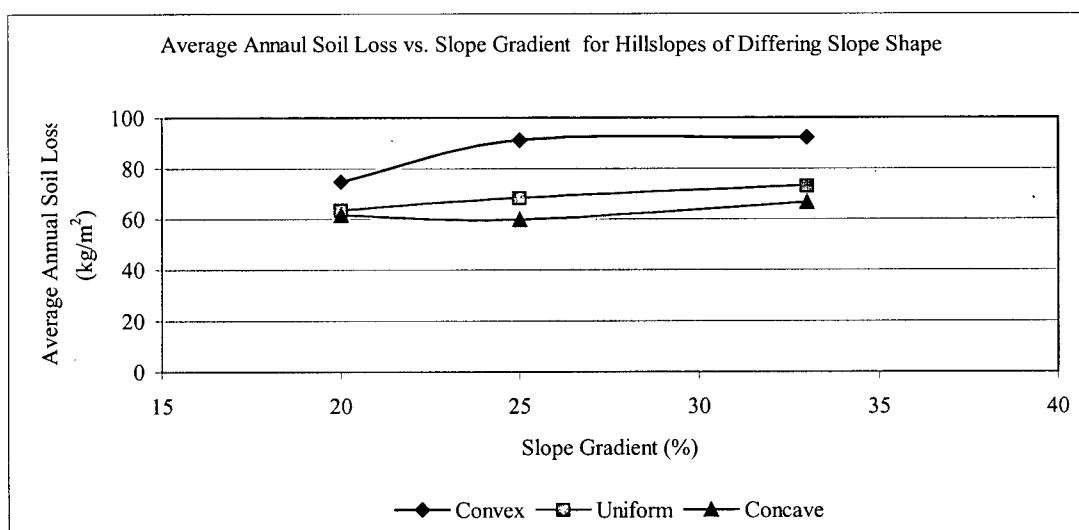


### **Figure 6.5 Comparison of Soil Loss for Different Slope Shapes**

The general observation that the concave slope shape results in a lower soil loss than that of the uniform slope shape is demonstrated continuously when comparisons of such parameters as interrill erodibility, rill erodibility, effective hydraulic conductivity and grain size distribution are made throughout the remaining sections (see Figure 6.12, Figures 6.14 through 6.16, Figures 6.18 through 6.20 and Figures 6.23 and 6.24).

Other researchers have found a similar effect of slope shape on runoff and soil loss as discussed in Section 3.7.3; however, the magnitudes are different likely due to the severity of the climate used in this example. The results reported here indicate that uniform and concave slopes have similar soil loss rates, which are both lower than those found on convex slopes. The WEPP model results show that erosion is not observed on convex plots at the upslope end, but as the flow gains velocity due to the convex shape, erosion is witnessed most severely at the downslope end of the plots. The results also indicate that deposition begins to take place farther upslope on concave and uniform slope profiles of the same slope gradient than on convex slope profiles.

#### **6.6.3.1.2 Slope Gradient**

The key constraint in mine waste management is the necessity to build the storage areas to contain the maximum amount of waste material possible while maintaining structural stability. Thus, often the waste facility height is fixed and as in this example, the pile slope is 3H:1V. Therefore, the slope gradient and length are intimately related and must be evaluated simultaneously. Figures 6.6 and 6.7 show the average annual runoff and soil loss versus bench length respectively for a single raise hillslope of uniform slope shape under various slope gradients.

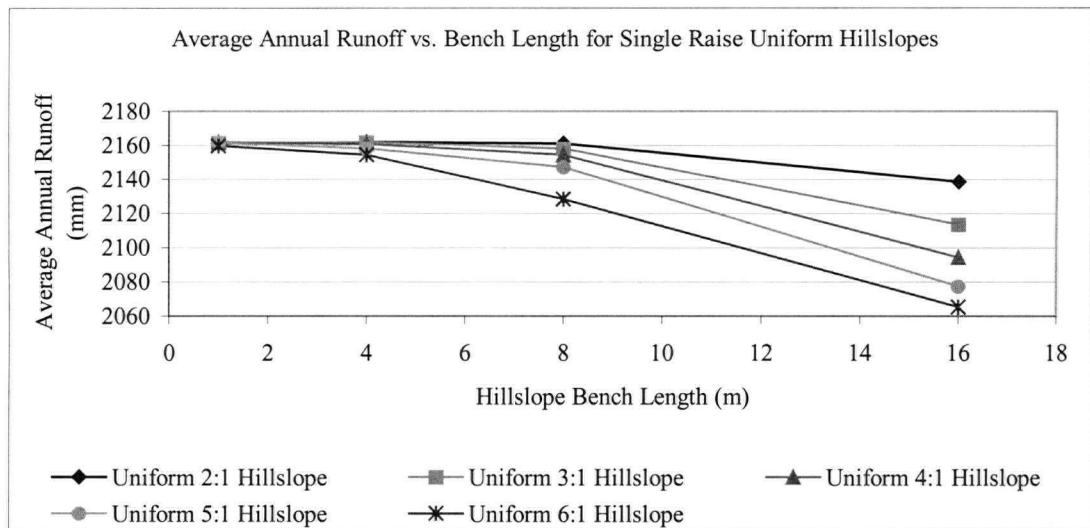


**Figure 6.6 Comparison of Runoff for Single Raise Uniform Hillslopes with Differing Slope Gradients and Bench Lengths**

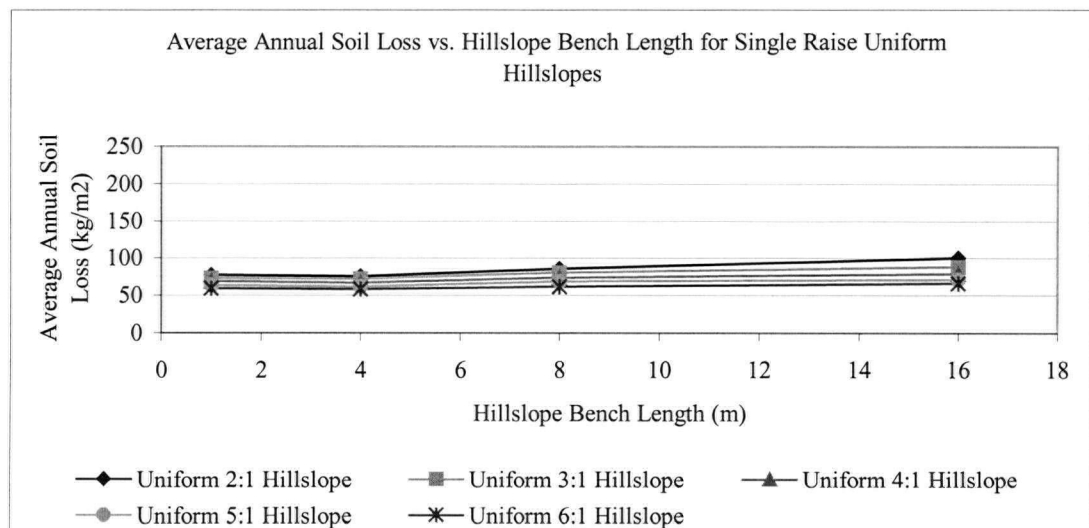


**Figure 6.7 Comparison of Soil Loss for Single Raise Uniform Hillslopes with Differing Slope Gradients and Bench Lengths**

In both cases, as the slope gradient increases, and consequently the slope length decreases, the average annual runoff and the average annual soil loss are increased

regardless of bench length. However, while the average annual runoff decreases as the bench length is increased for each slope gradient, the average annual soil loss is increased as the bench length is increased for each slope gradient.

The increase in average annual runoff that occurs as the slope gradient increases relates to the shorter distance over which the runoff must travel to reach the toe of the slope. The reduction in surface area caused by an increase in slope gradient for the same amount of rainfall applied to the hillslope surface, results in shorter travel time and a reduction in infiltration causing greater annual average runoff to be predicted. This reasoning also explains the reduction in annual average runoff for each increase in bench length for a given slope gradient. Again, as the bench length increases, the surface area over which the runoff travels also increases resulting in an increase in infiltration. Thus, the surface area is not only increased due to the reduction in slope, but also due to the increase in bench length and the effects on runoff are shown in Figure 6.6.

The increase in soil loss with an increase in bench length is due to the increase in surface area. However in contrast to runoff, the increased surface area provides more exposed soil available to be detached as shown in Figure 6.7.

When the dam configurations are considered as shown in the Figures 6.8 and 6.9, the relationships between runoff and soil loss with bench length for each of the slope gradients is linear.

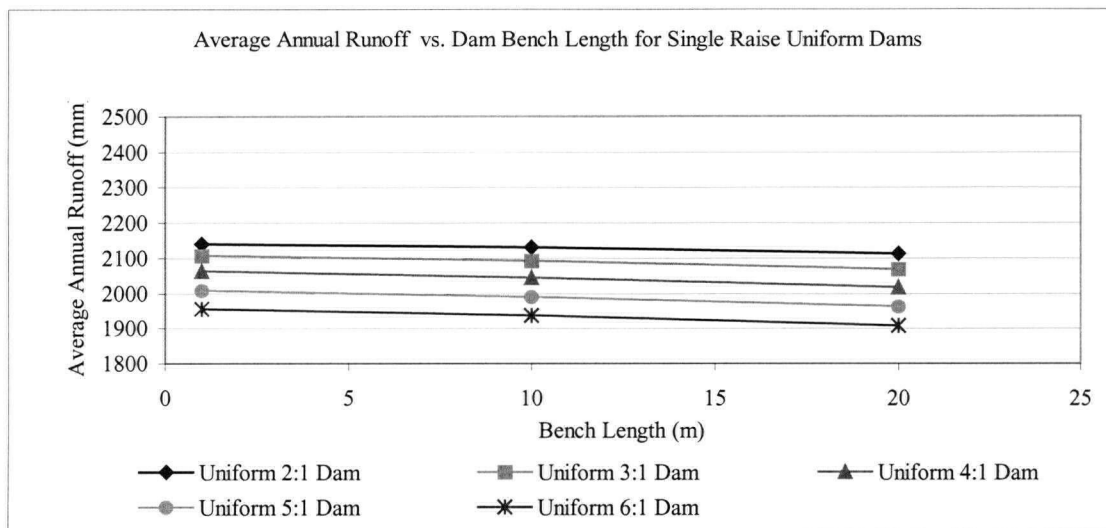


**Figure 6.8 Comparison of Runoff for Single Raise Uniform Dams with Differing Slope Gradients and Bench Lengths**

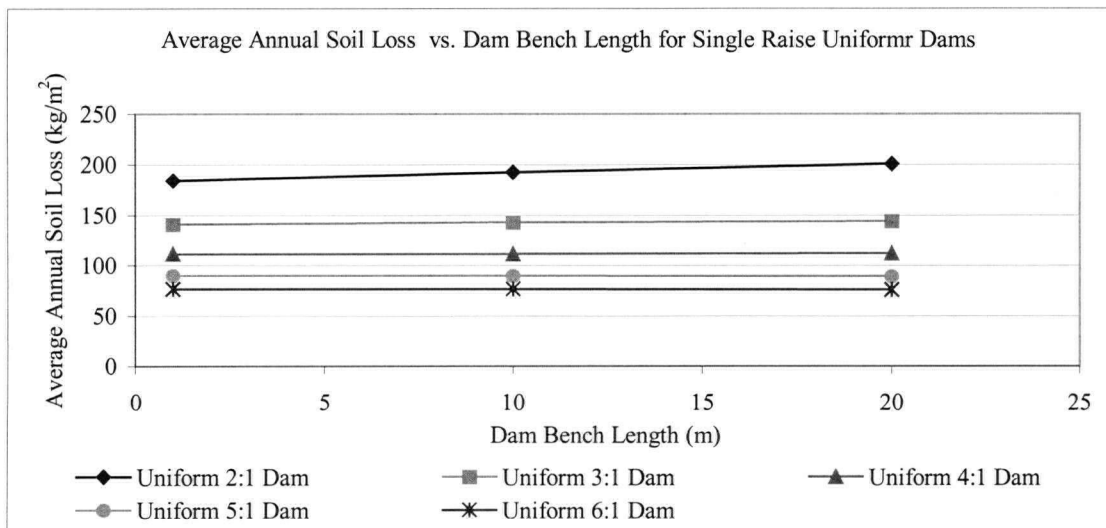


**Figure 6.9 Comparison of Soil Loss for Single Raise Uniform Dams with Differing Slope Gradients and Bench Lengths**

Again as the slope gradient is increased, there is an overall increase in both average annual runoff and soil loss for each bench length. The trend showing a decrease in



average annual runoff with increased bench length is again evident for the dam configurations. However, the linearity between the average annual runoff and the bench length that appears in the dam configuration is unexplained. Finally, the trend in average annual soil loss shown in Figure 6.9 for the dam configuration is similar to that of the hillslope configuration shown in Figure 6.7. Therefore, the factors contributing to this relationship hold for both profiles. However, the magnitudes of soil loss produced are not significantly increased when the downslope distance is increased between the hillslope and the dam configurations.

#### 6.6.3.1.3 Single vs. Multiple Raises

It was continuously observed throughout this sensitivity analysis, that the single raise hillslope and dam configurations produced a greater annual average runoff than the multiple raise configurations for all slope gradients as shown, for example, in Figure 6.10.

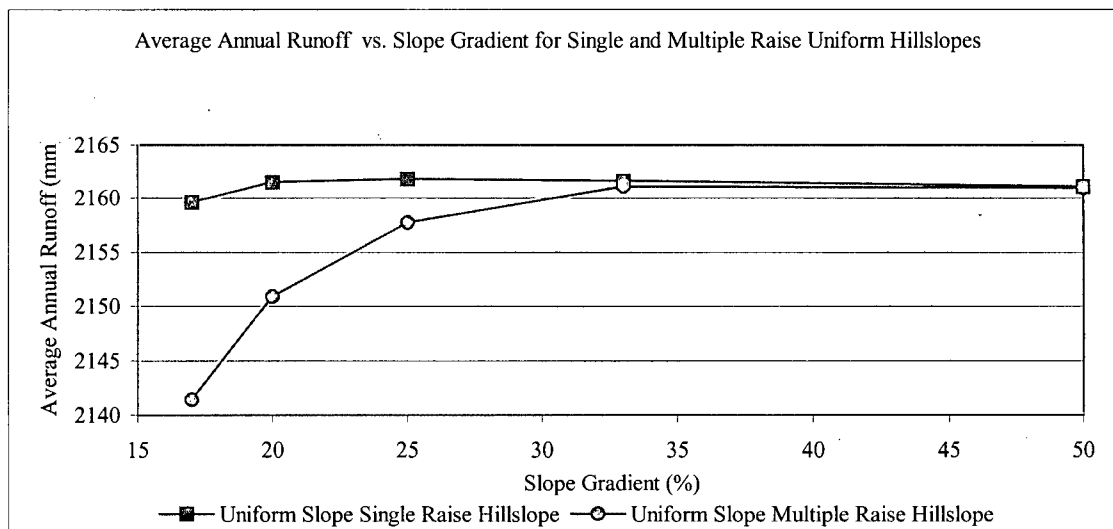


**Figure 6.10 Comparison of Runoff for Single and Multiple Raise Uniform Hillslope Configurations with Differing Slope Gradients**

The difference in average annual runoff between single and multiple raise configurations is again attributed to the difference surface area over which the runoff

travels. Under the single raise configurations, there is less surface area to promote infiltration and the surface area is reduced further when the hillslope of 4 m vertical lift was compared to the dam configuration of 40 m vertical lift.

Figure 6.11 shows the relationship between average annual soil loss for single and multiple raise hillslope configurations only. A similar relationship was noted when the single and multiple raise dam configurations were compared, but is not shown here. In Figure 6.11, it is evident that again due to the increased surface area provided in the multiple configurations, there is more soil available for detachment by overland flow causing greater soil loss values to be computed by the model.

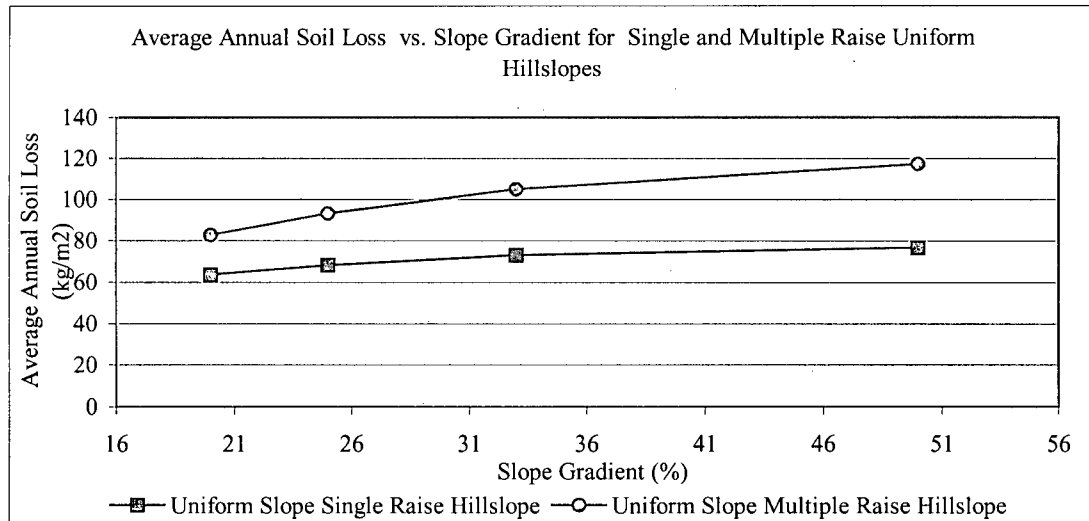


**Figure 6.11 Comparison of Soil Loss for Single and Multiple Raise Uniform Hillslope Configurations with Differing Slope Gradients**

In the previous discussion and Figures, the single and multiple raise hillslope and dam configurations were compared based on increasing the number of lifts and therefore increasing the total height. However, if one of the single raise dam configurations of 40 m high was instead built using two raises of equal height, the effects of terracing could be explored. The results of this analysis show no

difference in the average annual runoff produced between the terraced and un-terraced configuration. This is likely a result of the extreme climate used in the modeling. There was however a slight decrease in the soil loss for the terraced versus the un-terraced conditions demonstrating that terracing does provide a means of reducing soil particle movement.

When the uniform slope profiles for single and multiple raise dams and hillslopes are compared to those of concave slope profiles, the runoff and soil loss patterns are as expected and shown for soil loss only in Figure 6.12.

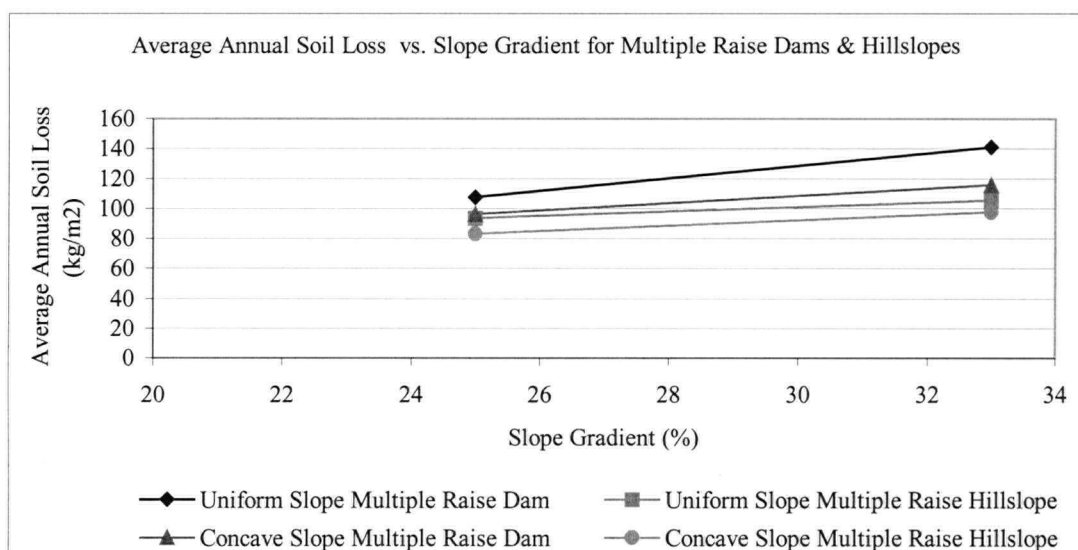


**Figure 6.12 Comparison of Soil Loss for Single and Multiple Raise Hillslopes and Dams of Uniform and Concave Slope Shapes with Differing Slope Gradients**

In both the hillslope and dam configurations under both single and multiple raise situations, the uniform slope shape produces a greater amount of soil loss than does the concave slope configuration for the slope gradients shown. This was discussed in Section 6.3.1.1.

### 6.6.3.2 Climatic Conditions

Using the uniform and concave 3H:1V single raise hillslope profiles, 100-year continuous simulation and single event based modes were used to assess average annual runoff and soil loss.

Under the continuous simulation conditions, a climate file representing an extreme climate in South East Asia was developed, as discussed in Section 6.6.2.2. Three additional climates were arbitrarily chosen for comparison and CLIGEN generated long-term climate files were created. These stations are listed in order of increasing rainfall amount and include Anacortes, Washington (652 mm/year), Key West, Florida (959 mm/year) and Hawaii Volcanoes National Park, Hawaii (4855 mm/year). Results of the simulations showed that average annual runoff and soil loss increased as the rainfall amount and intensity increased with each climate station as shown in Figures 6.13 and 6.14. However the difference in annual average runoff generated for each of the two slope shapes was negligible as shown in Figure 6.13.

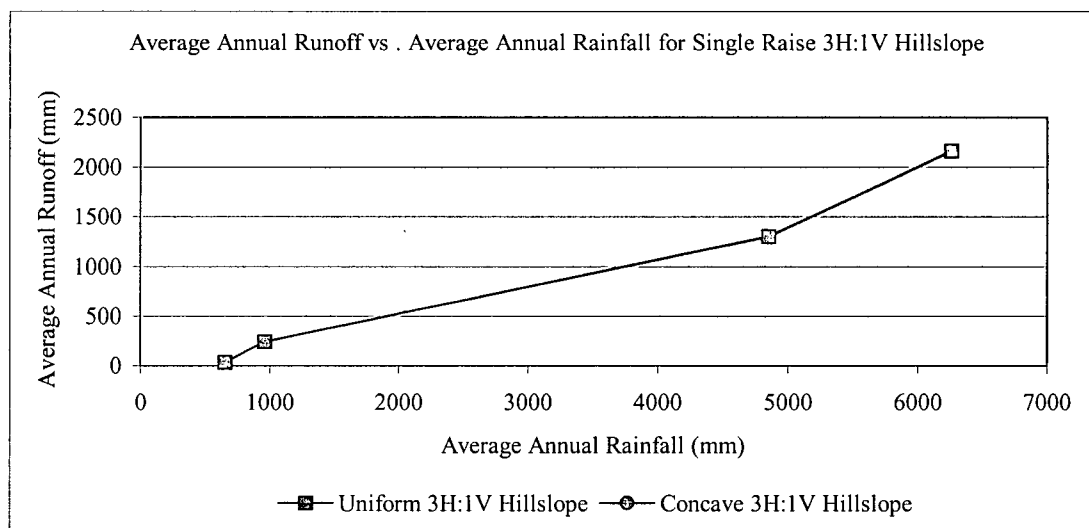


**Figure 6.13 Comparison of Runoff for Uniform and Concave Hillslope Under 100-year Continuous Simulation Climate Conditions**

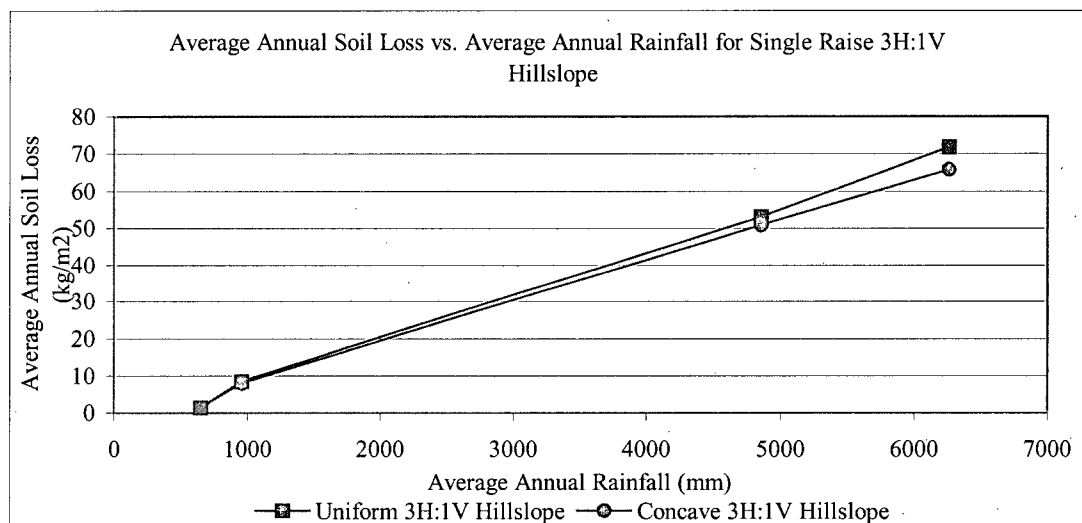


**Figure 6.14 Comparison of Soil Loss for Uniform and Concave Hillslopes Under 100-year Continuous Simulation Climate Conditions**

The soil loss occurring on the uniform and concave slope profiles diverge as the rainfall amount and intensity increase (see Figure 6.14). As reported previously, the uniform slope profiles consistently demonstrate greater annual average soil loss when compared to that of the uniform slope shape.

As indicated in Section 3.2.1, the rainfall intensity rather than the rainfall amount is the most significant in determining soil erosion. Therefore, using the single storm mode of the WEPP model, the rainfall intensity was varied to evaluate the effects on runoff and soil loss. The results of the single storm simulation show that the runoff is very similar for each of linear and concave slope profiles modeled and the single storm soil loss quantities are lower for the concave profiles than for the uniform profiles.

Figure 6.15 shows that as the peak rainfall intensity increases, there is an increase in the storm soil loss. It also reconfirms that uniform slopes contribute more soil loss than do concave slopes. It is interesting to note that the relationship shown in Figure 6.15 is non-linear indicating that under high rainfall intensities, the concave slope shape has a greater effect in reducing soil loss than does the uniform slope shape.

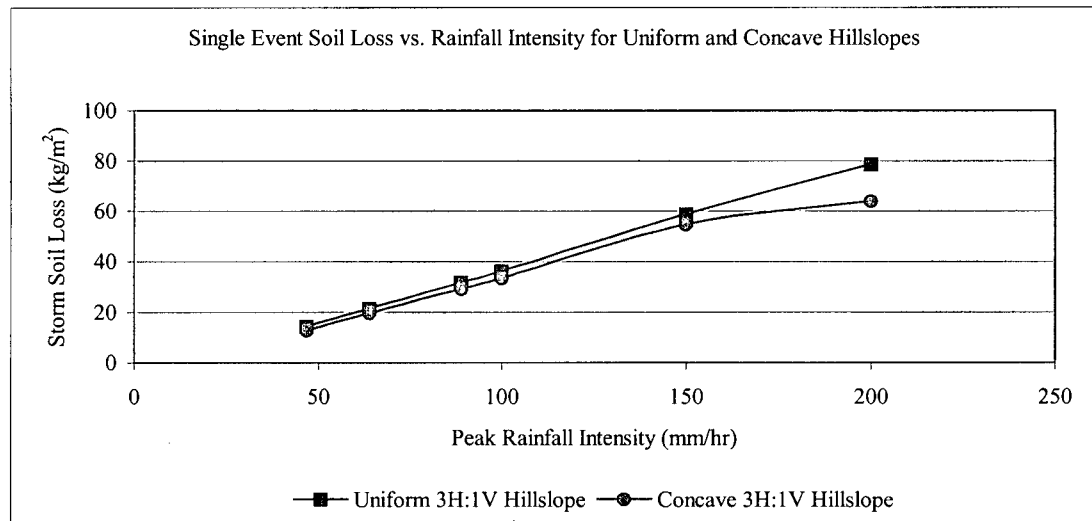


**Figure 6.15 Comparison of Single Event Soil Loss for Uniform and Concave Hillslopes**

### 6.6.3.3 Soil Parameters

Of the soil parameters that can be modified within the WEPP model, the following were used in the sensitivity analysis and are discussed in the sections that follow.

- Interrill Erodibility,  $K_i$ ;
- Rill Erodibility,  $K_r$ ;
- Critical Shear Stress,  $\tau_{cr}$ ;
- Effective Hydraulic Conductivity,  $K_e$ ; and
- Grainsize Distribution.

#### 6.6.3.3.1 Interrill Erodibility

Changes to the magnitude of the interrill erodibility factor,  $K_i$  do not have an effect on the amount of annual average runoff generated over the hillslope. The interrill erodibility factor attempts to explain variations in soil properties that affect soil detachment by raindrop impact. Changes in the average annual runoff occur as a result of structural characteristics such as slope shape, slope gradient and slope length. Results of the sensitivity analysis indicate that there is an optimum sediment composition that results in a minimum soil loss by interrill processes. Since the interrill erodibility factor is calculated based on the percentage of *VFS* in the sediment sample, a sample containing approximately 20 % *VFS* will be the most resistant to interrill soil loss for the climate conditions modeled here and as shown in Figure 6.16. Consequently, a soil with a different sediment composition will have an alternative optimum interrill erodibility factor.

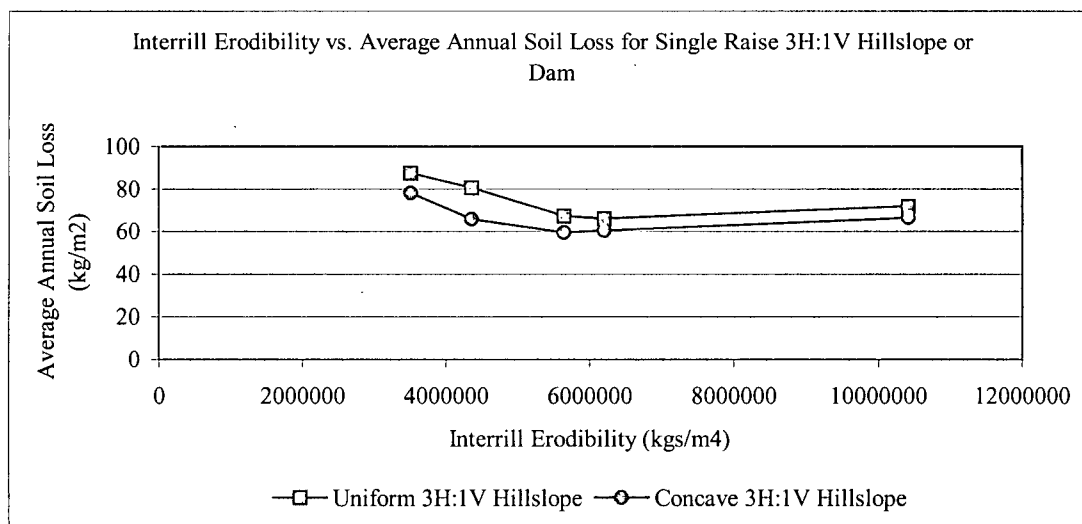


**Figure 6.16 Comparison of Interrill Erodibility and the Effect on Soil Loss for 3H:1V Hillslopes of Linear and Concave Configuration**

It was noted from the Main WEPP Output file that rill erosion occurs near the crest of the slope. This is due to the extreme rainfall conditions and the steep slope

gradient of the structural characteristics modeled here therefore facilitating the concentration of flow as it moves from the 8 m wide bench area to the slope face.

The location at which the rills begin to develop as shown in the Main WEPP Output file does not change regardless of the interrill erodibility factor or the slope shape. When the Main WEPP Output file is analyzed, it is clear that interrill erosion takes place in the upper 1 m of the slope lengths being modeled and the remaining slope length is dominated by rill erosion. Under such severe climatic conditions as modeled here rills begin to develop at the top of the slope and therefore, the effects of slope shape on the average annual soil loss are due largely to the effects of rill erosion.

Under agricultural slope gradients and moderate climates, it is expected that interrill erosion will dominate near the crest of the slope and rill erosion will begin at some point further downslope. Therefore, in order to evaluate the sensitivity of the interrill erodibility factor more effectively, short slopes were also modeled. Though these slopes do not exist at most mine waste stockpiles, they do provide a better indication of the sensitivity of the interrill erodibility factor for future use of the WEPP model. In this evaluation, the 3H:1V slope gradient was utilized and the horizontal slope distance was reduced 80 %. Results indicate that changing the interrill erodibility factor results in a greater change in average annual soil loss for short slopes than was observed for longer slopes since the effects that rill erosion have on soil loss are minimized by using short slope lengths.

In areas dominated by interrill erosion, rill erosion accounts for a smaller amount of the total soil loss. As a result, the sediment load of the overland flow is low relative to the transport capacity indicating, as discussed in Section 3.7.1, that interrill erosion is important on detachment limiting areas where rilling is not prevalent. It



should be noted however, that the effect of slope shape on soil loss due to variations in the interrill erodibility factor is negligible.

Since the equation used to determine the soil loss by interrill processes is based on the square of the rainfall intensity, the sensitivity of soil loss on interrill areas is more evident when the model is run in single event mode. For storms with intensities greater than 150 mm/hr, the quantities of soil loss from interrill areas are much greater than that caused by storms of for example 100 mm/hr as shown in Figure 6.17.

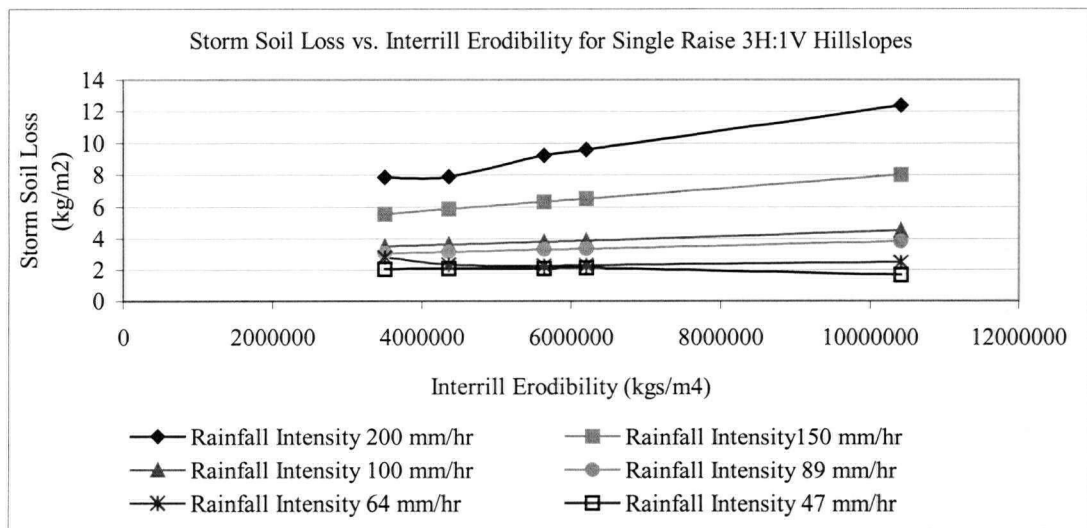


**Figure 6.17 Comparison of Interrill Soil Loss for Various Single Event Storm Intensities**

#### 6.6.3.3.2 Rill Erodibility

Like the interrill erodibility factor, changes in average annual runoff do not occur with changes in the rill erodibility factor,  $K_r$ , which attempts to explain the variation in soil properties that affect soil detachment by overland flow. Changes to the average annual soil loss with changes in the rill erodibility factor under 100-year continuous simulation conditions are shown in Figure 6.18.

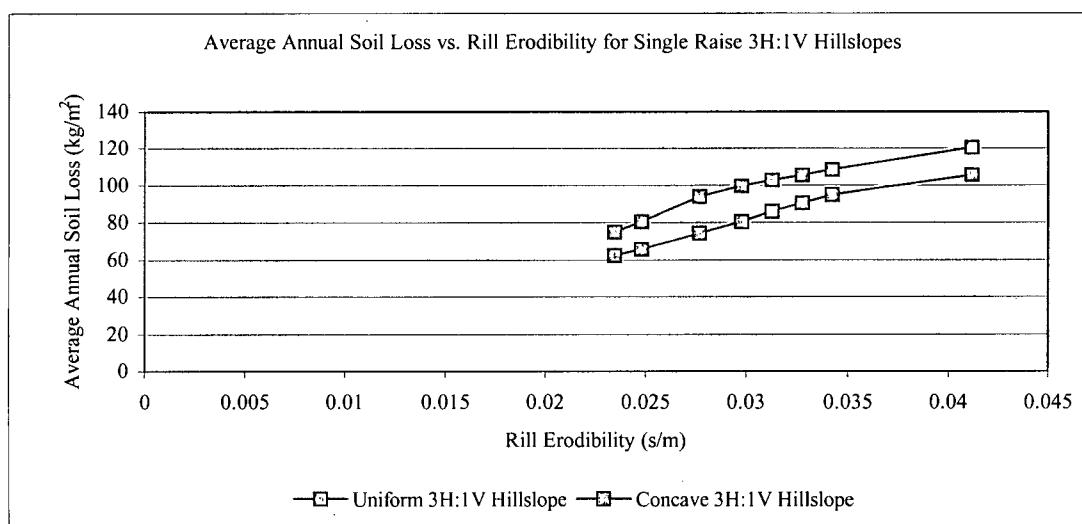


**Figure 6.18 Comparison of Soil Loss for Uniform and Concave Hillslopes for Differing Rill Erodibility Factors**

Soil loss is more sensitive to the rill erodibility factor than the interrill erodibility factor for this example when Figures 6.18 and 6.16 are compared. Although the rainfall used in this example is intense due to the climatic conditions a majority of the soil loss that is estimated by the WEPP model is due to rill erosion as determined when the Main WEPP Output file was inspected.

#### 6.6.3.3.3 Critical Shear Stress

Sediment detachment predictions are more sensitive to the interrill and rill erodibility parameters than the critical shear stress. In this case, where the rainfall rate is high and the critical shear stress is easily overcome by excess runoff, this parameter does not demonstrate significant sensitivity in the WEPP continuous simulation analysis. In Section 2.5.9, it was determined that the critical shear can be omitted from many overland flow equations when it is easily exceeded.

#### 6.6.3.3.4 Effective Hydraulic Conductivity

As expected, the model response to changes in the effective hydraulic conductivity,  $K_e$  shows the highest degree of sensitivity to runoff and soil loss of all of the empirical soil parameters. As the  $K_e$  increases, the amount of rainfall that enters the soil increases and therefore the runoff rate and soil loss decrease as shown in Figures 6.19 and 6.20.

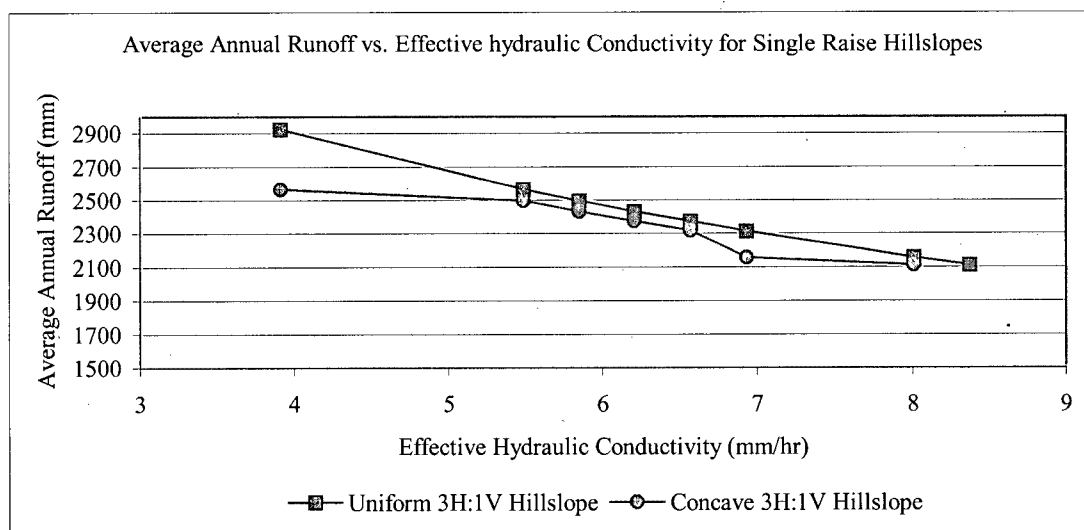


**Figure 6.19 Comparison of Runoff for Single Raise Uniform and Concave Hillslopes for Differing Effective Hydraulic Conductivity Values**

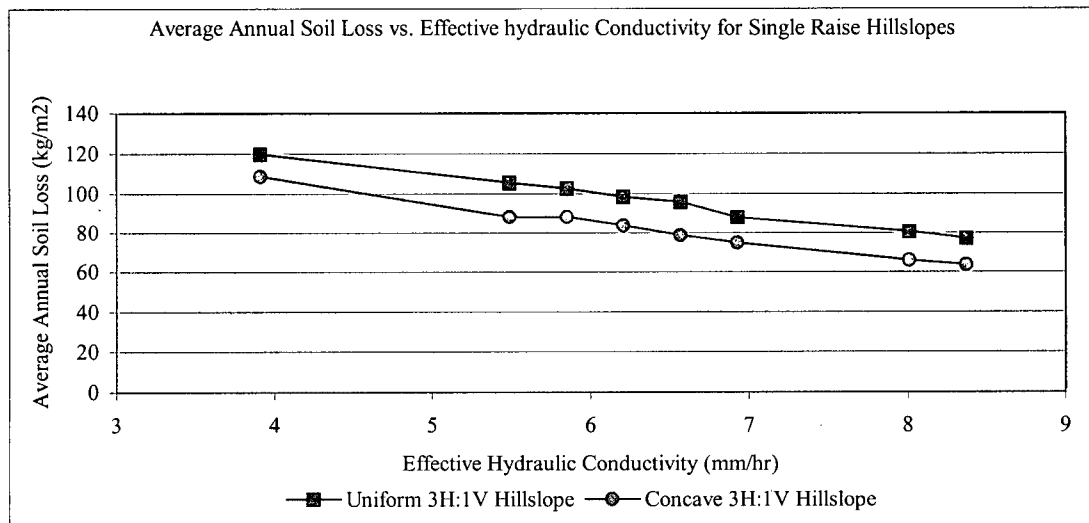


**Figure 6.20 Comparison of Soil Loss for Single Raise Uniform and Concave Hillslopes for Differing Effective Hydraulic Conductivity Values**

When the effects of effective hydraulic conductivity were investigated under single storm conditions, the parameter did not appear to be significantly sensitive (see Figure 6.21 and 6.22). However, under increasingly high rainfall intensities, there is a notable increase in soil loss produced for all effective hydraulic conductivity values tested.

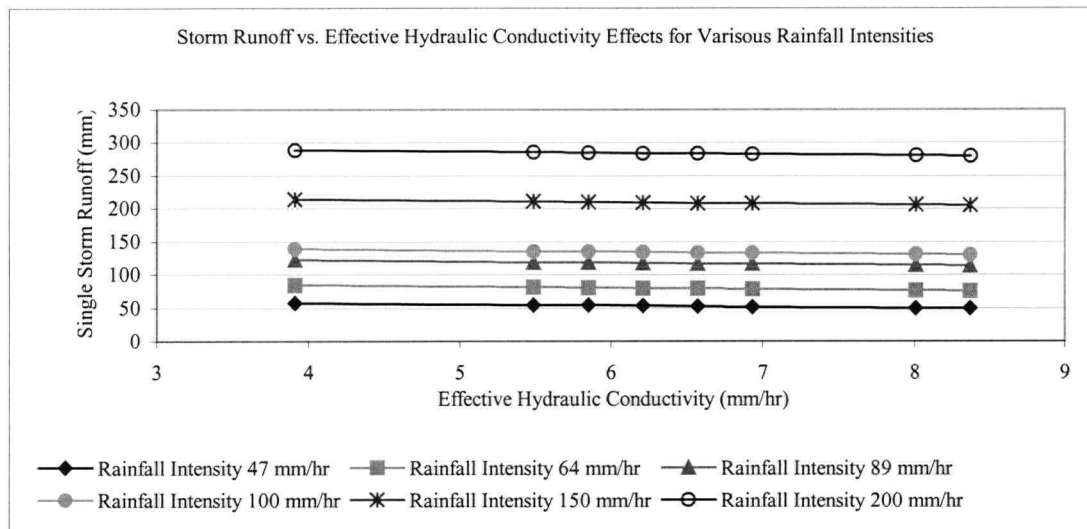


**Figure 6.21 Effect of Single Storm Rainfall Intensity on Runoff for Single Raise Uniform 3H:1V Hillslopes Under Differing Effective Hydraulic Conductivities**

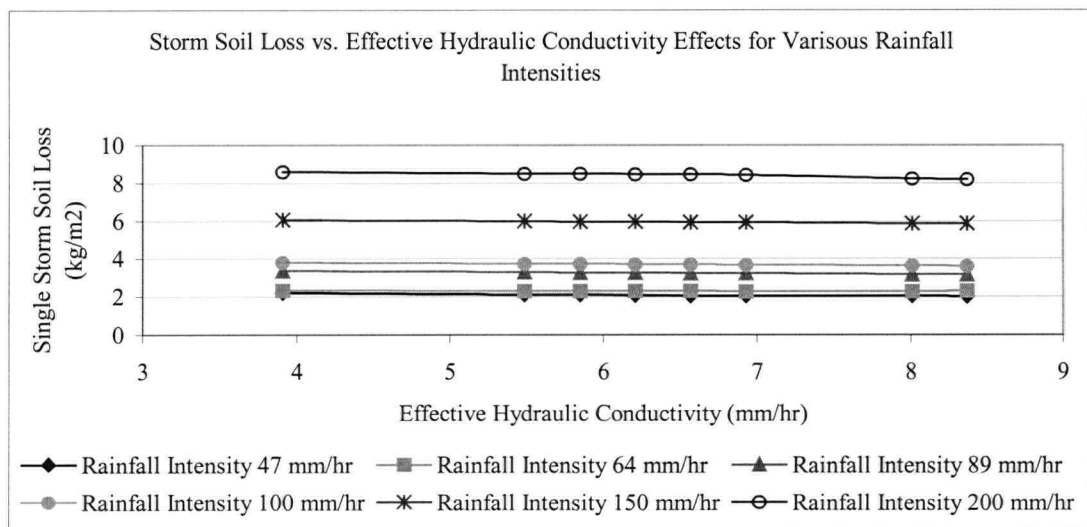


**Figure 6.22 Effect of Single Storm Rainfall Intensity on Soil Loss for Single Raise Uniform 3H:1V Hillslopes Under Differing Effective Hydraulic Conductivities**

#### 6.6.3.3.5 Grainsize Distribution

Since several of the model parameters are based on clay and sand fraction of the sediment, the sensitivity of the soil texture or grainsize distribution is high. The parameters that require grainsize information for further calculation are:

- Erodibility parameters;
- Infiltration parameters;
- Hydraulic friction factors;
- Rill widths; and
- Transportability of the sediment

As indicated in Figure 6.23, a peak in the average annual runoff occurs at approximately 80 % sand which corresponds to 20 % clay based on Equations 6.6 and 6.7 from Section 6.6.2.3 and this is consistent with the average annual soil loss displayed in Figure 6.24.

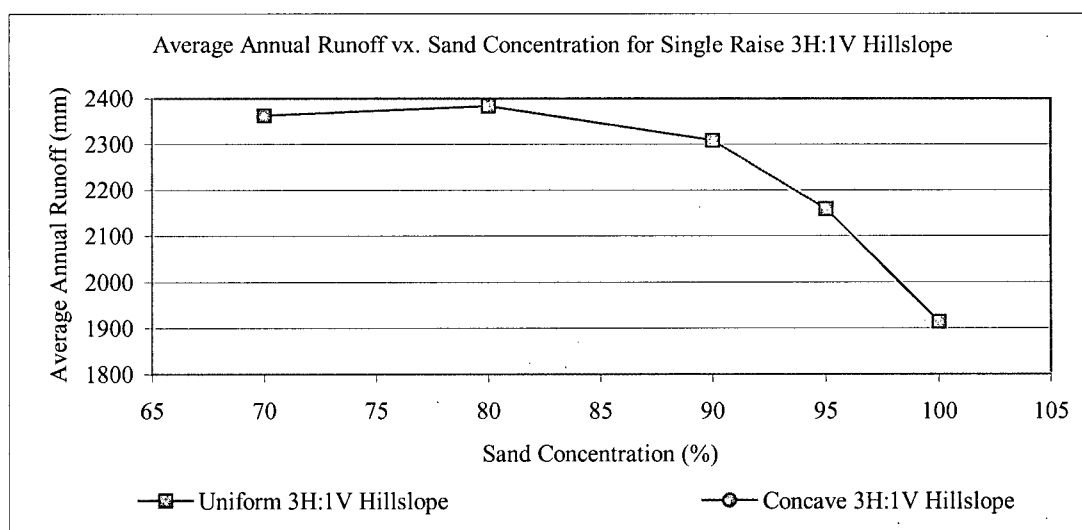


**Figure 6.23 Effects of Sand Concentration on Average Annual Runoff**

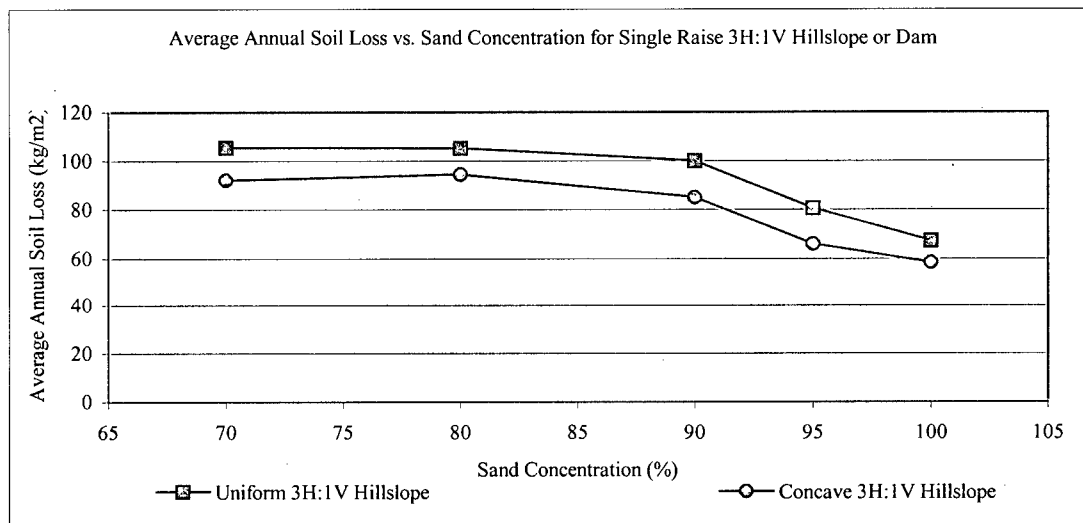


**Figure 6.24 Effect of Sand Concentration on Average Annual Soil Loss**

As the sand fraction in the mixture increases, the weight of each of the particles makes them less susceptible to detachment and transport by the overland flow. However, it appears that as the sand concentration decreases and consequently the clay fraction increases, the erosion of the media increases.

Determining the erodibility of a more clay rich media would require re-calculation of new erodibility factors to take into account high clay contents. As indicated in Section 6.6.2.3, the textural characteristics of the sediment used in this example required calculation of the erodibility parameters based on cropland soils with greater than 30 % sand. Therefore, variation within the range chosen (100 % sand to 70 % sand) is justified for sensitivity investigations in this example. However, due to the complex relationships between the soil characteristics and the variations that the erodibility parameters explain, re-calculation of the erodibility parameters would be required to investigate the sensitivity of a clay rich media (i.e. a cropland soil with < 30 % sand).



#### 6.6.3.3.6 Summary

The results of the sensitivity analysis shown here indicate that of the parameters tested, the climate provides the most change in runoff and soil loss. Sensitivity to runoff production was noted when the textural characteristics were varied as well as in variation of the effective hydraulic conductivity. Sensitivity to soil loss prediction was highest for the texture analyses under continuous simulation conditions. Of the empirical parameters, the effective hydraulic conductivity and rill erodibility showed the most sensitivity and as expected, the interrill erodibility is the parameter most affected by storm intensity when the single storm simulations were conducted. Of the structural characteristics investigated, the slope shape was the most significant in reducing the amount of soil loss predicted while the amount of runoff generated was not significantly different between the slope shapes tested. Increases in slope length due to increased bench length, single or multiple configurations, as well as the hillslope and dam profiles consistently decreased the amount of runoff generated and increased the amount of soil loss that occurred.

The values for soil loss predicted by the WEPP model for this example are significantly greater than those reported in the literature and quoted in Section 2.2 above. Since there are no means of verifying the results of this analysis and no means of calibrating the input parameters to those that would be expected in the field, no firm conclusions can be drawn regarding the values reported here. The only observations that can be made are the general trends in runoff and soil loss that occur due to variations in model parameters. Again no studies were published using the WEPP model on mine waste of similar origin and therefore the results of the calibration and validation studies shown here are for agricultural or rangeland applications.

One conclusion that can be drawn is that the climate encountered in this example pushes the limits of the capabilities of the WEPP model especially in the continuous simulation mode.

#### **6.6.3.4 WEPP Model Calibration**

Although not recommended, Favis-Mortlock (1998) reports that in some cases, the WEPP model is able to produce acceptable results without calibration. Due to the severe climate conditions and the homogeneity of the sediment used in this example, both of which force the limits of the capabilities of the model, calibration is mandatory any site with similar characteristics. The parameter that requires the most calibration effort is the effective hydraulic conductivity.

#### **6.6.3.5 WEPP Model Validation**

Validation of the WEPP Hillslope and Watershed models has taken place for a variety of model releases for a range of cropping and management conditions. The following provides some of the general conclusions from studies published determining the WEPP model accuracy in predicting runoff and soil loss.

When comparing the CLIGEN generated long-term weather files with the natural rainfall event pattern in Queensland, Australia, Yu and Rosewell (2001) find that WEPP under predicts the number of events that occurred each year. Under closer examination, it is shown that WEPP over predicts the number of events in the early part of the simulation and under predicts the number of events in the latter stages. When ranking the runoff and soil loss events to determine return periods, the under prediction of events is especially noticeable at lower recurrence intervals.

Tiwari *et al.* (2000) report that there is an apparent phenomenon whereby erosion models overestimate low values of measured soil loss and underestimate large values

of measured soil loss and this observation includes the WEPP model. Since runoff and soil loss values are directly related, this conclusion is further supported by a study by Risse *et al.*, (1993) who indicate that runoff from smaller events is over predicted and runoff for larger events is under predicted by WEPP. Conclusions from Zhang (1996) confirm this pattern of runoff and soil loss.

Risse *et al.*, (1995) offer the explanation that for small events a smaller proportion of the hillslope area is actually contributing runoff than for larger events. However, since the model considers that the entire hillslope is contributing to the runoff volume, the model will over predict the runoff for these smaller events. This idea of partial area response hydrology was mentioned as a limitation to the WEPP model in Section 5.4.

Using horizontal slope lengths of 20.73 m, 41.35 m and 62.08 m, Yu and Rosewell (2001) conclude that WEPP over predicts the amount of soil loss for plots of the two longer slope lengths. In addition, observed runoff amounts decreased as slope length increased; however in their study, WEPP did not adequately show this trend. In the above sensitivity analysis, the trend in a reduced runoff amount with increased slope length was evident. Since some researchers have indicated that the WEPP model gives more reliable estimates of relative rather than absolute rates of erosion (Favis-Mortlock, 1998), this conclusion is probably the most suitable means of viewing the model results provided here.

## CHAPTER 6 – LIST OF SYMBOLS

SYMBOL	DESCRIPTION
<i>SOALB</i>	soil albedo
<i>ORGMAT</i>	quantity of organic matter in the soil sample (%)
<i>VFS</i>	quantity of Very Fine Sand in the soil sample
<i>SIV</i>	United States standard sieve size
<i>CLAY</i>	quantity of clay in the soil sample (%)
<i>SAND</i>	quantity of sand in the soil sample (%)

## 7. CONCLUSIONS

The impact of mine sites is important for environmental protection and estimations of toxins migrating off-site is often required at many stages of the mine permitting process. Though chemical migration from tailings and waste rock dumps is the primary cause for concern, the physical migration of mine waste from storage sites has been seen to cause sedimentation problems in local streams, rivers and low-lying areas. Since soil erosion mechanics has been developed in the agriculture and forestry industries, questions have arisen as to the wider applicability of the prediction tools designed for these land uses. This thesis was undertaken to provide a detailed overview of the current status of the water erosion process, to explore the relationships between the factors that contribute to the accelerated erosion process, and to identify where possible the limits and threshold conditions that have been determined. These relationships, limits and thresholds were, where possible related to those encountered in the mining industry. Understanding the complexities involved in predicting accelerated erosion rates facilitated an evaluation of the current tools available again highlighting those most desirable to the mining industry. Finally an overview of the WEPP model and a sensitivity analysis using mine waste characteristics from a typical oxide/sulphide mine were undertaken.

The following conclusions are made based on the current status of knowledge of the erosion process in the literature.

- Erosion research has divided the processes into the mechanisms of soil detachment and transport and consequently equations describing each of these have been derived.
- The upland erosion process can be divided into four sub-processes:
  1. Detachment by Rainfall;
  2. Transport by Rainfall;
  3. Detachment by Runoff; and

#### 4. Transport by Runoff.

And each is significant depending on whether it occurs during the interrill or rill erosion process.

- Several empirical soil parameters are used to describe soil properties and consequently to predict the rate of erosion on interrill and rill areas.
- The equations developed for the estimation of transport capacity distinguish the erosion prediction tools from one another.
- A notable physically based detachment equation was determined by Owoputi (Owoputi, 1994) and the principles of this equation should be incorporated into state-of-the-art erosion prediction tools.

A review of the relationships that accelerate the upland erosion process by water show the following:

- Generally authors conclude that runoff velocity contributes to an increase in erosion rates. However, substantial research has not been undertaken to investigate the relationships between runoff and seepage or runoff and infiltration rates that complicate the runoff process.
- The soil texture plays a significant role in determining whether erosion will take place and is a simple factor to measure in the laboratory. However, many researchers caution that texture alone cannot be used to determine the rates of soil erosion.
- There is a trade-off between the amount of clay content in the soil and the erosion rates. Those soils high in clay content can experience high chemical strength that requires high flow shear stresses for particle detachment; however cohesionless sands may also require high flow shear stress to overcome their weight under the force of gravity.

- There are differences between agricultural soil properties and mining soil properties that cannot be accounted for in the erosion models currently available. Therefore it is necessary to determine the erodibility parameters of the mining material being tested prior to the use of any erosion prediction tool.
- The slope shape can have a significant effect on the amount of soil loss that occurs. Concave slopes are shown to have lower erosion rates compared with uniform, concave and complex slope shapes. However, when this theory was investigated using the WEPP model, the effects of slope shape on runoff were negligible.
- Literature reported values of the effects of vegetation cover indicate that a significant amount of soil loss can be prevented due to a small increase in vegetation cover

The review of the erosion models available and their applicability to the mining industry is as follows:

- Though the ease of application of the USLE makes it convenient for estimating average annual erosion rates, it is not recommended for use in the mining industry because the range of soils and slope gradients commonly encountered in mining situations fall outside those for which the USLE was originally designed.
- Though the RUSLE is likely the only equation that takes into account the variability in the soil types encountered in the mining industry, it is again only an extension of the USLE and provides estimates of average annual soil loss.
- The WEPP, GUEST and EUROSEM models are recommended for use in the mining industry due to their more physically based approach.
- It should be noted that the physical nature of these models is evident in their links between the modules of soil, climate, hydrology and vegetation and not

within the single modules themselves. As a result, these models still incorporate some empirical parameters to predict soil erosion rates.

- The WEPP model is advantageous in that it provides the means to evaluate erosion rates under both continuous simulation and event based conditions.
- The breadth of erosion models that have been designed for agricultural purposes is extensive. These models however have likely been developed for other purposes and use erosion as a means of determining, for example, the economic productivity of soil over the long term or the fate of agro-chemicals.

The sensitivity analysis conducted in South East Asian climate indicates the following:

- As slope length increases for each slope gradient the rate of runoff decreases.
- As slope length increases for each slope gradient the rate of soil loss increases.
- Of the soil erodibility parameters, the effective hydraulic conductivity and rill erodibility factors are the most sensitive to the prediction of soil loss as compared with the interrill erodibility factor and the critical shear stress.
- The effective hydraulic conductivity factor and the textural characteristics of the mine waste material have the most effect on the average annual runoff rate predicted.
- The interrill erodibility factor is the most sensitive to the change in rainfall intensities under single event conditions.
- When the climate is investigated, the severity of the climate factors including rainfall intensity resulting rainfall excess and the duration of runoff are significant in determining the amount of erosion that takes place under both single event and continuous simulation conditions.



## REFERENCES

- Ahrens, C. D. (1991). Meteorology Today An Introduction to Weather, Climate and the Environment. St. Paul, West Publishing Company.
- Al-Durrah, M. M. and Bradford, J. M. (1981). "New Methods of Studying Soil Detachment by Waterdrop Impact." Soil Science Society of America Journal **45**(1): 949-953.
- Al-Durrah, M. M. and Bradford, J. M. (1982). "Parameters for Describing Soil Detachment Due to Single Waterdrop Impact." Soil Science Society of America Journal **46**(4): 836-840.
- Alonso, C. V. (1981). "Estimating Sediment Transport Capacity in Watershed Modeling." Transactions of the American Society of Agricultural Engineers **24**(5): 1211-1220, 1226.
- Ariathurai, R. and Arulanandan, K. (1978). "Erosion Rates of Cohesive Soils." Journal of the Hydraulics Division **104**(HY2): 279-283.
- Arnold, J. G. and Williams, J. R. (1995). A Watershed Scale Model for Soil and Water Resources Management. Computer Models of Watershed Hydrology. V. P. Singh. Highland Ranch, Water Resources Publications: 847-908.
- ASCE (1975). Sedimentation Engineering. New York, ASCE.
- Baffaut, C. (1995). "Impact of CLIGEN Parameters on WEPP-Predicted Average Annual Soil Loss." Transactions of the American Society of Agricultural Engineers **39**(2): 447-457.
- Bagnold, R. A. (1966). An Approach to Sediment Transport Problem from General Physics.
- Ballard, T. (1999). Soil Science 200 Class Notes. Vancouver, University of British Columbia.
- Barfield, B. J. (1988). "Compaction Effects on Erosion of Mine Spoil and Reconstructed Topsoil." Transactions of the American Society of Agricultural Engineers **31**(2): 447-452.
- Bates, R. L. and Jackson, J. A. (1984). Dictionary of Geological Terms. New York, Doubleday.

Beasley, D. B. (1980). "ANSWERS: A Model for Watershed Planning." Transactions of the American Society of Agricultural Engineers **23**(4): 938-944.

Bhuyan, S. J. (2002). "Soil Loss Predictions with Three Erosion Simulation Models." Environmental Modelling and Software: With Environmental Data News **17**: 137-146.

Bouraoui, F. and Dillaha, T. A. (1996). "ANSWERS-2000: Runoff and Sediment Transport Model." Journal of Environmental Engineering **122**(6): 493-502.

Bradford, J. M. (1987). "Interrill Soil Erosion Processes: 1. Effect of Surface Sealing on Infiltration, Runoff and Soil Splash Detachment." Soil Science Society of America Journal **51**(6): 1566-1571.

Bradford, J. M. and Huang, C. (1993). "Comparison of Interrill Soil Loss for Laboratory and Field Procedures." Soil Technology **6**(2): 145-156.

Brady, N. C. and Weil, R. R. (1996). The Nature and Properties of Soils. Upper Saddle River, New Jersey, Prentice Hall.

Bubenzer, G. D. and Jones, B. A. (1971). "Drop Size and Impact Velocity Effects on Detachment of Soils Under Simulated Rainfall." Transactions of the Association of Agricultural Engineers **14**(1): 625-628.

Bubenzer, G. D. and Meyer, L. D. (1965). "Simulation of Rainfall and Soils for Laboratory Research." Transactions of the American Society of Agricultural Engineers **8**(1): 73 & 75.

Carroll, C. (2000). "Impact of Vegetation Cover and Slope on Runoff, Erosion and Water Quality for Field Plots on a Range of Soil and Spoil Materials on Central Queensland Coal Mines." Australian Journal of Soil Research **38**(2): 313-327.

Chen, C. N. (1974). Evaluation of Control of Erosion in Urbanising Watersheds. Proceedings of the National Symposium on Urban Rainfall and Runoff and Sediment Control, Lexington, USA, University of Kentucky.

China, S. S. (1985). "The Effect of Soil Air Entrapment on Soil Erosion During Simulated Rainfall." Transactions of the American Society of Agricultural Engineers **28**(5): 1598-1601.

Chorley, R. J. (1959). "The Geomorphic Significance of Some Oxford Soils." American Journal of Science **257**(1): 503-515.

Chu, S. T. (1978). "Infiltration During an Unsteady Rain." Water Resources Research **14**(3): 461-466.

Craig, R. F. (1992). Soil Mechanics. London, Chapman & Hall.

Curtis, W. R. (1971). "Terraces Reduce Runoff and Erosion on Surface-Mine Benches." Journal of Soil and Water Conservation **26**: 198-199.

Dunne, T. and Black, R. D. (1970). "An Experimental Investigation of Runoff Production in Permeable Soils." Water Resources Research **6**(2): 478-490.

Dunne, T. (1975). "Recognition and Prediction of Runoff Producing Zones in Humid Regions." Hydrological Sciences Bulletin **20**(3): 305-327.

El-Swaify, S. A. and Fownes, J. H. (1989). Erosion Processes and Models Applications in the Tropics. 6th International Soil Conservation Conference, Ethiopia & Kenya, Geographical Bernensia.

European Commission (2001). Modelling Within Storm Erosion Dynamics, Borselli, Lorenzo. **2003**.

Evans, K. G. (1991). Erosion Prediction Models and Factors Affecting the Application of the Universal Soil Loss Equation to Post-Mining Landscape in Central Queensland. Queensland Coal Symposium, Brisbane, Australia, The Australasian Institute of Mining and Metallurgy.

Evans, K. G. and Loch, R. J. (1996). "Using the RUSLE to Identify Factors Controlling Erosion Rates of Mine Soils." Land Degradation and Development **7**(3): 267-277.

Evans, K. G. (1997). "Laboratory Rainfall Simulator Studies of Selected Open-Cut Coal Mine Overburden Spoils From Central Queensland." Australian Journal of Soil Research **35**(1): 15-29.

Falk, J. A. (1985). Prediction of Gully Incision on Reclaimed Slopes. Department of Civil Engineering. Fort Collins, University of Colorado: 80.

Fan, J. C. and Wu, M. F. (2001). "Estimation of Interrill Soil Erosion on Steep Slopes." Transactions of the Association of Agricultural Engineers **44**(6): 1471-1477.

Farmer, E. E. (1973). "The Relative Detachability of Soil Particles by Simulated Rainfall." Soil Science Society of America Proceedings **37**(4): 629-633.

Favis-Mortlock, D. (1998). Evaluation of Field Scale Erosion Models on the UK South Downs. Modelling Soil Erosion By Water. J. Bourdman, Favis-Mortlock, David. Berlin, Springer-Verlag. **1**: 141-157.

Favis-Mortlock, D. (2002). RillGrow Soil Erosion Models, Favis-Mortlock, D. **2003**.

Flanagan, D. C. and Livingston, S. J. (1995). WEPP User Summary. West Lafayette, NSERL.

Flanagan, D. C. and Nearing, M. A. (1995). USDA - Water Erosion Prediction Project Hillslope Profile and Watershed Model Documentation. West Lafayette, NSERL.

Flanagan, D. C. and Nearing, M. A. (2000). "Sediment Particle Sorting on Hillslope Profiles in the WEPP Model." Transactions of the American Society of Agricultural Engineers **43**(3): 573-583.

Foster, G. R. (1982). Modeling the Erosion Process. Hydrologic Modeling of Small Watersheds. C. T. Haan. St. Joseph, American Society of Agricultural Engineers: 533.

Foster, G. R. and Meyer, L. D. (1972a). Mathematical Simulation of Upland Erosion By Fundamental Erosion Mechanics. Present and Prospective Technology for Prediction Sediment Yields and Sources, Oxford, Mississippi, USDA-ARS.

Foster, G. R. and Meyer, L. D. (1972b). "Transport of Soil Particles by Shallow Flow." Transactions of the American Society of Agricultural Engineers **15**(1): 99-102.

Foster, R. L. and Martin, G. L. (1969). "Effect of Unit Weight and Slope on Erosion." Journal of the Irrigation and Drainage Division **95**(IR4): 551-561.

Gilley, J. E. (1982). Soil Erosion By Sheet Flow. Department of Agricultural and Chemical Engineering. Fort Collins, University of Colorado: 146.

Gilley, J. E. and Finkner, S. C. (1985). "Estimating Soil Detachment Caused by Raindrop Impact." Transactions of the American Society of Agricultural Engineers **28**(1): 140-146.

Gilley, J. E. (1977). "Runoff and Erosion Characteristics of Surface Mined Sites in Western North Dakota." Transactions of the American Society of Agricultural Engineers **20**(1): 697-700.

Govers (1987). Empirical Relationships for the Transport Capacity of Overland Flow. Erosion, Transport and Deposition, Jerusalem, IAHS.

Graphic Maps (2001). World Atlas.com. **2002**.

Grosh, J. L., , Jarrett, A.R. (1994). "Interrill Erosion and Runoff on Very Steep Slopes." Transactions of the American Society of Agricultural Engineers **37**(4): 1127-1133.

Guy, B. T. (1987). "The Roles of Rainfall and Runoff in the Sediment Transport Capacity of Interrill Flow." Transactions of the Association of Agricultural Engineers **30**(5): 1378-1386.

Hirschi, M. C. and Barfield, B. J. (1988). "KYERMO - A Physically Based Research Erosion Model Part I: Model Development." Transactions of the American Society of Agricultural Engineers **31**(3): 804-813.

Holtan, H. N. (1961). A Concept for Infiltration Estimates for Watershed Engineering. Washington, D.C., U.S. Department of Agriculture, Agricultural Research Service: 41-51.

Horton, R. E. (1933). "The Role of Infiltration in the Hydrologic Cycle." Transactions, American Geophysical Union **14**(1): 446-460.

Horton, R. E. (1945). "Erosional Development of Streams and Their Drainage Basins: Hydrophysical Approach to Quantitative Morphology." Bulletin of the Geological Society of America **56**(1): 275-370.

Huang, C.-h. and Laflen, J. M. (1996). "Seepage and Soil Erosion for a Clay Loam Soil." Soil Science Society of America Journal **60**: 408-416.

Hudson, N. (1993). Field Measurements of Soil Erosion and Runoff. Rome, Food and Agriculture Organization of the United Nations.

Jetten, V. (n.d.). LISEM: Limburg Soil Erosion Model. **2003**.

Julien, P. T. and Simons, D. R. (1985). "Sediment Transport Capacity of Overland Flow." Transactions of the Association of Agricultural Engineers **28**(3): 755-762.

Katholieke Universiteit Leuven (2002). WaTEM Homepage, Johann Boon. **2003**.

Kirkby, M. J. (1980). Soil Erosion. Chichester, Wiley.

Knisel, K. G. (1980). CREAMS: A Field Scale Model for Chemicals, Runoff and Erosion From Agriculture Management Systems. West Lafayette, USDA-ARS.

Laflen, J. (2002). Use of WEPP in a Mining Context.

Laflen, J. M., Elliot, W.J., Simanton, J.R., Holzhey, C.S., Kohl, K.D. (1991). "WEPP Soil Erodibility Experiments for Rangeland and Cropland Soils." Journal of Soil and Water Conservation(1): 39-44.

Laflen, J. M., Flannagan, Dennis.C., Ascough II, C., Weltz, Mark A., Stone, Jeffry J. (1994). The Wepp Model and Its Applicability for Predicting Erosion on Rangelands. Variability in Rangeland Water Erosion Processes: Proceedings of a Symposium, Soil Science Society of America Journal.

Laflen, J. M. (1997). "WEPP-Predicting Water Erosion Using A Process Based Model." Journal of Soil and Water Conservation: 96-102.

Laflen, J. M. and Roose, E. J. (1998). Methodologies for Assessment of Soil Degradation Due to Water Erosion. Methods of Assessment of Soil Degradation. R. Lal, W. H. Blum, G. Valentine and B. A. Stewart. Boca Raton, CRC Press LLC: 31-55.

Laflen, J. M. and Schertz, D. L. (1990). WEPP Modeling for the User. Transferring Models to Users: Hyatt Regency Denver, Denver, Colorado, November 4-8, 1990, Denver, Colorado, USA, American Water Resources Association.

Lal, R. (1990). Soil Erosion in the Tropics Principles and Management. New York, McGraw Hill Inc.

Lane, L. J. (1989). National Water Conference : Proceedings of the Specialty Conference / Sponsored by the Irrigation and Drainage Division and the Water Resources Planning and Management Division of the American Society of Civil Engineers and the Delaware Section of ASCE. National Water Conference: Proceedings of the Specialty Conference, Newark, Delaware, American Society of Civil Engineers.

Lattanzi, A. R. (1974). "Influences of Mulch Rate and Slope Steepness on Interrill Erosion." Soil Science Society of America Journal **38**(1): 946-950.

Loch, R. J. (1984). "Field Rainfall Simulator Studies on Two Clay Soils of the Darling Downs, Queensland. III An Evaluation of Current Methods for Deriving Soil Erodibilities (K Factors)." Australian Journal of Soil Research **22**(4): 401-412.

Loch, R. J. and Donnollan, T. E. (1982b). "Field Rainfall Simulator Studies on Two Clay Soils of the Darling Downs, Queensland. II Aggregate Breakdown, Sediment Properties and Soil Erodibility." Australian Journal of Soil Research **21**(1): 47-58.

Loch, R. J. (2001). "A Multi-Purpose Rainfall Simulator for Field Infiltration and Erosion Studies." Australian Journal of Soil Research **39**(3): 599-610.

Marshall, T. J. (1996). Soil Physics. Cambridge, Press Syndicate of the University of Cambridge.

Meinardus, A. (1996). EPIC, Dagitz, Steve. **2003**.

Meyer, L. D. (1981). "How Rain Intensity Affects Interrill Erosion." Transactions of the American Society of Agricultural Engineers **24**(6): 1472-1475.

Meyer, L. D. (1985). Interrill Erosion Rates and Sediment Characteristics. Soil Erosion and Conservation. S. A. S. A. El-Swaify, W. C. Moldenhauer and A. Lo. Ankeny', Soil Conservation Society of America: 793.

Meyer, L. D. (1975). "Effect of Flow Rate and Canopy on Rill Erosion." Transactions of the American Society of Agricultural Engineers **18**(5): 905-911.

Meyer, L. D. and McCume, D. L. (1958). "Rainfall Simulator for Runoff Plots." Agricultural Engineering **39**: 644-48.

Meyer, L. D. and Wischmeier, W. H. (1969). "Mathematical Simulation of the Process of Soil Erosion by Water." Transactions of the American Society of Agricultural Engineers **12**(4): 754-758.

Misra, M. K. and Rose, C. W. (1995). "An Examination of the Relationship Between Erodibility Parameters and Soil Strength." Australian Journal of Soil Research **33**: 715-732.

Moore, I. D. and Burch, G. J. (1986). "Sediment Transport Capacity of Sheet and Rill Flow: Application of Unit Stream Power Theory." Water Resources Research **22**(8): 1350-1360.

Morgan, R. P. C. (1998). The European Soil Erosion Model (EUROSEM): documentation and user guide, Silsoe College, Cranfield University: 89.

Nakano, M. (1986). "Computer Analysis on Effects of Land Parcel Shape Upon Rill Network Formation." Journal of Irrigation Engineering and Rural Planning **10**: 34-39.

Neal, J. H. (1938). "Effect of Degree and Length of Slope on Rainfall Characteristics on Runoff and Soil Erosion." Agricultural Engineering **19**(5): 213-217.

Nearing, M. A. (1998). "Primary Verification and Adaptation of the WEPP Model for Ukrainian Conditions: Problems, Possible Solutions, and Perspectives." Eurasian Soil Science **31**(3): 88-91.

Nearing, M. A. (1990). "Sensitivity Analysis of the WEPP Hillslope Profile Erosion Model." Transactions of the American Society of Agricultural Engineers **33**(3): 839-849.

Nearing, M. A. (1989). "A Process-based and Soil Erosion Model for USDA-Water Erosion Prediction Project Technology." Transactions of the American Society of Agricultural Engineers **32**(5): 1587-1593.

Nearing, M. A. (1994). Modelling Soil Erosion. Soil Erosion Research Methods. R. Lal. Delray Beach, St. Lucie Press: 340.

Nearing, M. A. and Nicks, A. D. (1998). Evaluation of the Water Erosion Prediction Project (WEPP) Model for Hillslopes. Modelling Soil Erosion by Water. J. Bourdman, Favis-Mortlock, David. Berlin, Springer-Verlag. **1**: 43-53.

Nichols, M. L. and Sexton, H. D. (1932). "A Method of Studying Soil Erosion." Agricultural Engineering **13**(1): 101-103.

Olson, O. C. and Wischmeier, W. H. (1963). "Soil Erodibility Evaluations for Soils on the Runoff and Erosion Stations." Soil Science Society of America Proceedings **27**(1): 590-592.

Owoputi, L. O. (1994). A Physically Based Study of the Mechanism of Sediment Detachment in the Soil Erosion Process. Department of Civil Engineering. Saskatoon, University of Saskatchewan: 247.

Owoputi, L. O. (1995). Erosion From an Engineered Mine Waste Rock Cover Under an Extreme Rainfall Event. 1995 Annual Conference of the Canadian Society of Civil Engineers, Ottawa, Ontario.

Pearce, A. J. (1986). "Storm Runoff Generation in Humid Headwater Catchments1. Where Does the Water Come From?" Water Resources Research **22**(8): 1263-1272.



Press, F. a. R. S. (1985). Earth. New York, W.H. Freeman and Company.

Renard, K. G. (1994). The Revised Universal Soil Loss Equation. Soil Erosion Research Methods. R. Lal. Delray Beach, St. Lucie Press: 340.

Risse, L. M. (1993). "Determining the Green-Ampt Effective Hydraulic Conductivity From Rainfall-Runoff Data for the WEPP Model." Transactions of the American Society of Agricultural Engineers **37**(2): 411-418.

Risse, L. M. (1995). WEPP: Validation and Application. Carrying the Torch for Erosion Control: An Olympic Task: Proceedings of Conference XXVI, Atlanta, Georgia, USA, International Erosion Control Association.

Rose, C. W. (1961). "Rainfall and Soil Structure." Soil Science **91**(1): 49-54.

Rose, C. W. (1997). Modeling Erosion by Water and Wind. C. LLC: 57-87.

Rymshaw, E. (1997). "Processes of Soil Movement on Steep Cultivated Hill Slopes in the Venezuelan Andes." Soil and Tillage Research **44**(3-4): 265-272.

Schroeder, S. A. (1987). "Slope Gradient Effect on Erosion of Reshaped Spoil." Soil Science Society of America Journal **51**: 405-409.

Selby, M. J. (1993). Hillslope Materials and Processes. Oxford, Oxford University Press.

Sheng, T. C. (1989). Modelling of the Hydrological Response of Catchments to Land Use Change. Hydrology and Water Resources Symposium 1989: Comparisons in Austral Hydrology. E. M. O'Loughlin, D. I. Short and W. R. Dawes. Christchurch, New Zealand, University of Canterbury: 335-340.

Sheridan, G. J. (2000a). "Use of Laboratory-scale Rill and Interrill Erodibility Measurements for the Prediction of Hillslope-Scale Erosion on Rehabilitated Coal Mine Spoils and Overburden." Australian Journal of Soil Research **38**(2): 285-97.

Sheridan, G. J. (2000b). "Estimation of Erosion Model Erodibility Parameters from Media Properties." Australian Journal of Soil Research **38**(2): 265-84.

Singer, M. J. (1978). "In-situ Study of Podzolization of Tephra and Bedrock." Soil Science Society of America Journal **40**(1): 105-111.

Sloan, P. G. and Moore, I. D. (1984). "Modeling Subsurface Stormflow on Steeply Sloping Forested Watersheds." Water Resources Research **20**(12): 1815-1822.

Smith, R. E. (1995). KINEROS - A KINematic Runoff and EROSION Model. Computer Models of Watershed Hydrology. V. P. Singh. Highlands Ranch, Water Resources Publications: 697-732.

Stolte, W. J. (1990). "The Impact of Seepage on Soil Erosion." Transactions of the American Society of Agricultural Engineers **33**(2): 475-479.

Terzaghi, K. (1925). "Principles of Soil Mechanics II, Compressive Strength of Clays." Engineering News Record **96**(20): 799-.

Thornton, C. J. (1999). Gully Intrusion into Reclaimed Slopes: A long-term Time Averaged Calculation Procedure. Department of Civil Engineering. Fort Collins, Colorado State University: 111.

Tiscareno-Lopez, M. (1993). "Sensitivity Analysis of the WEPP Watershed Model for Rangeland Applications I: Hillslope Processes." Transactions of the American Society of Agricultural Engineers **36**(6): 1659-1672.

Tiwari, A. K. (2000). "Evaluation of WEPP and Its Comparison with USLE and RUSLE." Transactions of American Society of Agricultural Engineers **43**(5): 1129-1135.

Toy, T. R. and Foster, G. R., Eds. (1998). Guidelines for the Use of the Revised Universal Soil Loss Equation (RUSLE) Version 1.06 on Mined Lands, Construction Sites and Reclaimed Land. Denver, Western Regional Coordinating Centre Office of Surface Mining.

Truman, C. C. and Bradford, J. M. (1993). "Relationships Between Rainfall Intensity and the Interrill Soil Loss-Slope Steepness Ratio as Affected by Antecedent Water Content." Soil Science **156**(6): 405-413.

Turner, A. K. (1985). Rainfall Intensity and Overland Flow in Relation to Soil Erosion Studies for Tropical Lands. Soil Erosion Management. E. T. Craswell, J. V. Remenyl and L. G. Nallana. Canberra, Australian Centre for International Agricultural Research: 24-31.

United States Forest Service (2002). Forest Service WEPP interfaces, Bill Elliot. **2002**.

Uri, N. (2001). "A Note on Soil Erosion and Its Environmental Consequences in the United States." Water, Air and Soil Pollution **129**(1): 181-197.

USDA-ARS (n.d.). AGNPS Web Site, Sedimentation Laboratory. **2003**.

Warrington, D. (1989). "Slope and Phosphogypsum's Effect on Runoff and Erosion." Soil Science Society of America Journal **53**(4): 1201-1205.

Watson, D. A. and Laflen, J. M. (1986). "Soil Strength, Slope and Rainfall Intensity Effects on Interrill Erosion." Transactions of the American Society of Agricultural Engineers **29**(1): 98-102.

Williams, D. (2002a). Erosion and Vegetation.

Williams, D. J. (2002b). "Prediction of Erosion from Steep Mine Waste Slopes." International Journal of Environmental Management and Health **12**(1): 35-50.

Williams, J. R. (1972). Sediment-Yield Prediction With Universal Equation Using Runoff Energy Factor. Present and Prospective Technologies for Predicting Sediment Yields and Sources, Oxford, Mississippi, USDA-ARS-S40.

Williams, J. R. (1995). The EPIC Model. Computer Models of Watershed Hydrology. V. P. Singh. Highlands Ranch, Water Resources Publications: 909-1000.

Wischmeier, W. H. (1971). "A Soil Erodibility Nomograph for Farmland and Construction Sites." Journal of Soil and Water Conservation **26**(5): 189-192.

Wischmeier, W. H. and Smith, D. D. (1958). "Rainfall Energy and its Relationship to Soil Loss." Transactions of the American Geophysical Union **39**(1): 25-291.

Wischmeier, W. H. and Smith, D. D. (1978). Prediction Rainfall Erosion Losses A Guide to Conservation Planning, USDA.

Yalin, Y. S. (1963). "An Expression of Bedload Transportation." Journal of the Hydraulic Division **89**(HY3): 221-250.

Yamamoto, T. and Anderson, H. W. (1973). "Splash Erosion Related Soil Erodibility Indexes and Other Forest Soil Properties in Hawaii." Water Resources Research **9**(1): 336-345.

Yang, C. T. (1972). "Unit Stream Power and Sediment Transport." Journal of the Hydraulics Division **98**(HY10): 1805-1826.

Young, R. A. and Onstad, C. A. (1976). "Predicting Particle-Size Composition of Eroded Soil." Transactions of the American Society of Agricultural Engineers **19**(6): 1071-1075.

Young, R. A. (1987). AGNPS, Agricultural Nonpoint Source Pollution Model: A Watershed Analysis Tool. Washington, USDA-ARS.

Young, R. A. and Wiersma, J. L. (1973). "The Role of Rainfall Impact in Soil Detachment and Transport." Water Resources Research **9**(6): 1629-1636.

Yu, B. (2000). "A Validation Test of WEPP to Predict Runoff and Soil Loss From a Pineapple Farm on a Sandy Soil in Subtropical Queensland, Australia." Australian Journal of Soil Research **38**(3): 537-554.

Yu, B. and Rose, C. W. (1999). "Application of A Physically Based Soil Erosion Model, GUEST, In the Absence of Data on Runoff Rates I. Theory and Methodology." Australian Journal of Soil Research **37**(1): 1-11.

Yu, B. (1997). "Toward A Framework For Runoff and Soil Loss Prediction Using GUEST Technology." Australian Journal of Soil Research **35**(5): 1191-1212.

Yu, B. and Rosewell, C. J. (2001). "Evaluation of WEPP for Runoff and Soil Loss Prediction at Gunnedah, NSW, Australia." Australian Journal of Soil Research **39**: 1131-1145.

Yu, B. (1999). "Application of A Physically Based Soil Erosion Model, GUEST, In the Absence of Data on Runoff Rates II. Four Case Studies From China, Malaysia and Thailand." Australian Journal of Soil Research **37**(1): 13-31.

Yulianti, J. S. (1996). Uncertainty Analysis in NonPoint Source Water Quality Management. Department of Civil and Geological Engineering. Winnipeg, University of Manitoba: 218.

Zeleeke, G. (1995). BPCDG: Breakpoint Climate Data Generator for WEPP Using Observed Standard Weather Data Sets. **2002**.

Zhang, X. C. (1996). "Evaluation of WEPP Runoff and Soil Loss Predictions Using Natural Runoff Plot Data." Transactions of the American Society of Agricultural Engineers **39**(3): 855-863.

Zingg, A. W. (1940). "Degree and Length of Land Slope as it Affects Soil Loss in Runoff." Agricultural Engineering **21**(2): 59-64.

---

## **APPENDIX I**

MODEL PARAMETER	UNITS	BASELINE VALUE	LOWER BOUND	UPPER BOUND
Climate		SEA	PNW	HI
Continuous Simulation		X	X	X
Single Storm		X	X	X
Tr-55		-	-	-
Years Of Simulation		100	100	100
Soil				
Texture		S	S	S
Albedo		0.6	0.1	0.7
Initial Saturation	%	70	50	80
Interrill Erodibility ( $K_i$ )	kg s/m <sup>2</sup>	4361520	3506005	10412000
Rill Erodibility ( $K_r$ )	s/m	0.0248	0.0235	0.0412
Critical Shear ( $\tau_{cr}$ )	Pa	2.242	2.242	3.57
Effective Hydraulic Conductivity ( $K_e$ )	mm/hr	8.01	3.91	8.37
Soil Layer 1				
Depth	mm	1700	-	-
Sand	%	90	70	100
Clay	%	10	0	30
Organics	%	0	-	-
CEC	meq/100g soil	2	-	-
Rock	%	0	-	-
Management		No Veg		
Initial Plant		Fallow	-	-
Bulk Density After Las Tillage	g/cm <sup>3</sup>	1.6	-	-
Initial Canopy Cover (%)	%	0	-	-
Days Since Last Tillage	Days	3652	-	-
Days Since Last Harvest	Days	3652	-	-
Initial Frost Depth	cm	0	-	-
Initial Interrill Cover	%	0	-	-
Initial Residue Cropping System		Fallow	-	-
Cumulative Rainfall Since Last Tillage	mm	48557	-	-
Initial Ridge Height After Last Tillage	cm	0	-	-
Initial Rill Cover (%)	%	0	-	-
Initial Roughness After Last Tillage	cm	0.5	-	-
Rill Spacing	cm	500	-	-
Rill Width Type		Temporary	-	-
Initial Snow Depth	cm	0	-	-
Initial Depth To Thaw	cm	0	-	-
Depth Of Secondary Tillage	cm	0	-	-
Depth Of Primary Tillage Layer	cm	0	-	-
Initial Rill Width	cm	0	-	-
Initial Total Dead Root Mass	kg/m <sup>2</sup>	0	-	-
Initial Total Submerged Residue Mass	kg/m <sup>2</sup>	0	-	-